Tracing Water and Nitrate Movement through Soils with Bromide

by

Ketema Tilahun Zeleke

Thesis

submitted in the fulfilment of the requirement of the degree of

Doctor of Philosophy

in the Faculty of Natural and Agricultural Sciences

Department of Geohydrology

University of the Free State

Bloemfontein

Republic of South Africa

January 2003

Promoter: Prof. J.F. Botha, Ph.D.

Co-promoter: Prof. A.T.P. Bennie, Ph.D.

ACKNOWLEDGMENTS

It is my sincere desire to acknowledge the following organizations and persons who contributed significantly towards the finishing of this thesis.

The Alemaya University (Ethiopia) for the leave given to me during this study and the Agricultural Research and Training Project of the University for the financial support during this study.

My promoter, Prof. J.F. Botha from the Institute for Groundwater Studies and my co-promoter, Prof. A.T.P. Bennie from the Department of Soil, Climate and Crop Sciences for their continuous guidance, support and encouragement during the field experiment, data analysis and modelling, and writing of this thesis.

The academic and administrative staff members of the Institute for Groundwater Studies for their assistance on various academic and administrative matters. The Department of Soil, Climate and Crop Sciences and the staff members of the former Department of Soil Sciences are acknowledged for providing me with their facilities at the experimental site and the cooperation rendered during the field experiment and laboratory analysis.

My mother Medemdemia Desalegn, my sisters and brothers whose prayer and encouragement was always supporting me. All my relatives and in-laws who took care of my family are also acknowledged.

My wife Hirut Assefa, my two sons Abenezer (Ab) and Nathan (Nati) for their patience during my long absence from home during this study. Had it not been for my wife's loving support throughout my past and present studies, I would have not been able to achieve this goal.

My Lord and Savior Jesus Christ, whose comfort, encouragement, guidance and mercy is always with me.

TABLE OF CONTENTS

Chapter 7

Conclusions and Recommendations 134

LIST OF FIGURES

Chapter 2

Field Determination of the Hydraulic Properties of a Bainsvlei Soil 10

Chapter 3

Steady State Transport of Bromide in the Field under Simulated Rainfall 33

Chapter 4

Transient State Transport of Bromide and Nitrate in the Field 67

Chapter 5

Comparison of Bromide and Nitrate Transport under Bare and Cropped Soil Conditions 91

Chapter 6

Application of the Solute Transport Parameters 119

LIST OF TABLES

Chapter 2

Field Determination of the Hydraulic Properties of a Bainsvlei Soil 10

Chapter 3

Steady State Transport of Bromide in the Field under Simulated Rainfall 33

Chapter 4

Transient State Transport of Bromide and Nitrate in the Field 67

Chapter 5

Comparison of Bromide and Nitrate Transport under Bare and Cropped Soil Conditions 91

Chapter 6

Application of the Solute Transport Parameters 119

LIST OF SYMBOLS

LATIN SYMBOLS

c volumetric concentration of dissolved solute.....[ML^{-3}]
c_i background solute concentration in the soil.....[ML^{-3}]
c_o volumetric input concentration of dissolved solute.....[ML^{-3}]
d Willmott's index of agreement .....[1]
f(v,D)joint probability density function (pdf) for v and D .....[1]
m_{ij} solute mass recovered from depth i at time j..... [M]
m_k total mass of Br recovered from the soil profile of depth z at position k ..... [M]
q Darcy velocity .....[LT^{-1}]
q_m maxium roo water extraction at z = 0 ..... [T^{-1}]
q_r root water extraction..... [T^{-1}]
s concentration of the adsorbed phase.....[MM^{-1}]
t time ..... [T]
t_o duration of solute application..... [T]
var [ ]variance .....[1]
v_s solute velocity .....[LT^{-1}]
v_w seepage velocity .....[LT^{-1}]
z soil depth..... [L]
z_p depth of peak concentration ..... [l]
z_r root depth ..... [L]
A area of field .....[L^2]
A_r water input (P+I) ..... [L]
C temperature dependent soil-limiting evaporation coefficient .....[1]
C_{p+i} bromide concentration of input water.....[ML^{-3}]
C_r bromide concentration of deep percolating water .....[ML^{-3}]
CV coefficient of variation.....[1]
D dispersion coefficient..... [L^2T^{-1}]
D_x dispersion coefficient in one of (x) the transverse direction..... [L^2T^{-1}]
D_y dispersion coefficient in the other (y) transverse direction..... [L^2T^{-1}]
D_z dispersion coefficient in the flow (z) direction ..... [L^2T^{-1}]
E_T evapotranspiration ..... [L]
E_V evaporation..... [L]
EV_p energy-limiting or potential evaporation ..... [L]
EV_s soil-limiting evaporation..... [L]

H hydraulic head ..... [L]
I irrigation..... [L]
K_d distribution coefficient for linear adsorption..... [$M^{-1}L^3$]
K_o steady state hydraulic conductivity .....[LT^{-1}]
K_s saturated hydraulic conductivity .....[LT^{-1}]
$K(\theta)$ hydraulic onductivity as a function of soil water content.....[LT^{-1}]
M1 first moment (breakthrough time) ..... [T]
M2 second moment (variance) .....[1]
P precipitation..... [L]
Q_r A_r-R..... [L]
R retardation factor .....[1]
$\hat{R}$ estimated deep percolation using the root water extraction models.....[LT^{-1}]
R_r deep percolation .....[LT^{-1}]
Y_D dispersion coefficient in lognormal distribution .....[1]
Y_v velocity variable in lognormal distribution.....[1]

GREEK SYMBOLS

α dispersivity..... [L]
α_L longitudinal dispersivity..... [L]
α_T transverse dispersivity..... [L]
λ_s first-order decay coefficient for the solid phase..... [T^{-1}]
λ_w first-order decay coefficient for the liquid phase ..... [T^{-1}]
μ mean of the logtransformed variable .....[1]
γ_s zero-order production term for the solid phase ..... [$MM^{-1}T^{-1}$]
γ_w zero-order production term for the liquid phase..... [$ML^{-3}T^{-1}$]
η consatnt that relates q_r to q_m in the root water extraction model.....[1]
θ volumetric water content..... [L^3L^{-3}]
$\overline{\theta}$ depth-averaged soil water content..... [L^3L^{-3}]
θ_o steady state soil water content..... [L^3L^{-3}]
θ_r residual water content..... [L^3L^{-3}]
θ_s saturated water content ..... [L^3L^{-3}]
ρ_b bulk density.....[ML^{-3}]
ρ_{vD} correlation coefficient between Y_v and Y_D .....[1]
σ_D standard deviation of the logtransform of D.....[1]
σ_v standard deviation of the logtransform of v.....[1]
Δ difference (e.g. ΔS is change in soil water storage).....[1]
<..> ensemble average, e.g., <c(z,t)> is the ensemble average concentration

ABBREVIATIONS

BTC	breakthrough curve
CAN	calcium ammonium nitrate
CDE	convective-dispersive equation
CXTFIT	concentration-distance-time fitting
DAP	days after crop planting
ERFC	complementary error function
NIR	net infiltrated rain
STM	stream tube model
USDA	united states department of agriculture
3DADE3	dimensional advection-dispersion equation

CHAPTER 1

INTRODUCTION

1.1 GENERAL

The world population is increasing at an alarming rate with a corresponding increase in the need for food and fibre to feed and cloth the population. Agriculture is a major provider for these human needs. With this ever-increasing pressure on agriculture, horizontal and vertical expansions are the only options to satisfy these needs. However, with the expansion of agriculture to more fragile lands, deforestation, erosion and desertification might follow. Vertical expansion, the intensification of agriculture through irrigation, fertilizer, pesticide, and herbicide application is the option that many nations are following presently. However, this often causes non-degradable compounds of these agrochemicals to contaminate the water resources. Groundwater, by virtue of its location and the very slow rate of motion, is very prone to the danger of pollution by leaching of these agrochemicals through the soil. Therefore, the intense application of these chemicals has created concern and awareness of agrochemicals as non-point sources of groundwater contamination. The same applies, of course, to other contaminants originating in the unsaturated zone. Deep leaching of agrochemicals, besides being a threat to the groundwater quality, also presents an economic loss to the farmer. A proper understanding and management of this zone is therefore essential for protecting and improving the quality of groundwater supplies and saving on agricultural costs.

The major agrochemicals threatening groundwater quality are NO_3^--N, pesticides and herbicides. Nitrate can originate from a number of non-point and point sources, including fertilizers, mineralization of organic matter, geological origins, septic tanks, and animal manures. Agricultural-nitrate contamination of groundwater depends upon climate, fertilizer management, soil, crop, and farming systems. In areas where rainfall is higher than evaporation, water, which infiltrated the soil, moves to the groundwater taking NO_3^--N with it. Nitrate losses are likely to be more when all the nitrogen is applied in one application compared to split applications. Nitrogen losses from fertilizers can be reduced by matching the quantity of fertilizer applied with the nitrogen need of a crop.

1.2 TRACER STUDIES AND MODELLING

Knowledge about the rate at which NO_3^--N is leached through the soil is very important to implement different fertilizer management practices. However, NO_3^--N transport is a

very complex process in which chemical, physical, and biological components interact. Tracer studies of conservative (chemically non-reactive) chemicals, such as chloride and bromide are consequently often used to study the movement of agrochemicals in general, and NO_3^--N in particular, towards the groundwater. However, comparisons of Br^- and NO_3^--N transport is often drawn from experiments conducted in a laboratory on small soil columns. While laboratory tracer experiments provide unique opportunities to study conceptual mechanisms affecting solute transport, they should always be augmented with field studies, since the ultimate purpose is to predict actual transport in the field. The focus therefore increasingly shifts from laboratory to field-scale tracer studies as it is not possible to fully study the transport processes with repacked laboratory columns of 10 cm diameter, because several factors affect the field-scale flow and transport processes. Some of the most important of these processes include: soil properties, such as texture and structure (Bronswijk *et al*., 1995; Kelly and Pomes, 1998), irrigation methods (sprinkling or flooding) (Bowman and Rice, 1986; Jaynes *et al*., 1988), land use (tilled or untilled) (Fleming and Butters, 1995) and the presence of a crop (Iragavarapu *et al*., 1998). In addition, there is high spatial (both horizontal and vertical) and temporal variation of the transport and flow processes (Biggar and Neilsen, 1976; Williams *et al*., 1998). For these reasons, the true picture of solute transport processes can be attained only from tracer experiments conducted in the field, preferably in the presence of crops.

Field studies are not only very laborious, but also expensive. There has been a tendency in recent years to couple such field studies with computer models to simulate field-scale solute transport through the unsaturated zone. Many of these studies are based on the classical convective-dispersive equation (CDE). This model was developed on the basis of solute transport experiments in soil columns in laboratories (Biggar and Neilson, 1976) and assumes constant solute transport parameters (velocity and dispersion coefficient). In general, this equation is able to simulate solute transport in one-dimensional laboratory soil columns accurately (Porro *et al*., 1993) and has been applied with some success in homogenous field soils (Jaynes, 1991). Experimental investigations, however, have shown that most field soils are heterogeneous (Biggar and Nielsen, 1976; Sudicky, 1986), because of factors such as the spatial variability of soil properties in the field and the existence of preferential flow paths. Laboratory-verified models are therefore not able to simulate field-scale solute transport very accurately (Sposito *et al*., 1986). This observation led to the introduction of the stochastic stream tube model (STM), which views the field as a series of independent vertical soil columns (Jury and Roth, 1990; Dagan, 1993). This model tries to account for the field variability by describing transport in each tube with the CDE in which the model parameters are considered realizations of a stochastic process with a bivariate lognormal probability distribution function (pdf). The

stream tube model is therefore, in principle, able to account for horizontal heterogeneities in the soil, but not vertical heterogeneities.

Both the CDE and STM are parametric models of the physical system and values of the model parameters (e.g. the velocity and dispersion coefficient) need to be estimated before the model can be applied, the so-called inverse problem. In this study, the CXTFIT package of Toride *et al*. (1995) was used to estimate solute transport parameters from the concentration data observed during a number of tracer studies in the field. This package has the advantage that it can also be used to directly simulate solute distributions as functions of space and time for observed model parameters. The package also allows one to analyse transport under intermittent, transient flow conditions by using cumulative drainage, instead of time, as an independent variable. As stated by Leij and Bradford (1994), one of the advantages of an analytical model is that it can be used to perform a sensitivity analysis of the model parameters.

1.3 PURPOSE OF THE STUDY

There is no documented study on solute transport properties of the Bainsvlei and related soils, which cover large parts of the central South Africa and many of the soils of Ethiopia. As such, there is a need for a controlled field experiment through which NO_3^--N movement in relation to conservative tracers is compared and solute transport models tested. The main aim of this study was therefore to conduct controlled field experiments and compare Br^- and NO_3^--N transport under steady state, transient state, and field crop conditions on these soils and to compare the transport parameters determined from the deterministic convective-dispersive equation with that of the stochastic stream tube model.

1.4 SCOPE OF THE STUDY

Solute transport in soils is controlled by a combination of factors including soil type, climate, land-use, and the solute itself. In this study an attempt was made to study the movement of Br^- and NO_3^--N in bare soils and soils planted with crops under continuous and intermittent irrigation practices and natural rainfall in two different climatic regions. The first set of experiments was performed on the experimental farm of the Department of Soil, Climate and Crop Sciences at the University of the Free State, situated approximately 10 km north-west of Bloemfontein and the second at the experimental farm of Alemaya University in Ethiopia. The soil profiles of both study areas consist mainly of fine sandy loam covered by sandy top layers.

1.4.1 Soil Properties

Soil hydraulic properties are usually determined in a laboratory from disturbed or undisturbed soil samples. Laboratory methods are easy, quick and less expensive. However, soil hydraulic properties are affected by soil structure, pore size and geometry, which are easily damaged when taking the samples. The hydraulic properties of soils should therefore be determined *in situ*, whenever possible.

Unsaturated soil hydraulic conductivity and water retention are important parameters in the flow and mass transport studies of the vadose zone. The first step in the investigation was therefore to determine the hydraulic properties of the Bainsvlei soil profile. As discussed in Chapter 2, the water content and matric potential of a 160 cm deep soil profile was monitored for about one month during the redistribution period following an initially steady state soil water flux condition. Textural class, bulk density, hydraulic conductivity and water retention of the soil profile were determined *in situ*. An exponential equation of the form

$$K(\theta) = K_0 \exp\left[\beta(\theta - \theta_0)\right]$$

was used to express the hydraulic conductivity as a function of the water content of the soil. The parameters K_0 and β were determined from measured values of $\theta(z, t)$ using simplified models described by Libardi *et al*. (1980) based on Richards' equation. The values of K_0 determined from the Flux method and the CGA method were higher than that of the other simplified methods described by Libradi *et al*. (1980), while the Flux method yielded the highest β-values and the CGA method the lowest.

The K-θ relation for different layers of the soil profile was established using the simplified methods of Libardi *et al*. (1980), the internal drainage model of Hillel *et al*. (1972) and the model of van Genuchten (van Genuchten, 1980; Botha, 1996). In the simplified methods, the calculated K_0 and β values were used to determine the unsaturated hydraulic conductivities of the soil layers. The estimated values of K using the CGA model were consistently higher than the other models at all depths.

The index of agreement introduced by Willmott (1981) was used to compare the K-values derived from Libardi's simplified models and van Genuchten's model with the K- values derived from the internal drainage model of Hillel. This comparison showed that the K-θ relationship of the Bainsvlei soil is better described by the van Genuchten and internal drainage models than the simplified Libardi's models, for which the index of agreement decreased with depth. This behaviour of Libardi's models is probably caused by a

deviation of hydraulic gradient values from unity at deeper depths—a basic assumption of these models.

1.4.2 Steady State Transport of Bromide

The first set of experiments performed at the Bainsvlei test site concerned a field-scale tracer study of bromide under steady state conditions. Two experiments carried out for this purpose are described in Chapter 3. The first experiment with a rainfall intensity of 5.41 mm h^{-1} was conducted for 96 hours and the second with a rainfall intensity of 3.27 mm h^{-1} for 124 hours. A rainfall simulator was used in both experiments to apply water on a (120 x 120) cm^2 area. The inner (100 x 100) cm^2 of the area under the simulator was isolated with sheets of metal inserted to a depth of 20 cm into the soil that extended 20 cm above the soil surface. It was assumed that the soil column achieved a steady state when the four tensiometers installed at depths of 30 cm, 45 cm, 90 cm, and 120 cm, showed little or no changes in the matric potential. A conservative tracer Br^- was then applied as KBr at a rate of 13.5 g Br^- m^{-2}. Soil samples were taken to a maximum depth of 160 cm at 20 cm interval using a cylindrical auger of 4.2 cm diameter. The soil was dried and crushed to pass a 2 mm sieve for Br^- analysis. Then 50 g of soil was mixed with 50 ml of water and shaken for one hour on a laboratory shaker. The solution was filtered and its Br^- concentration determined using ion chromatography. Bromide recovery at a particular time of sampling was determined by integrating the Br^- mass recovered from the series of soil cores, taken over the sampling depth of 160 cm. These results indicated that almost 100% in the first experiment and 95.6% in the second experiment during the time before the Br^- begin to leach to depths exceeding the sampling depth.

Solute transport parameters were determined by fitting the observed bromide profiles to the CDE and STM models with the package CXTFIT. This yielded the values of 2.24 cm h^{-1} and 2.20 cm h^{-1} respectively for the pore-water velocities associated with the rainfall intensity of 5.41 mm h^{-1}, which is similar to the 2.05 cm h^{-1} and 2.02 cm h^{-1}, derived from the observed velocities of the concentration peak and solute centre of mass, and the pore-water velocity of the infiltrating water, 2.08 cm h^{-1}. These results indicate that the Br^- experience very little if any preferential flow in this relatively homogeneous and weakly structured soil during the experiment. This conclusion was confirmed by the sensitivity analysis of the parameters, which indicated that variations in the dispersion coefficient have almost no effect on the movement of the centre of mass, but completely control the width of the solute plume.

1.4.3 Transient State Transport of Bromide

In practice, soils in the field always experience transient conditions due to the intermittent nature of evaporation, transpiration, rainfall and irrigation. Tracer experiments are, nevertheless, usually carried out under steady state conditions. A second set of experiments were therefore performed in which Br^- was applied to a plot of (200 x 200) cm^2, which was then irrigated intermittently with sprinklers for one month. The soil profile was again sampled to a maximum depth of 160 cm at intervals of 20 cm.

Although it is possible to model transient conditions with numerical models, these models often require large sets of data. However, it has been suggested (Wierenga, 1977; Jury *et al*., 1982; Sharma and Taniguchi, 1991; Meyer-Windel, 1999) that the analytical models used in the study of steady state solutions may be applied to transient conditions, if the time variable in these models is replaced by the cumulative drainage. This approach was consequently also used to fit the soil Br^- concentrations observed during this study to the CDE and STM models with CXFIT. The average coefficients of determination yielded by these fits (r^2 = 0.868 and 0.872) clearly support this procedure, especially if the duration of the experiment and the heterogeneity of natural soils is taken into account.

The average pore-water velocities of 2.22 cm d^{-1} and 2.32 cm d^{-1} and average dispersion coefficients of 20.67 and 18.02 cm^2 d^{-1} determined from these fits are considerably lower than the fitted values for the steady state experiments. This means that the Br^- moved considerably slower under the intermitted application of water than in the steady case, a conclusion supported by the observed behaviour of the solute peaks.

1.4.4 Comparison of Seasonal Leaching of Bromide and Nitrate

Bromide is commonly used as a substitute for NO_3^--N in studies of the movement of fertilizers through a soil profile. Since, there were no comparative evaluation of the transport and leaching properties of Br^- and NO_3^--N for the Bainsvlei soil under local soil and rainfall conditions, another experiment was conducted to compare the leaching of Br^- and NO_3^--N in this soil. In this experiment, also discussed in Chapter 4, a bare and level plot of (245 x 245) cm^2 was isolated from its surroundings using galvanized sheet metal and solutions of KBr and KNO_3 at the rates of 13.5 g Br^- m^{-2} and 20 g N m^{-2} were applied uniformly to the plot at the beginning of the experiment. The rainfall was measured with two rain gauges next to the plot and the soil sampled five times during the season to a maximum depth of 160 cm at intervals of 20 cm. The soil water content of the profile was measured at the same times of soil sampling with a neutron probe. The Br^- and NO_3^--N concentrations were determined from the extracts from the soil samples using ion

chromatography. The movement of the solutes was again analysed with CDE and STM models using CXTFIT. These results indicated that the Br^- and NO_3^--N exhibited similar transport properties in the Bainsvlei soil, and that Br^- can be used with confidence as a substitute for NO_3^--N in this soil.

Approximately 67% and 48% of the applied Br^- and NO_3^--N respectively leached below the sampling depth of 160 cm at the end of the season. This behaviour can be ascribed to the relatively high deep percolation rate—the flux of water at the sampling depth—that was approximately equal to 56% of rainfall. These results indicate that agricultural non-point sources pose a considerable risk for the contamination of groundwater sources in this sandy textured soil. This conclusion is supported by the current levels of NO_3^--N (27.96 mg L^{-1}) in the groundwater at the site.

1.4.5 Bromide and Nitrate Transport under Bare and Cropped Soil Conditions

Nitrogen fertilizer is an important agricultural input in any crop production system. However, leaching of this fertilizer is a threat to the environment and an economic loss to the farmer. Since nitrogen experiences complex and interdependent transformations in the soil, its leaching in soils is often studied with conservative tracers. However, only a few studies, which compare the movement of a conservative tracer with that of NO_3^--N, have been done under cropped soil conditions. In this study, described in Chapter 5, a field experiment was conducted to compare Br^- and NO_3^--N transport under bare and maize planted soil conditions at the experimental site of the Alemaya University at Dire Dawa in East Ethiopia.

The experiment was performed from March 2001to May 2001 on six plots of (500 x 500) cm^2, on land which was not cultivated before. Three of the plots were left bare and three planted with maize. The inner (300 x 300) cm^2 of each plot was isolated from the surrounding area with metal sheets and used for soil sampling. At the beginning of the experiment, potassium bromide and calcium ammonium nitrate were applied at rates of 200 kg ha^{-1} (135 kg Br ha^{-1}) and 800 kg ha^{-1} (224 kg N ha^{-1}) respectively. Since the natural rainfall was not sufficient to sustain the maize, the plots were irrigated from time to time during the experiment. Soil and plant samples were taken eleven times during the experiment to determine the Br^- and NO_3^--N concentrations with ion chromatography. The soil was sampled every 20 cm to a maximum depth of 160 cm. At harvest, the leaf, stalk and grain parts of the plant were analysed separately.

The mass of Br^- recovered (as a percentage of the mass applied) from the soil of the bare and maize plots was 98.5% and 86.8% respectively and 308.8% and 124.5% for nitrogen.

The lower recovery of Br^- from the maize plots can probably be ascribed to crop uptake, while the high recovery of nitrogen can be attributed to the very high background concentration of nitrogen in all six soil profiles. This high background nitrogen concentrations is caused by the high evaporation and low precipitation in this semi-arid region, with the result that dissolved solids only leached to the shallow depths. Since the land was not cultivated before and covered only by shallow rooted grasses, nitrogen had ample time to accumulate in the top soil layers.

The average pore-water velocities obtained from a study of the water balances on bare and maize plots were 0.96 cm d^{-1} and 1.51 cm d^{-1} respectively, and that determined from fitting the CDE model to the observed Br^- concentration profiles 1.47 cm d^{-1} and 1.78 cm d^{-1} respectively. This may be an indication that some preferential flow occurred in the soil. This conclusion is supported by the velocities estimated from the positions of the peak concentrations and mass centres of 1.32 cm d^{-1} and 1.95 cm d^{-1} in the case of Br^- and 1.47 cm d^{-1} and 1.78 cm d^{-1} in the case of NO_3^--N. This inferred preferential flow may have been caused by small cracks that developed in the soil, especially the bare soil, during the wetting and drying of the soil and flow along the plant roots and root holes in the maize plots. These mechanisms may also have been responsible for the occurrence of Br^- peaks at an average depth of 90 cm in the bare plots and 130 cm in the maize plots at the end of the experimental period. The Br^- concentration profiles display distinct peaks on both the bare and the maize plots, but the NO_3^--N concentration always increased with depth, probably because of its high background concentration. These results suggest that while Br^- might not be used to determine the loss of NO_3^--N from the plant-soil system, it can be useful to study the movement of NO_3^--N in a natural soil column.

The plant tissue Br^- and NO_3^--N concentrations decreased continuously during the growing season due to the accumulation of biomass and the consequential dilution of the solutes. The total mass uptake over the growing season amounted to 64.4% of the original mass supplied as fertilizer in the case of nitrogen and 8.1% in the case of bromide. The cumulative mass of bromide taken up by the crop increased steadily with time during the season, but that of nitrogen showed a strong dependence on the vegetative stage of the plant. It may therefore be more beneficial to both crops and the contamination of groundwater if fertilizers are applied intermittently during the growing season of the plant and not as a batch at the time of planting.

Tracers are often used to estimate deep percolation rates of water, in addition to their application in solute transport studies. A common assumption made in such investigations is that the pore-water velocity of water remains constant through the soil profile. While

this assumption may be valid at depths below the root zone, it is rather unlikely that the pore-water velocity will be constant within the root zone. The deep percolation rates derived from constant pore-water velocity models may consequently be largely in error. A study of the deep percolation rates calculated from a constant velocity model and one in which the plant water extraction in the root zone follows an exponential law, showed that this is indeed the case. As could have been expected, the difference between the two sets of velocities decrease with depth.

The mass balance of the applied Br^- and its average concentration at a depth of 100 cm was also used to determine the deep percolation at this depth. The deep percolation determined according to the Br^- mass balance was about 15% lower than the one determined using soil water balance approach.

1.4.6 Application of the Solute Transport Parameters

A major advantage of modelling solute transport in soils is the ability of the models to describe the behaviour of the solute at different times and depths, without performing expensive and tedious field observations. Examples of such applications is discussed in Chapter 6, where the mass transport parameters derived from the field investigations described in Chapters 4 and 5 were used to simulate the arrival time of a conservative tracer at the groundwater table.

Although one-dimensional solute transport in the vadose zone may be a reasonable assumption for most practical purposes, solute transport in the soil is always a three-dimensional phenomenon. The three-dimensional analytical model 3DADE of Leij and Bradford (1994) and the mass transport parameters determined from the steady state experiment described in Chapter 3 was consequently used to simulate three-dimensional transport, assuming that the transverse dispersion coefficient is equal to one tenth of the longitudinal dispersion coefficient derived from the field observations. This model indicated that the Br^- concentration remained uniform only in the inner (80 cm x 80 cm) of the (100 cm x 100 cm) plot used in the experiments. Samples taken too far from the centre of an experimental plot could therefore introduce significant variations in observed concentrations and errors in results derived from one-dimensional models. Since the distribution of the dissolved solids in the soil is non-linear, samples should never be taken too far from the centre of experimental plots in field studies of solute transport analysed with one-dimensional models.

CHAPTER 2

FIELD DETERMINATION OF THE HYDRAULIC PROPERTIES OF A BAINSVLEI SOIL

2.1 INTRODUCTION

Water movement and retention within the soil is an important component of agricultural and environmental processes such as irrigation, subsurface drainage, and waste disposal. The rates at which these processes occur depend upon the water transmission characteristics of the subsurface of the earth, particularly the hydraulic conductivity. It is therefore essential to know the hydraulic conductivity of the soil and rocks that comprises the earth's subsurface when investigating such phenomena. This restraint presents a severe problem in field investigations of such phenomena, particularly in the unsaturated or vadose zone of the earth where the hydraulic conductivity is extremely sensitive to changes in the matric pressure head of the soil and therefore its water contents, θ and there is no universal expression that describes this relation. One approach to circumvent this problem would be to determine the relation experimentally in the field. This approach has the advantage that it can be applied simultaneously at several soil depths under natural conditions that include overburden pressure, swelling and shrinkage and the effects of water quality (Kutilek and Nielsen, 1994). However, such measurements are rather time consuming, expensive, and only yield information for a particular soil at a particular point in the soil. It has consequently become practice to base investigations of the vadose zone on empirical and semi-empirical models of the flow of water in the subsurface of the earth derived from observations of the redistribution of water in the field (Libardi *et al*., 1980; Sisson *et al*., 1980; Chong *et al*., 1981). The latter approach was consequently also applied in this investigation. Hydraulic conductivities were determined for different layers of a Bainsvlei soil near Bloemfontein (South Africa) using matric pressure heads and water contents measured during redistribution period of an initially steady state soil profile.

The discussion below begins with a description of the simplified models used in the investigation in Section 2.2. This is followed by a discussion of the experimental site and the field investigations to test the validity of a number of models proposed for the estimation of hydraulic conductivities in Section 2.3. The models are evaluated in Section 2.4 by fitting them to the observed field data and by comparing the estimates with one another.

2.2 SIMPLIFIED MODELS

2.2.1 General

The models conventionally used in field investigations of the vadose zone can be conveniently divided into two classes—those that concentrate on the hydraulic conductivity as such and models that tend to give a more general description of the distribution of water.

The first group of models is perhaps best represented by the empirical model of Libardi *et al*. (1980), the power function models of Chong *et al*. (1981) and the semi-empirical internal drainage model of Hillel *et al*. (1972). The best-known model in the second group, especially in saturated-unsaturated flow, is probably that of van Genuchten (1980).

2.2.2 The Empirical Model of Libardi *et al*

The basic premise of this model is that the hydraulic conductivity of the soil, K, at a given water content, θ, is related to the steady-state values of the two parameters, K_0 and θ_0, through the equation

$$K(\theta) = K_0 \exp[\beta(\theta - \theta_0)] \qquad (2.1)$$

where β is a parameter that describes the drainage characteristics of the soil. The parameter θ_0 can be measured in the field with the neutron probe, for example, but the other two parameters must be determined otherwise.

According to Davidson *et al*. (1969), the accuracy of the approximation in Equation (2.1) depends, essentially, on how closely the assumption of a unit hydraulic gradient is met during the drainage period. The assumption was consequently checked continuously during this investigation by measuring the matric head with tensiometers installed at different depths.

Libardi *et al*. (1980) proposed five methods to determine the coefficients K_0 and β in Equation (2.1) based on the following assumptions:

(a) The soil water flux at the beginning of the drainage (time $t = 0$) is constant throughout the soil profile and negligible at the surface ($z = 0$) for $t > 0$.

(b) The average soil water content, $\bar{\theta}$, to a depth z and the actual soil water content, θ, at the depth z are related by the equation

$$\bar{\theta} = a\theta + b \qquad (2.2)$$

where *a* and *b* are coefficients that have to be determined by regression.

(c) The hydraulic head, *H*, which is the sum of the matric pressure head, *h* and the elevation of the observation point, *z*, satisfies the assumption of a unit hydraulic gradient during the redistribution ($dH/dz = 1$).

The methods are:

1 The θ–method

This method is based on the assumption that

$$\theta_0 - \theta = \frac{1}{\beta}\ln(t) + \frac{1}{\beta}\ln\left(\frac{\beta K_0}{az}\right) \tag{2.3}$$

Graphs of $\theta_0 - \theta$ as a function of ln(*t*) for each depth *z* should therefore display straight lines with slopes $(1/\beta)$ and the intercepts $(1/\beta)\ln(\beta K_0/az)$, from which β and K_0 can be determined, if θ_0 is known.

2 The θ-method of Lax

This method is similar to the θ-method, except that $\theta_0 - \theta$ is now expressed as

$$\theta_0 - \theta = \frac{1}{\beta}\ln(t) + \frac{1}{\beta}\ln\left(\frac{\beta K_0}{z}\right) \tag{2.4}$$

The method therefore does not depend on the parameter *a* in Equation (2.2).

3 The Flux method

In this method $\theta_0 - \theta$ is expressed as

$$\ln\left|z\frac{\partial\bar{\theta}}{\partial t}\right| = \ln\left(z\theta'\right) = -\beta\left(\theta_0 - \theta\right) + \ln K_0 \tag{2.5}$$

A graph of $\ln\left|z\theta'\right|$ as a function of $(\theta_0 - \theta)$ should therefore display a straight line with slope $-\beta$ and intercept $\ln K_0$. $\bar{\theta}$ is rate of change of depth-averaged soil water content.

4 The CGA method (Chong *et al.*, 1981)

In this method β and K_0 are determined from the relations:

$$K_0 = -zA^{1/B} B\overline{\theta_0}^{(B-1)/B} \tag{2.6}$$

and

$$\beta = a(B-1)/B\overline{\theta_o} \tag{2.7}$$

where $\overline{\theta}_0$ is the average soil water content to a depth z at time $t = 0$ with A and B parameters determined from the relation (Gardner *et al*., 1970; Chong *et al*., 1981)

$$\overline{\theta} = At^B \tag{2.8}$$

5 The W-method of Lax

This method is based on the expression

$$\frac{W(z,t)}{z} = \theta_0 - \frac{1}{\beta}\left[1 - \ln\left(\frac{z}{K_0\beta}\right)\right] - \frac{1}{\beta}\ln(t) \tag{2.9}$$

where

$$W(z,t) = \int_0^z \theta dz \tag{2.10}$$

is the total water content above a depth z. The parameter β for a given depth is then given by the reciprocal of the slope of the graph of $W(z, t)/z$ as a function of $\ln(t)$, while K_0 is given by

$$K_0 = \frac{z}{\beta}\exp[\beta(\theta_0 - e) - 1] \tag{2.11}$$

where e is the y-intercept on the graph of $W(z, t)/z$ as a function of $\ln(t)$ at $t = 1$.

Detailed derivations of these equations can be found in Libardi *et al*. (1980), Sisson *et al*. (1980), Chong *et al*. (1981) and Jones and Wagenet (1984).

2.2.3 The Power Function Models of Chong *et al*

Nielsen *et al*. (1973) use the assumption that the redistribution of soil water in a uniform soil profile after infiltration and without evaporation induces a unit hydraulic gradient in the soil water profile (Black *et al*., 1969), to show that the rate of change of soil water content during the infiltration satisfies the equation

$$K_L(\overline{\theta}) = -Z\frac{d\overline{\theta}}{dt} \tag{2.12}$$

where Z is the soil depth under consideration, $K_Z(\bar{\theta})$ the hydraulic conductivity and $\bar{\theta}$ the average soil water content at depth Z and t the time. Equation (2.8) can now be used to express this equation first as a function of t

$$K_Z(t) = -ZABt^{B-1} \tag{2.13a}$$

and then as a function of $\bar{\theta}$

$$K_Z(\bar{\theta}) = -ZBA^{(1/B)}\bar{\theta}^{[(B-1)/B]} \tag{2.13b}$$

The assumption that the matric pressure head at the depth Z assumes during the redistribution period the form (Chong *et al*., 1981)

$$h = Mt^N \tag{2.14}$$

where M and N are constants, allows one to express the hydraulic conductivity also in the form

$$K_Z(h) = -ZABM^{[(B-1)/N]}h^{[(B-1)/N]} \tag{2.15}$$

2.2.4 The Internal Drainage Model

The model of internal drainage (Hillel *et al*., 1972) is essentially based on the general equation describing the flow of water in a vertical soil profile

$$\frac{\partial\theta}{\partial t} = \frac{\partial}{\partial z}\left[K(\theta)\frac{\partial H}{\partial z}\right] \tag{2.16}$$

where

$$H = h + z$$

is the hydraulic head and z is positive downward. This equation can be immediately integrated over the depth z to obtain

$$\int_0^z \frac{\partial\theta}{\partial t}dz = \left(K\ \frac{\partial H}{\partial z}\right)_z - \left(K\ \frac{\partial H}{\partial z}\right)_0 \tag{2.17}$$

Since z does not depend on t, this equation can be expressed through Equation (2.10) as

$$\left(\frac{dW}{dt}\right)_z = K\left(\frac{\partial H}{\partial z}\right)_z = q \tag{2.18}$$

if it is assumed that no water enters or leaves the soil surface during drainage, in which case q may be rearranged as the total water flux at the depth z and Equation (2.18) expressed as

$$K(\theta)\Big|_z = \frac{q}{\partial H/\partial z}\Bigg|_z \tag{2.19}$$

2.2.5 The Model of van Genuchten

The model of van Genuchten (1980) differs from the preceding models in that it does not describe the hydraulic conductivity as such, but rather the water retention curve of a soil. The model is conventionally expressed in the form

$$\Theta = \frac{\theta - \theta_r}{\theta_s - \theta_r} = [1 + (\alpha h)^n]^{-m} \tag{2.20}$$

where Θ, θ_r and θ_s are known as is the reduced, residual and saturated soil water content respectively, while α, n, and m are constants characteristic of a given soil. In his original paper van Genuchten equates the parameter m with 1-1/n, but later suggests that it should be considered as an independent parameter (van Genuchten and Nielsen, 1985). However, Botha (1986) has found that the original suggestion is more appropriate for South African soils, in which case the hydraulic conductivity of the soil assumes the form (van Genuchten, 1980; Botha, 1996)

$$K(\Theta) \equiv K_s \sqrt{\Theta}[1 - (1 - \Theta^{1/m})^m]^2 \tag{2.21}$$

where K_s is the saturated hydraulic conductivity of the soil.

Equation (2.20) is only valid for either the desorption or sorption leg of the soil water retention curve, but can be easily adapted to account for scanning curves (Luckner and Shestakow, 1991).

2.3 FIELD EXPERIMENTS

2.3.1 General

The application of the models discussed above to South African Soils was investigated through a series of field experiments conducted at the experimental station of the Department of Soil, Climate, and Crop Sciences at the University of the Free State in Bloemfontein South Africa. The site, located at 26.1^o S and 29.0^o E with an altitude of 1372 m, is underlain by a cultivated Bainsvlei amalia sandy loam soil which covers most of the South African land mass (Soil Classification Working Group, 1991). It is

characterized by orthic topsoil and red apedal/soft plinthic subsoil. The area is semi-arid with a mean annual rainfall of 510 mm.

2.3.2 Experimental Procedures

A (100 x 100) cm^2 plot was isolated from the surrounding soil by a metal frame 40 cm high inserted to a depth of 20 cm into the soil. Rainfall was applied to a (120 x 120) cm^2 area on and around the plot at a rate of 5.41 mm/h continuously for one week using a rainfall simulator constructed according to the design of Claassens and van der Watt (1993). The soil water content was measured, as a function of depth and time, with a neutron probe through a steel tube inserted to a depth of 200 cm at the centre of the plot. The matric potential was measured with four tensiometers installed at depths of 30 cm, 45 cm, 90 cm and 120 cm, around the access tube. It was assumed that the water distribution attained a steady state when the deepest tensiometer indicated a constant matric-pressure head. The water application was discontinued after one week and the plot was covered with a plastic sheet to prevent evaporation. The soil water content and matric pressure heads were then measured at selected time intervals for about one month. As the experiment was conducted at the end of the rainy season, the surrounding area was wet enough to neglect the radial flow of water. In addition, the sand content of the soil is high (> 75%) and the soil is homogenous in the depth range investigated, which supported the vertical flow of the applied water.

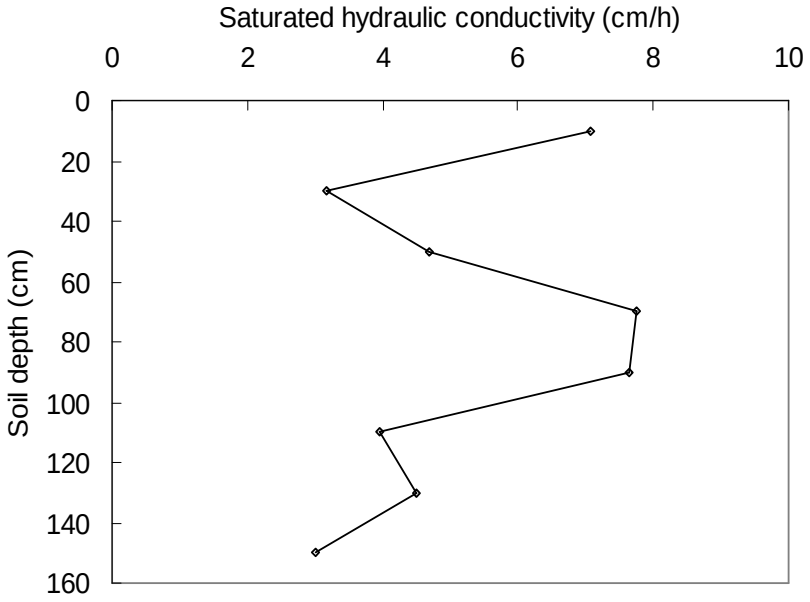

Figure 2-1 The saturated hydraulic conductivities observed in the soil profile of the test site at various depths.

The saturated hydraulic conductivity, saturated water content, bulk density, and soil texture were determined from a soil profile opened adjacent to the plot, after completion of the experiment. The saturated hydraulic conductivity *(K_s)* at different depths of the soil profile was determined with a double ring infiltrometer (Bouwer and Jackson, 1974), which consisted of two concentric metal rings with diameters of 10.5 cm and 13.0 cm respectively. Successive soil layers were removed each time measurement is completed on the upper layer. The rings were carefully inserted into the soil to a depth of 5.0 cm. The value of K_s was determined using Darcy's law and the volume of water required to keep the inner ring at a constant head of 2.0 cm. The saturated water content was determined from soil samples taken immediately after the water disappeared from the inner ring, when the measurement was terminated. The saturated hydraulic conductivity values for the different depths of the soil profile are shown in Figure 2-1.

Table 2-1 Particle size distribution and bulk density of the soil profile at the test site

Depth	Sand (%)				Silt	Clay	Soil Texture	Bulk density
(cm)	Coarse	Medium	Fine	Total	(%)	(%)		(g cm^{-3})*
0-20	0.4	6.8	63.8	91	4	5	Sand	1.64±0.05
20-40	0.4	7.7	78.9	87	2	11	Loamy sand	1.72±0.07
40-60	0.3	5.5	70.2	74	6	20	Sandy loam	1.62±0.04
60-80	0.4	5.5	72.1	76	6	18	Sandy loam	1.58±0.05
80-100	0.2	4.8	73.0	76	4	20	Sandy loam	1.64±0.06
100-120	0.3	4.8	73.9	78	4	18	Sandy loam	1.67±0.08
120-140	0.3	5.4	71.3	76	4	20	Sandy loam	1.68±0.08
140-160	0.2	2.8	73.0	76	4	20	Sandy loam	1.71±0.04
150-180	0.2	5.3	77.7	83.1	4	14	Sandy loam	
180-210	0.3	5.9	65.0	71.2	4	24	Sandy loam	
210-240	0.1	5.8	68.0	73.9	4	22	Sandy loam	
240-270	0.1	4.9	73.0	78.0	4	18	Sandy loam	
270-300	0.1	5.5	74.0	79.6	2	16	Sandy loam	

* Mean of 8 values ± standard deviation

2.3.3 Drainage Patterns

The soil profile was opened after the completion of the infiltration experiment and soil samples were taken at every 20 cm to a depth of 160 cm to determine the soil texture. The soil particle distribution was determined with the hydrometer method. Bulk densities were determined at the same intervals using a cylindrical metal core sampler (4.8 cm in diameter and 5.2 cm in length) driven horizontally into the vertical trench. The soil texture and bulk densities for the different soil layers (0-160 cm) are given in Table 2-1. The soil texture for deeper depths (150-300 cm) determined by Bennie *et al*. (1998) from

a soil profile on the same farm indicates sandy loam texture also at deeper depths.

An interesting feature of the soil profile is the high bulk density in the 20-40 cm layer; probably due to subsoil compaction by tillage that caused a reduction in the total pore volume and a change of the pore size distribution. This could explain a decrease in the saturated hydraulic conductivity at a depth of 30 cm in Figure 2-1. Below this depth, the hydraulic conductivity increased up to a depth 100 cm before it began to decrease most likely caused by the increase in bulk density with depth. The influence of the bulk density of a soil on the flow of water in the soil has been observed previously. Meek *et al*. (1992), for example, observed a 86% decrease in hydraulic conductivity of a sandy loam soil when its bulk density increased from 1.6 to 1.8 g cm^{-3}. Agrawal *et al*. (1987) also found that an increase of 0.15 g cm^{-3} in the bulk density of a sandy soil, caused a decrease of 42% in infiltration rate through the soil and a decrease of 56% in its hydraulic conductivity. Patel and Singh (1980) also observed a drastic decrease in hydraulic conductivity with depth as the bulk density of a coarse-textured soil increased from 1.5 to 2.0 g cm^{-3}.

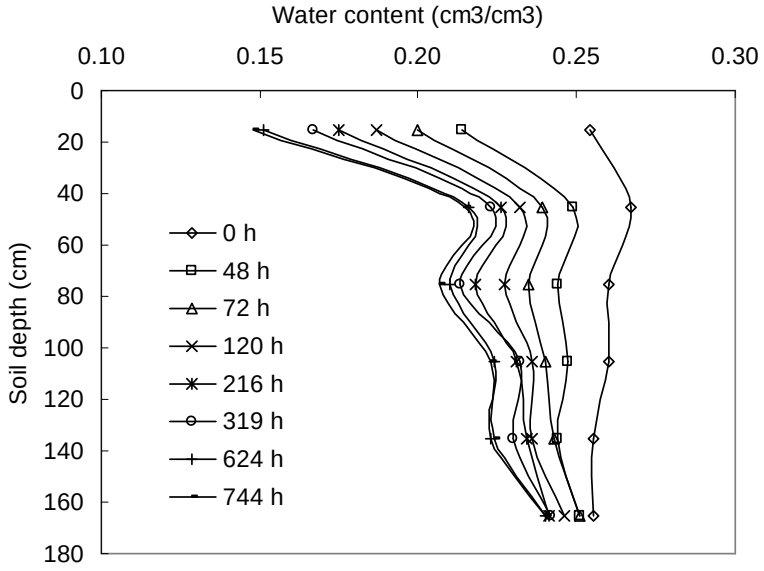

Figure 2-2 The soil water-content profiles observed at the test site during the redistribution of the infiltrated water.

The soil water content profile during redistribution, given in Figure 2-2, shows that the soil water content was almost the same throughout the profile at time $t = 0$. This indicates that steady state flux conditions existed at that time. Under these conditions, water drains at the same rate from all depths under a unit hydraulic gradient. However, this was not the

case during the redistribution period where the water drained faster from the top 30 cm sandy layer and more slowly from the deeper layers as can be seen from the soil water-content profiles in Figure 2-3. The slower drainage rate at the lower depths can be attributed to the increased clay content of the layers that caused water to accumulate in these layers and retarded the flow of water from the layers.

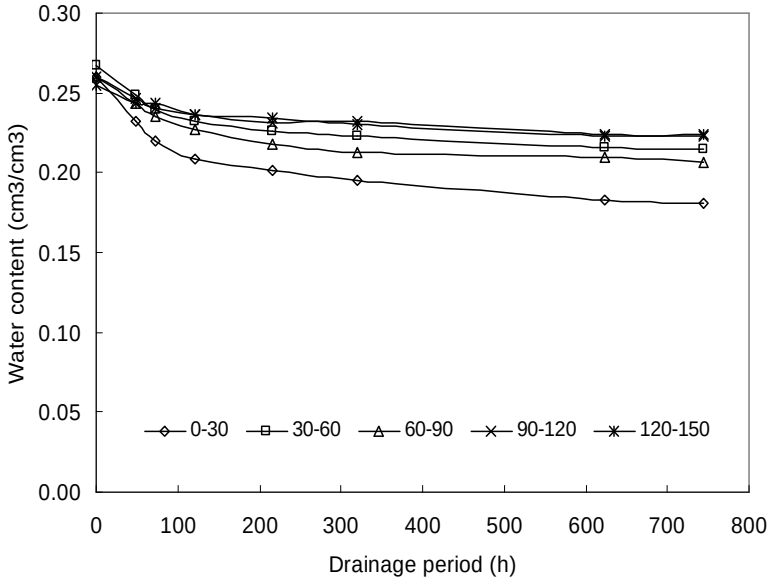

Figure 2-3 Drainage curves at different depths of the soil profile during redistribution.

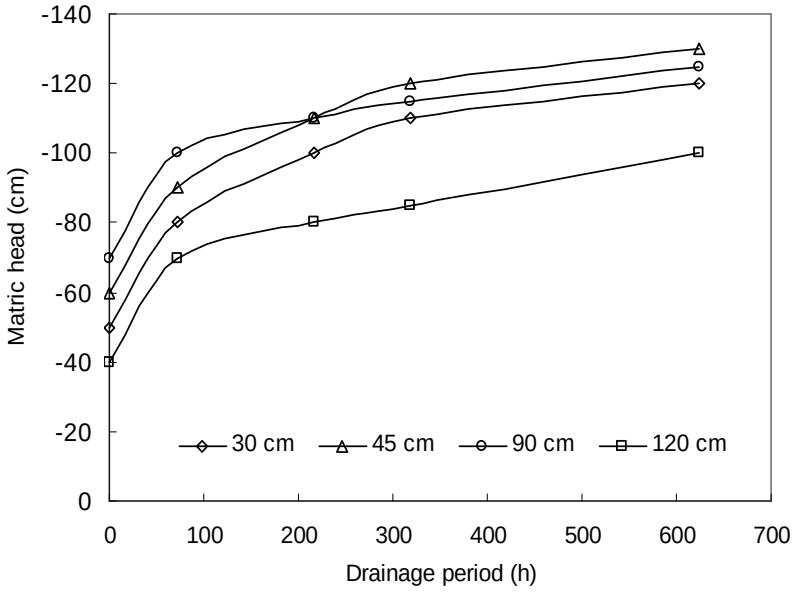

Figure 2-4 Matric head during redistribution.

The changes in the matric head during the redistribution period are given in Figure 2-4. The change in the head was faster at the early stages of redistribution and decrease during the later stages. This was due to the higher drainage rate of water in the larger pores during the early periods. The corresponding hydraulic head profiles are given in Figure 2-5.

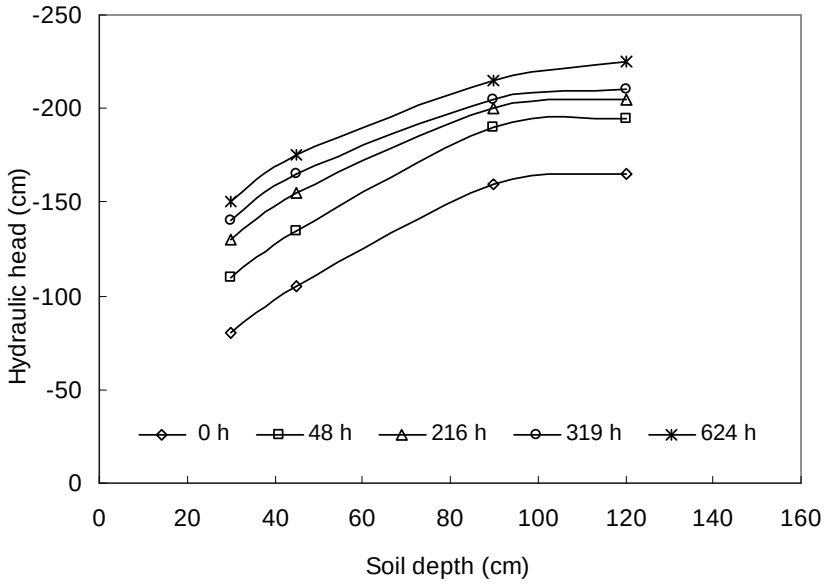

Figure 2-5 Hydraulic head profiles during redistribution.

2.3.4 The Hydraulic Gradient

It follows from the preceding discussion that if the five simplified methods are used to determine K_0 and θ_0 the accuracy with which Equation (2.1) can describe the hydraulic conductivities in the soil profile will ultimately depend on how closely the hydraulic gradient satisfies the assumption of a unit hydraulic gradient during the redistribution period.

The hydraulic gradients used in this investigation were derived from Figure 2-5 and are presented in Figure 2-6. Although the hydraulic gradients generally remained constant during the drainage period, none of them really satisfied the assumption of a unit gradient. It is therefore highly unlikely that Equation (2.1) will be able to describe the hydraulic gradient at the test site very accurately, if one of the five simplifies models are used to derive the values for K_0 and θ_0. Nevertheless, it was thought that it may still be interesting to compare the values of K_0 and θ_0 derived from these five simplified models with one another and the values of $K(\theta)$, derived from the internal drainage method.

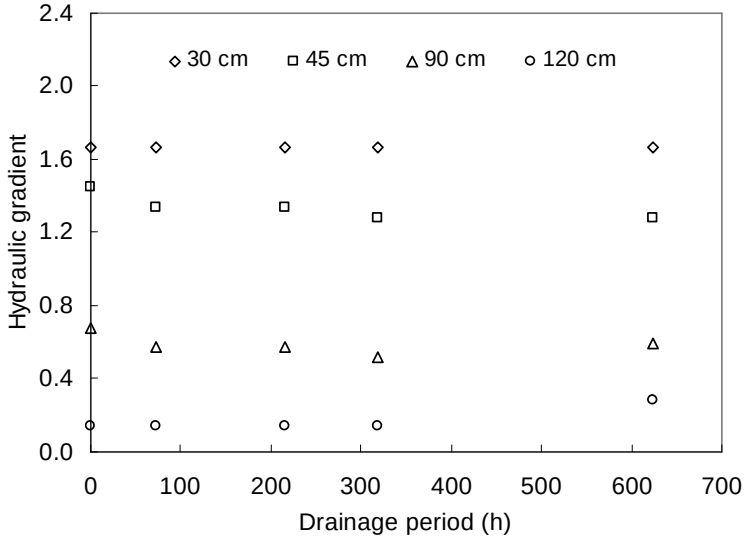

Figure 2-6 Hydraulic head gradients at different depths during the redistribution of the water at the test site.

2.4 ESTIMATION OF THE HYDRAULIC CONDUCTIVITY

2.4.1 Estimates of K_0 and β with the Simplified Methods

The computation of the coefficients K_0 and β with any of the five simplified methods discussed in Section 2.2.2 generally require a regression of the changes in water content (θ_o-θ) and the logarithm of the time, as illustrated in Figure 2-7 for the θ-method. The figure also illustrates how the drainage properties varied with depth. The graphs for the other four methods are very similar and will not be repeated here. The values of K_0 and β derived from the regression analysis of all the five simplified methods are presented in Table 2-2.

It is interesting to note that β-values in Table 2-2 increased with depth for all the methods. The values of K_0, on the other hand, increase from a depth of 30 cm to 45 and then decrease continuously with depth except for values derived with the Flux and the CGA methods, which all increase continuously with depth. The large variations in the estimated values of K_0 and β in Table 2-2 is not peculiar to this study, but have also been observed by Jones and Wagenet (1984) and Fuller and Moolman (1989). Indeed, Jones and Wagenet (1984) observed K_0 and β values that varied by two orders of magnitude for some of the methods.

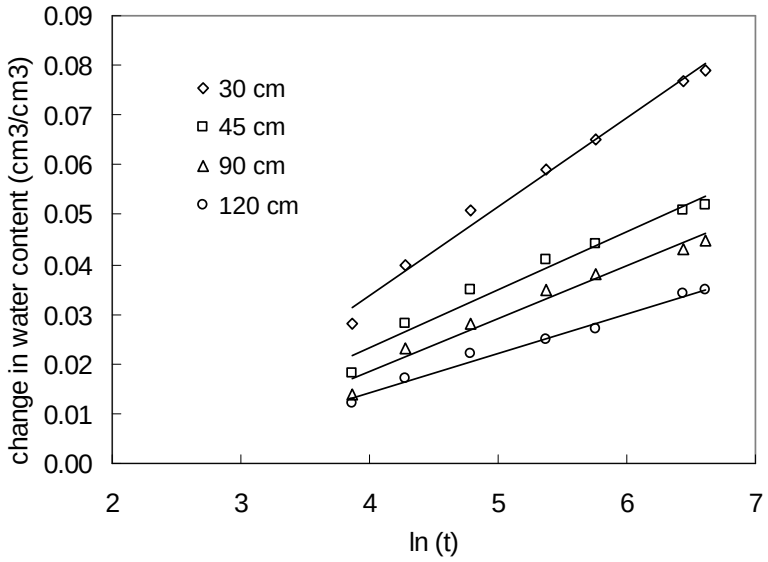

Figure 2-7 Regression lines of the fit between the changes in water content (θo-θ) and the logarithm of the time for the θ-method at different depths of the soil profile.

Table 2-2 Calculated values of K_0, β and the regression coefficients using the simplified methods discussed in Section (2.2) at different depths of the soil profile

Depth	**K_0**	β	**r^2**	**Depth**	**K_0**	β	**r^2**
(cm)	**(cm h^{-1})**			**(cm)**	**(cm h^{-1})**		
	θ-Method				**Lax-θ Method**		
30	0.076	56.2	1.000	30	0.076	56.2	0.988
45	0.094	86.2	0.998	45	0.075	86.2	0.968
90	0.057	94.3	0.998	90	0.045	94.3	0.972
120	0.015	125.0	0.996	120	0.010	125.0	0.986
	Flux Method				**CGA-Method**		
30	0.200	69.0	0.942	30	0.070	31.7	0.992
45	0.279	107.2	0.947	45	0.139	40.7	0.986
90	0.333	115.6	0.904	90	0.200	42.2	0.986
120	0.401	152.7	0.931	120	0.227	42.8	0.986
	Lax-W Method						
30	0.028	56.2	0.988				
45	0.044	63.5	0.984				
90	0.029	75.6	0.982				
120	0.021	82.6	0.984				

The methods, moreover, do not seem to behave consistently. For example, Libardi *et al*. (1980) found that estimates of K_0 using the θ, Flux and CGA methods were comparable, while Jones and Wagenet (1984) found that the CGA method yielded higher and the Lax-W method lower estimates of K_0 than the other three methods. However, in the work of Fuller and Moolman (1989), the Flux method yielded the highest values and the Lax-W method the lowest values of K_0. In this study, the magnitudes of K_0 at each depth follow approximately the following progression: Flux > CGA > θ ≈ Lax-θ > Lax-W. One reason for this behaviour is probably the relation between θ and the time used by the different methods.

2.4.2 Hydraulic Conductivity Estimates Derived from the Simplified Methods

Estimates of the hydraulic conductivities computed from Equation (2.1) and the coefficients K_0 and β in Table 2-2 are presented in Table 2-3, which show that the conductivities decrease sharply with time, because of the decrease in soil water content with time, see Figure 2-2. The hydraulic conductivities at any depth and time are very similar, except for those computed from the CGA coefficients, which are consistently higher at all depths.

Table 2-3 Hydraulic conductivity calculated from K_0 and β values obtained using the simplified methods

		Method				
Depth	**Time**	θ	**Lax-θ**	**Flux**	**CGA**	**Lax-W**
(cm)	**(h)**	**Hydraulic conductivity (cm h^{-1})**				
30	72	0.0080	0.0080	0.0127	0.0197	0.0030
	216	0.0028	0.0028	0.0034	0.0108	0.0010
	319	0.0020	0.0020	0.0023	0.0089	0.0007
	624	0.0010	0.0010	0.0010	0.0061	0.0004
45	72	0.0084	0.0067	0.0139	0.0445	0.0074
	216	0.0027	0.0022	0.0034	0.0262	0.0033
	319	0.0021	0.0017	0.0025	0.0232	0.0027
	624	0.0012	0.0009	0.0012	0.0174	0.0017
90	72	0.0072	0.0057	0.0262	0.0790	0.0055
	216	0.0021	0.0017	0.0058	0.0457	0.0021
	319	0.0017	0.0014	0.0046	0.0420	0.0018
	624	0.0010	0.0008	0.0023	0.0326	0.0011
120	72	0.0018	0.0012	0.0299	0.1097	0.0052
	216	0.0007	0.0004	0.0088	0.0779	0.0027
	319	0.0005	0.0003	0.0065	0.0715	0.0023
	624	0.0002	0.0001	0.0022	0.0530	0.0013

2.4.3 The Power Function Models of Chong *et al*

The observed soil water contents and matric heads during redistribution were next fitted to the simplified power function relationships of Chong *et al*. (1981), given in Equations (2.8) and (2.14). The observed and fitted results for the 45 cm depth are presented graphically in Figures 2-8 and 2-9 and the parameters for all depths are also presented in Table 2-4.

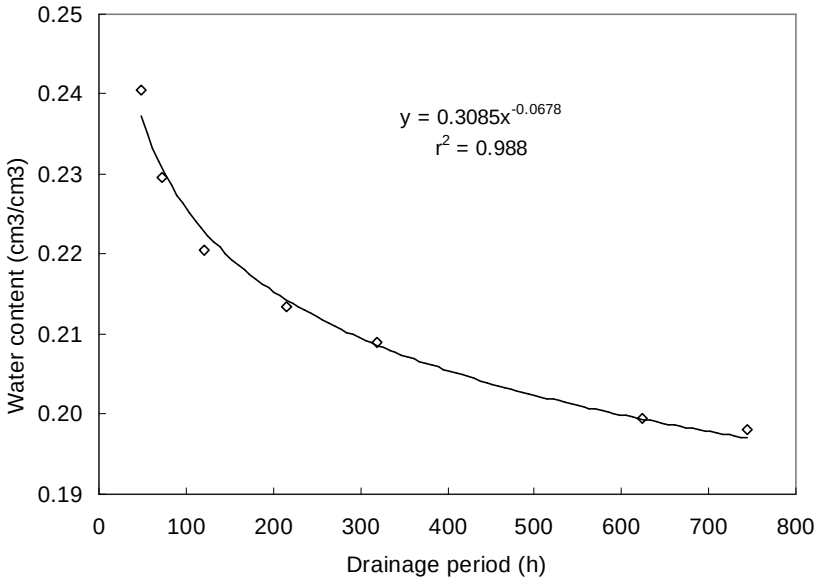

Figure 2-8 Calculated $\bar{\theta}(t)$ curve obtained by regression of Equation (2.8) at 45 cm soil depth.

Table 2-4 The parameters *A*, *B*, *M* and *N* of Equations (2.8) and (2.14) for the soil profile at the test site

Depth	$\bar{\theta} = At^B$			$h = Mt^N$		
(cm)	**A**	**B**	**r²**	**M**	**N**	**r²**
30	0.3216	-0.0874	0.993	41.853	0.1657	0.945
45	0.3085	-0.0678	0.988	63.403	0.1111	0.952
90	0.3021	-0.0603	0.986	67.630	0.0969	0.954
120	0.2960	-0.0535	0.988	31.386	0.1800	0.948

It is interesting to note that the coefficients *M* and *N* do not show any pattern with depth, but that the coefficient *A* decreases with depth while *B* increases with depth. The correlation coefficients, r^2, for the various fits also all exceed 0.95, which implies that the two empirical power functions given in Equations (2.8) and Equation (2.14) are excellent approximations of the $\bar{\theta}(t)$ and $h(t)$ relation for the Bainsvlei soil profile at the experimental site.

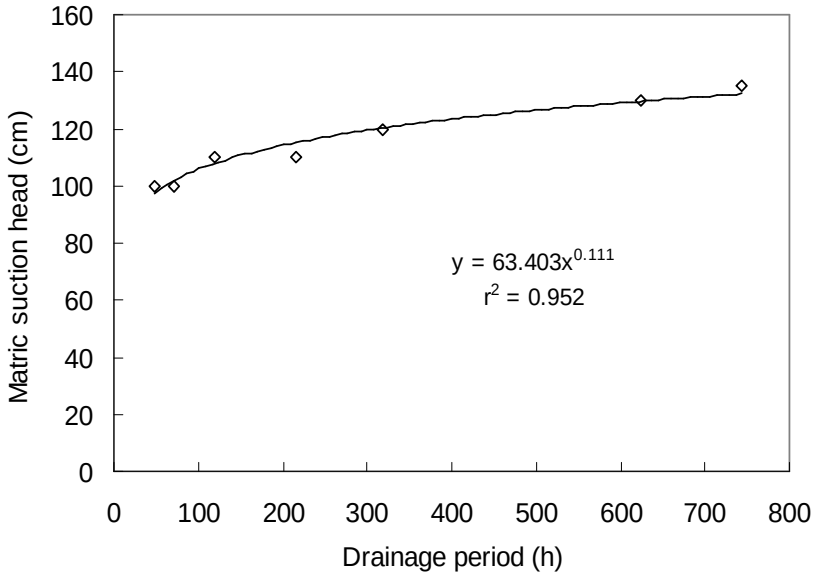

Figure 2-9 Observed and calculated *h(t)* curve obtained by regression of Equation (2.14) at 45 cm soil depth.

Table 2-5 The hydraulic conductivities, $K(t)$, $K(\bar{\theta})$ and $K(h)$ computed from Equations (2.13a), (2.13b) and (2.15) respectively, for different depths in the soil profile at the experimental site during the period of redistribution or drainage

Time	Depth (cm)			
(h)	30	45	90	120
		K(t) (cm h^{-1})		
72	0.0081	0.0098	0.0176	0.0210
216	0.0024	0.0030	0.0055	0.0066
319	0.0016	0.0020	0.0036	0.0044
624	0.0008	0.0010	0.0018	0.0022
		K($\bar{\theta}$) (cm h^{-1})		
72	0.0075	0.0190	0.0435	0.0654
216	0.0024	0.0077	0.0193	0.0321
319	0.0017	0.0059	0.0153	0.0264
624	0.0008	0.0033	0.0095	0.0168
		K(h) (cm h^{-1})		
72	0.0120	0.0118	0.0227	0.0174
216	0.0028	0.0047	0.0080	0.0080
319	0.0015	0.0020	0.0031	0.0056
624	0.0008	0.0009	0.0020	0.0022

The hydraulic conductivity values calculated using Equations (2.13a, b and 2.15) as a function of time, depth-averaged water content and matric heads during redistribution are presented in Table 2-5. As one would have expected, the conductivity decreased with time as the soil is continuously losing water from the quickly draining top layer towards the slowly draining deeper layers. The estimated hydraulic conductivities using these equations therefore seem to satisfy the basic physical principles that control the motion of the soil water.

2.4.4 The Internal Drainage Method

The water flux through each depth increment (Table 2-6) was calculated by integrating the water content-time curve (Figure 2-3) with respect to depth. The first step taken in applying the internal drainage method was to compute the slopes $d\theta/dt$ of the water contents from the water content-time curves in Figure 2-3 for the different depths and integrate the slopes over depth to obtain q in Equation (2.18), as illustrated in Table 2-6. The hydraulic conductivities were then computed simply by dividing q with the hydraulic gradients in Figure 2-6, with results given in Table 2-7. An interesting feature of the computed fluxes, q, in Table 2-6 decreased with time at a given depth and increased with depth for a given time.

Table 2-6 Calculation of soil water flux ($D\theta = \partial\theta/\partial t$, $q = \sum(\partial\theta/\partial t)\Delta z$) at different depths and times during redistribution

Time	Depth	Dθ	DθΔz	q
t (h)	*z* (cm)	(h^{-1})	(cm h^{-1})	(cm h^{-1})
72	0-30	0.00058	0.0175	0.0175
	30-60	0.00042	0.0125	0.0300
	60-90	0.00033	0.0099	0.0399
	90-120	0.00017	0.0051	0.0449
216	0-30	0.00013	0.0039	0.0039
	30-60	0.00006	0.0018	0.0057
	60-90	0.00007	0.0021	0.0079
	90-120	0.00003	0.0009	0.0088
319	0-30	0.00008	0.0024	0.0024
	30-60	0.00003	0.0009	0.0033
	60-90	0.00002	0.0006	0.0039
	90-120	0.00002	0.0006	0.0045
624	0-30	0.00005	0.0015	0.0015
	30-60	0.00002	0.0006	0.0021
	60-90	0.00002	0.0006	0.0027
	90-120	0.00002	0.0008	0.0035

The semi-log graphs presented in Figure 2-10 show that the hydraulic conductivities given in Table 2-7 display an exponential relation with the soil water contents θ of the form

$$K = a \exp(b\theta) \tag{2.22}$$

which is identical to Equation (2.1), if

$$\alpha = K_0 \exp(-\beta\theta_0) \quad \text{and} \quad b = \beta \tag{2.23}$$

Table 2-7 Computation of the hydraulic conductivities with the internal drainage method (DH = $\partial H/\partial z$) at different depths of the soil profile and times during redistribution

Depth	Time	q	DH	K	θ
***z* (cm)**	***t* (h)**	**(cm h^{-1})**		**(cm h^{-1})**	
30	72	0.0175	1.67	0.0105	0.220
	216	0.0039	1.67	0.0023	0.201
	319	0.0024	1.67	0.0014	0.199
	624	0.0015	1.67	0.0009	0.183
45	72	0.0300	1.34	0.0224	0.239
	216	0.0057	1.34	0.0043	0.226
	319	0.0033	1.28	0.0025	0.223
	624	0.0021	1.28	0.0016	0.216
90	72	0.0399	0.57	0.0700	0.239
	216	0.0079	0.57	0.0138	0.225
	319	0.0039	0.52	0.0073	0.223
	624	0.0027	0.59	0.0046	0.217
120	72	0.0449	0.14	0.3207	0.242
	216	0.0088	0.14	0.0628	0.233
	319	0.0045	0.14	0.0314	0.231
	624	0.0035	0.28	0.0125	0.224

As shown by the list of the coefficients in Table 2-8 that fit the hydraulic conductivities the best, in the least squares sense, the values of b are indeed of the same order as that of β in presented in Table 2-2 and that they also increase with depth. However, the actual values of the coefficients differ considerably from one another. Nevertheless, the results do suggest that it may be possible to represent the hydraulic conductivities of the soil profile at the test site by an equation of the form given by Equations (2.1) or Equation (2.22). Such relations will not be single-valued functions of the soil water content θ over the whole soil profile though, but must be determined for every soil depth in which one is interested.

Table 2-8 The coefficients a and b in Equation (2.22) that fit the hydraulic conductivities in Table 2-7 as functions of θ the best, in the least squares sense, for the different soil layers

Depth (cm)	a (cm h^{-1})	b	r^2
0-30	$3 \cdot 10^{-7}$	45.0	0.982
30-60	$3 \cdot 10^{-14}$	112.4	0.989
60-90	$2 \cdot 10^{-14}$	119.4	0.993
90-120	$4 \cdot 10^{-20}$	178.2	0.997

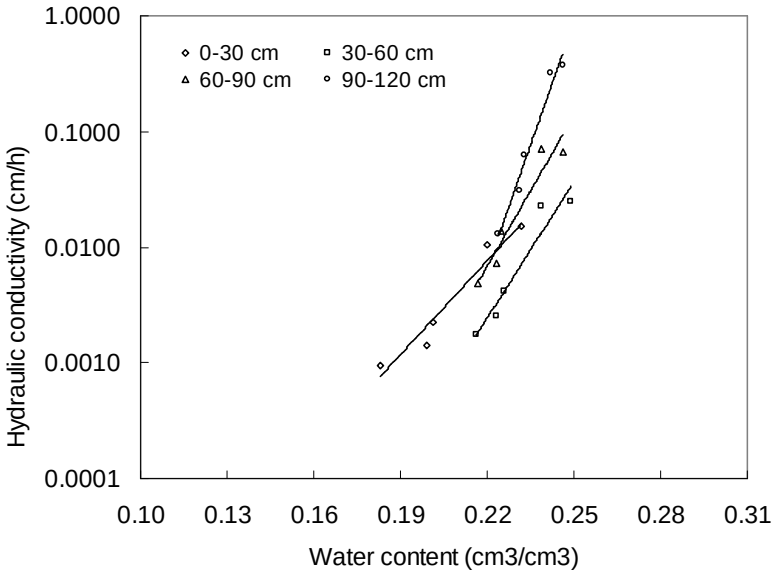

Figure 2-10 Graphs of the hydraulic conductivities of the different soil layers in Table 2-7 as functions of the water contents.

2.4.5 Comparison of the Estimated Hydraulic Conductivities

As shown by the preceding discussion there is a very close connection between the hydraulic conductivities estimated by the simplified methods and the method of internal drainage. It was thus thought worthwhile to compare the estimated hydraulic conductivities, derived from the simplified methods with that derived from the internal drainage method more quantitatively. This will be done through the index of agreement, d, of Willmott (1981), which is a descriptive measure, bounded by the inequality $0<d<1$ that can be used to cross-compare the different models. Wilmot expresses this index as

$$d = 1 - \frac{\sum_{i=1}^{N} (e_i - o_i)^2}{\sum_{i=1}^{N} (|E_i| + |O_i|)^2} \quad (E_i = e_i - \bar{o},\ O_i = o_i - \bar{o}) \qquad (2.24)$$

where o_i is the i-th observation of a given variable, e_i its value estimated by a model, N the number of observations and $\bar{o}$ the average of the N observed values. For this purpose, the values obtained with the method of internal drainage in Table 2-7 were considered as 'observed' and the values estimated with the simplified methods and exponential function methods in Tables 2-3 and 2-5 as 'estimated'.

The indexes of agreement for the eight methods of estimation in Table 2-9 show that the agreement between the 'observed' and 'estimated' values decrease with depth for all the methods. It is difficult to explain this behaviour of the indexes, except to note that the internal drainage model, unlike the other estimators, does not require a unit hydraulic gradient. It is therefore natural to ascribe the behaviour of the indices in Table 2-9 to the behaviour of the hydraulic gradients in Figure 2-6, which not only deviate completely from unity, but decrease steadily from approximately 1.67 at a depth of 30 cm to 0.14 at 120 cm. The average d-values in Table 2-9 can in this case be used to arrange the 'estimation' models in the following order of increasing sensitivity for deviations from the unit hydraulic gradient

$$K(\bar{\theta}) \rightarrow Flux \rightarrow K(h) \rightarrow K(t) \rightarrow \theta \rightarrow \text{Lax-}\theta \rightarrow \text{CGA} \rightarrow \text{Lax-}W$$

The power functions of Chong *et al*. (1981) are therefore less sensitive to deviations from the hydraulic gradient than the values derived from the simplified methods of Libardi *et al*. (1980), except for his flux-method.

Table 2-9 Willmott's index of agreement for the hydraulic conductivities at the test site derived from the five simplified methods in Section 2.2.2 in Table 2-3 and the power function models of Section 2.2.3 in Table 2-5 compared with the values derived from the internal drainage method in Table 2-7

Depth				**Method**				
(cm)	θ	**Lax-θ**	**Flux**	**CGA**	**Lax-W**	**K(t)**	**K($\bar{\theta}$)**	**K(h)**
30	0.962	0.962	0.977	0.639	0.588	0.992	0.981	0.961
45	0.660	0.592	0.903	0.567	0.580	0.796	0.956	0.876
90	0.500	0.491	0.671	0.768	0.487	0.580	0.886	0.629
120	0.461	0.460	0.497	0.444	0.463	0.485	0.522	0.478
Average	**0.540**	**0.514**	**0.690**	**0.593**	**0.510**	**0.620**	**0.788**	**0.661**

2.4.6 The Model of van Genuchten

The model of van Genuchten (1980) has been included in this discussion for two reasons. The first is that it does not require special conditions, such as a unit hydraulic gradient, and the second because it is the model most widely used in the investigations of

saturated-unsaturated flow. The fact that the present investigation was mainly concerned with the desorption leg of the water retention curve further favours the model as can be seen from the graphs of the observed soil water contents and matric heads. The non-linear least squares routines RETC of van Genuchten (1985) and RIEN of Botha (1988) were therefore used to fit Equation (2.20) to the observed values in Figure 2-11. In addition to the field-measured data, some laboratory-measured values were added (including the permanent wilting point 15 000 cm matric head). The coefficients derived from these fits are given in Table 2-10. The saturated water content was not fitted and the residual water content fit led to zero values. The hydraulic conductivities calculated using Equation (2.21) are presented in Table 2-11.

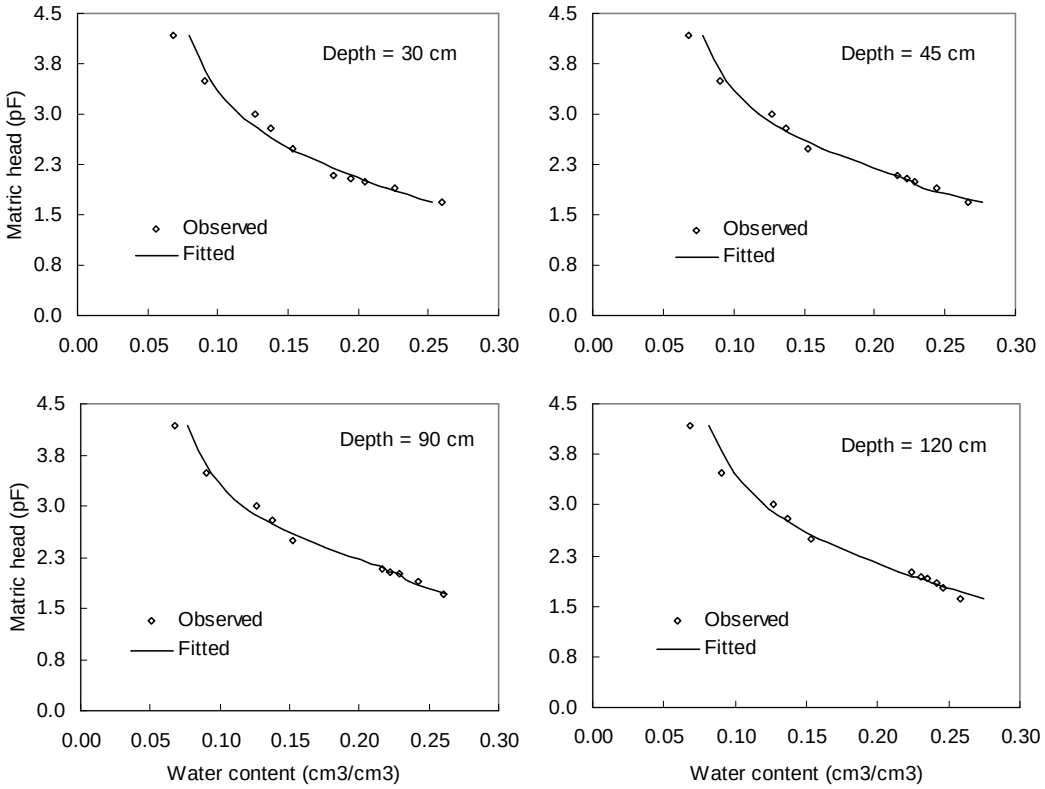

Figure 2-11 Graphs of the van Genuchten model fitted estimation to the observed water retention curve at different depths of the soil profile.

The saturated hydraulic conductivity of the soil profile, used in Equation (2.21), was measured as discussed in Section 2.3.2 and was found to be 3.16, 4.69, 7.65 and 4.24 cm/h at 30, 45, 90 and 120 cm depths of the soil profile. Table 2-12 compares the hydraulic conductivities determined by the method of internal drainage in Equation (2.22) and the method proposed by van Genuchten (1980) and Botha (1996) given by Equation (2.21). The comparison was done using the Willmott's index of agreement (*d*) discussed

in Section 2.4.5.

Table 2-10 The soil water retention curve parameters of van Genuchten model at different depths of the soil

Soil Depth	Parameters				r^2
(cm)	α	n	θ_s	m	
30	0.058	1.458	0.390	0.314	0.979
45	0.038	1.517	0.420	0.341	0.988
90	0.0251	1.524	0.370	0.344	0.991
120	0.046	1.445	0.370	0.308	0.985

Table 2-11 Hydraulic conductivities calculated with Equation (2.21) using the coefficients derived from water retention curve fits and the saturated hydraulic conductivities at the respective depths

Depth	Time	θ	K
z (cm)	t (h)	(cm^3 cm^{-3})	(cm h^{-1})
30	72	0.220	0.0105
	216	0.201	0.0023
	319	0.199	0.0014
	624	0.183	0.0009
45	72	0.239	0.0224
	216	0.225	0.0043
	319	0.223	0.0025
	624	0.216	0.0016
90	72	0.239	0.0700
	216	0.225	0.0138
	319	0.223	0.0073
	624	0.217	0.0046
120	72	0.242	0.3207
	216	0.233	0.0628
	319	0.231	0.0314
	624	0.224	0.0125

Comparing the average index of agreements in Table 2-9 with the ones in Table 2-12, it can be seen that the hydraulic conductivities determined using the coefficients derived from the water retention fits, Equation (2.21), were in better agreement with the conductivities calculated using the internal drainage method than the conductivities determined using the Simplified methods do. The average index of agreement was 0.843 (Table 2-12) for conductivities determined using Equation (2-21) while the highest index of agreement for the simplified methods was obtained for the $K(\bar{\theta})$ method with the average value of 0.788 (Table 2-9). The lowest index of agreement was obtained at the

120 cm depth. This might be because of the overestimation of the hydraulic conductivity by the Internal drainage method itself at this depth due to the low hydraulic gradient.

Table 2-12 Willmott's index of agreement between the hydraulic conductivities calculated using van Genucten model, Equation (2.21) and the internal drainage method, Equation (2.22)

Depth (cm)	30	45	90	120	Average
Index of agreement (*d*)	0.998	0.821	0.875	0.678	0.843

2.5 CONCLUSIONS

In the soil profile studied, at about the tillage depth there exists a flow-limiting layer of high bulk density, high water holding capacity and low hydraulic conductivity. The magnitudes of K_0 estimated using the simplified methods were approximately Flux > CGA > θ ≈ Lax-θ > Lax-W. The lowest and the highest values of β were obtained with the CGA and the Flux methods respectively. The hydraulic conductivity (K) values estimated using the CGA method were consistently higher than the other methods at all depths. Evaluation of the simplified models based on the 'Willmott's index of agreement (d)' indicated that the simplified methods could be arranged as *K($\bar{\theta}$), Flux, K(h), K(t), θ, Lax-θ, CGA,* and *Lax-W* arranged from the highest to the lowest average '*d*' value. This shows that generally, the power-function-based methods (Chong *et al*., 1981) estimated the hydraulic conductivity of this soil better than the simplified methods of Libardi (Libardi *et al*., 1980). The index of agreement obtained between the hydraulic conductivities determined using the van Genuchten model and the internal drainage method was better than the agreement between the conductivities determined using the simplified methods and the internal drainage method. This shows that the van Genucten model describes the K-θ relationship of this soil better than the simplified methods. The K-θ relationships obtained at four depths were different which implies that the soil profile cannot be characterized in its entirety by a single-valued K-θ function.

Determining the actual evapotranspiration of a crop is an important aspect in efficient agricultural water management, since over-irrigation could lead to a wastage of water and the leaching of fertilizers, while under-irrigation could cause crop water stress and a reduction in yield. The actual crop evapotranspiration can be determined from the soil water balance. The deep percolation component in the soil water balance is the most difficult one to quantify. The K-θ relation determined in this study can be used in the determination of this component using the Darcy's principle. All it requires is the measurement of soil water content using neutron probe. The K-θ relation can also be used in numerical models to study leaching of solutes in this soil.

CHAPTER 3

STEADY STATE TRANSPORT OF BROMIDE IN THE FIELD UNDER SIMULATED RAINFALL

3.1 INTRODUCTION

The rate at which agrochemicals move with percolating water from the soil surface to the groundwater is important in the management of agricultural lands and the subsurface of the earth. Although considerable progress has been made in describing the transport of water and chemicals under laboratory conditions (Nielsen *et al*., 1986), the results have not been carried to the field because of the natural heterogeneity of soils. At the field scale, even the most basic solute transport process, the mean convection rate, cannot be described with reasonable accuracy (Ashraf *et al*., 1997).

A basic assumption in these investigations is that the transport of solutes through soils can be described by the hydrodynamic dispersion equation

$$\frac{\partial}{\partial t}(\theta c + \rho_b s) + \mathbf{q}\cdot\nabla c = \nabla\cdot[\theta \mathbf{D}\nabla c] - \lambda_w \theta c - \lambda_s \rho_b s + \gamma_w \theta + \gamma_s \rho_b \qquad (3.1)$$

where c is the concentration of the solution, s the fraction of the solute adsorped by the soil, θ the volumetric water content, $\mathbf{D}$ the dispersion coefficient, $\mathbf{q}$ the volumetric flux of water, also known as the Darcy velocity, ρ_b the bulk density of the porous medium, t the time and ∇ the gradient operator. The constants λ_w and λ_s are rate constants for first order decay in the liquid and solid phases of the soil and γ_w and γ_s similar constants for zero-order production in the two phases.

There are no known solutions of the general hydrodynamic equation given in Equation (3.1), but there are a number of analytical solutions if the Darcy velocity and the dispersion coefficient are constants. These solutions will be referred to here as the classical convective-dispersive equation solutions or CDE models. Although CDE models perform well for laboratory soil columns and homogenous field soils, the models are not always able to describe transport processes in heterogeneous field soils accurately (Jury and Fluhler, 1992).

For many solute transport processes through the unsaturated zone (e.g., movement to shallow groundwater or transport within the root zone) the lateral dimension of the field is much greater than the maximum depth of solute movement over the time of interest.

Furthermore, field investigations indicate that the fluid velocity in the field is highly variable, but can be characterized with a lognormal distribution (Biggar and Nielsen, 1976; Butters and Jury, 1989). A number of models, which ignore lateral mixing and treat solute movement as though it occurred in isolated stream tubes with different transport parameters, see Figure 3-1, have therefore been proposed for applications in the field. In these models the local (or stream tube) parameters are treated as random, lognormal distributed variables, with zero correlation length normal to the vertical direction of flow. The area-averaged solute concentration can then be calculated by averaging the local transport model over all possible values of the random parameters. Models of this kind include parallel soil columns obeying local convection-dispersion (Dagan and Bresler, 1979; Bresler and Dagan, 1981; Amoozegard-Fard *et al*., 1982; Jaynes *et al*., 1988) and travel-time transfer functions (Jury, 1982; Jury *et al*., 1986).

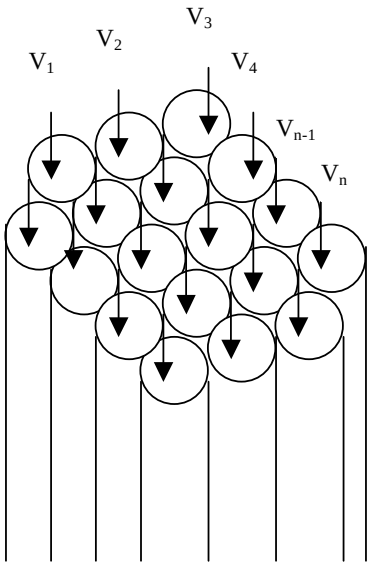

Figure 2-1 Schematic illustration of the stream tube model.

Bresler and Dagan (1979) and Dagan and Bresler (1979) were the first persons to describe the downward movement of nonreactive solutes on the field scale with these *stochastic stream tube models (STM)*, which consider field soils as composed of a series of vertical parallel columns. Amoozegar-Fard *et al*. (1982) demonstrated the effect of a random velocity, *v*, and dispersion coefficient, *D*, on the field scale concentration with Monte Carlo simulation. The theoretical background of the stochastic stream tube models has, recently been discussed in detail by Toride and Leij (1996a and b), who also developed procedures for its application to both reactive and nonreactive solutes under

chemical equilibrium and nonequilibrium conditions.

The main difference between deterministic convective-dispersive and the stochastic stream tube models can be briefly summarized as follows. The stream tube models consider the field as a series of independent vertical soil columns with discrete concentration values in the horizontal plane and with no horizontal mixing (Jury and Roth, 1990; Dagan, 1993; Toride and Leij, 1996a). The deterministic models, conversely, assume that the concentration across the horizontal plane is uniform and perfectly mixed across both the vertical and horizontal planes (Jury and Fluhler, 1992).

Deterministic convective-dispersive models have been used for years in many fields where the transport of contaminants is important and are well understood (Javandel *et al*., 1984). Unfortunately, the same cannot be said of stream tube models. Indeed, there are only a limited number of data sets that can be analysed with the stream tube model (Toride *et al*., 1995), and almost no attempt made to relate the performance of the stochastic stream tube models to the deterministic models through field tracer experiments. Moreover, there is no information available on the role that the various parameters play in the two types of models, or how sensitive the models are to changes in the convection and dispersion components of solute transport. One of the main purposes of the present investigation is to investigate these properties of the two types of models in more detail.

The experimental results from the in-field tracer transport were analysed with the CXTFIT program of Toride *et al*. (1995). The solute transport parameters for steady one-dimensional flow were estimated by fitting the observed bromide concentration field data, obtained from the leaching experiments, to the convective-dispersive and the stream tube models.

The objectives of this study were: (i) to conduct a steady state field experiment to quantify the transport of bromide in the Bainsvlei soil of South Africa, analyse the data with the deterministic convective-dispersive and a stochastic stream tube models; (ii) to perform a sensitivity analysis of the transport parameters and (iii) to determine the effect of rainfall intensity on the solute transport process in this soil.

The discussion below begins with a brief introduction of the two types of models in Section 3.2. This is followed by a discussion of the field experimental procedure and laboratory analysis in Section 3.3. The results and discussion of the deterministic and stochastic modelling, the transport parameters and their sensitivity analysis are presented in Section 3.4.

3.2 CONVECTIVE-DISPERSIVE AND STREAM TUBE MODELS

3.2.1 General

The hydrodynamic dispersion equation, Equation (3.1), is known in the literature on mathematical physics as a three-dimensional partial differential equation, which means that it describes the transport of a dissolved solid in all three dimensions of space and in time. However, convective dispersion and stream tube models to be discussed here are all based on the one-dimensional version of the equation

$$\frac{\rho_b}{\theta}\frac{\partial s}{\partial t}+\frac{\partial c}{\partial t}=D\frac{\partial^2 c}{\partial z^2}-v\frac{\partial c}{\partial z}-\lambda_w c-\frac{\lambda_s \rho_b}{\theta}s+\gamma_w+\frac{\gamma_s \rho_b}{\theta} \tag{3.2}$$

where

$$v=q/\theta$$

is known as the *pore-water velocity* of the water and the other symbols have the same meaning as above. The present discussion will consequently be limited to this equation.

3.2.2 The Deterministic One-Dimensional Convective-Dispersive Model

To solve Equation (3.2) analytically requires that one must prescribe suitable initial and boundary conditions for the system under study and an expression that relates the adsorbed concentration, *s*, to the solute concentration, *c*. In this study, the initial condition was assumed to be of the form

$$c(z,0)=c_i \tag{3.3}$$

where c_o is constant. At the soil surface a third- or flux type boundary condition was used.

$$\left(c-\frac{D}{v}\frac{\partial c}{\partial z}\right)_{z=0}=c_o \quad (0 \le t \le t_o)$$
$$=0 \quad (t>0) \tag{3.4}$$

where t_o is the duration of solute application at the inlet boundary ($z = 0$) and

$$\left.\frac{\partial c}{\partial z}(z,t)\right|_{z\to\infty}=0 \tag{3.5}$$

at the outlet boundary ($z \to \infty$). The relation between *s* and *c* will be described by the linear isotherm for the adsorption

$$s=K_d c \tag{3.6}$$

where K_d is known as the equilibrium distribution or partition coefficient. Substitution of this in Equation (3.2) yields

$$R\frac{\partial c}{\partial t} = D\frac{\partial^2 c}{\partial z^2} - v\frac{\partial c}{\partial z} - \mu c + \gamma \tag{3.7}$$

where the *retardation factor, R*, is defined as

$$R = 1 + \frac{\rho_b K_d}{\theta} \tag{3.8}$$

and the rate coefficients λ and γ are given by

$$\begin{aligned} \lambda &= \lambda_w + \lambda_s \rho_b K_d / \theta \\ \gamma &= \gamma_w + \gamma_s \rho_b / \theta \end{aligned} \tag{3.9}$$

Equation (3.7) reduces in the case of a conservative tracer, for which K_d = 0, and the assumption that $\lambda_\omega = \gamma_w = \gamma_s = 0$, to

$$\frac{\partial c}{\partial t} = D\frac{\partial^2 c}{\partial z^2} - v\frac{\partial c}{\partial z} \tag{3.10}$$

This equation, often referred to as the convective-dispersive equation (CDE) for a conservative tracer, states that the downward flux of solute consists of a convection term (the term containing *v*) and a dispersion term proportional to the vertical gradient of the concentration.

There exist a large number of analytical solutions for Equation (3.10) (Lapidus and Amundson, 1952; Danckwerts, 1953; Brenner, 1962; Cleary and Andrian, 1973; Lindstrom *et al*., 1976; van Genuchten and Alves, 1982). The present discussion will however be restricted to the following solution given by van Genuchten and Alves (1982), which is also used in the computer package CXTFIT of Toride *et al*. (1995).

$$\begin{aligned} c(z,t) &= c_i + (c_o - c_i)A(z,t) && 0 < t \le t_o \\ c(z,t) &= c_i + (c_o - c_i)A(z,t) - c_o A(z, t - t_o) && t > t_o \end{aligned} \tag{3.11}$$

where

$$\begin{aligned} A(z,t) = {} & \frac{1}{2} erfc\left[\frac{z - vt}{2(Dt)^{1/2}}\right] + \left(\frac{v^2 t}{\pi D}\right)^{1/2} \exp\left[-\frac{(z - vt)^2}{4Dt}\right] \\ & - \frac{1}{2}\left(1 + \frac{vz}{D} + \frac{v^2 t}{D}\right)\exp\left(\frac{vz}{D}\right) erfc\left[\frac{z + vt}{2(Dt)^{1/2}}\right] \end{aligned} \tag{3.12}$$

It should be kept in mind that the concentration given in Equation (3.11) applies strictly speaking only along a line in the vertical direction. However, it could in principle be used to represent the transport in the field if the various parameters in Equation (3.12) are interpreted as averages over the horizontal area of the field.

3.2.3 The Stream-Tube Model

The stream tube model is based on the following assumptions (Jury and Roth, 1990; Dagan, 1993):

(a) The flow field can be divided into an ensemble of separate, non-overlapping, vertical columns, see Figure 3-1.

(b) The flow in a stream tube is independent of the flow in the other tubes and does not interact with them, in other words the flow is one-dimensional.

(c) The hydraulic properties controlling solute transport may vary horizontally across the field, but not with depth.

(d) Mass transport in each stream tube can be described deterministically through a suitable solution of the convective-dispersive equation.

(e) The parameters in the convective-dispersive model are realizations of a stochastic variable across the ensemble of stream tubes.

(f) The mean solute concentration for a given flow field is the ensemble average of the local concentrations in all stream tubes.

The parameters often considered as stochastic variables in stream tube models are the pore-water velocity, v, in combination with either the dispersion coefficient, D, the distribution coefficient, K_d. The corresponding parameters for the local scale transport in each stream tube are obtained from the bivariate lognormal joint probability density function (pdf) of the relevant parameters (Toride and Leij, 1996a and b). For example, the joint pdf for v in conjunction with D, $f(v,D)$ is given by

$$f(v,D) = \frac{1}{2\pi\sigma_v\sigma_D v D\sqrt{1-\rho_{vD}}} \exp\left(-\frac{Y_v^2 - 2\rho_{vD}Y_vY_D + Y_D^2}{2(1-\rho_{vD}^2)}\right) \qquad (3.13)$$

with

$$Y_v = \frac{\ln v - \mu_v}{\sigma_v}, \quad Y_D = \frac{\ln D - \mu_D}{\sigma_D}$$
$$\rho_{vD} = \langle Y_vY_D \rangle = \int_0^\infty\int_0^\infty Y_vY_D f(v,D)\,dv\,dD \qquad (3.14)$$

the correlation coefficient between Y_v and Y_D and (μ_u, σ_u) the mean and standard

deviation of the transformed variable, ln u (u = v, D).

An interesting situation arises in the case where v and D are perfectly correlated, i.e., ρ_{vD} = ±1, as suggested by the widely used relation for the dispersivity

$$\alpha = D/v \tag{3.15}$$

By using the ensemble averages of v and D

$$<v> = \exp\left(\mu_v + \frac{1}{2}\sigma_v^2\right) \quad \text{and} \quad <D> = \exp\left(\mu_D + \frac{1}{2}\sigma_D^2\right) \tag{3.16}$$

it can be shown that (Toride and Leij, 1996a)

$$D(v) = \left(\frac{v}{<v>}\right)^{\rho_{vD}\sigma_D/\sigma_v} <D> \exp\left(\frac{\rho_{vD}}{2}\sigma_v\sigma_D - \frac{1}{2}\sigma_D^2\right) \tag{3.17}$$

which reduces in the case of a perfect correlation between v and D (σ_v = σ_D and ρ_{vD} = 1) to

$$D(v) = \frac{<D>}{<v>}v \tag{3.18}$$

This means that the dispersivity α in Equation (3.15) is constant (= <D>/<v>) for all stream tubes. However, σ_D is usually greater than σ_v. For example, Biggar and Nielsen (1976) studied the spatial variability of v and D for a field soil and found that ρ_{vD} = 0.795, <v> = 44.2 cm d^{-1} with σ_v = 1.25, and <D> = 367.6 cm^2 d^{-1} with σ_D = 1.74.

Field-scale transport in the stochastic stream tube model can be modelled by averaging the local-scale concentration in a stream tube over all stream tubes

$$<c(z,t)> = \frac{1}{A}\int_A c(z,t)dA = \int_0^\infty\int_0^\infty c(z,t;v,D)f(v,D)dvdD \tag{3.19}$$

where A denotes the area of the field. The field scale resident concentration, $\hat{c_r}$, which represents the resident concentration averaged over the entire horizontal plane at a particular depth, is equal to the ensemble average given in Equation (3.19)

$$\hat{c}_r(z,t) = <c_r(z,t)> \tag{3.20}$$

3.2.4 Transverse Dispersion

The one-dimensional convection dispersion equation, Equation (3.10), cannot account for

dispersion transverse to the direction of flow. However, it can be conveniently quantified in the stream tube model through the variance of the local resident concentration between stream tubes across the horizontal given by Bresler and Dagan (1981) as

$$\begin{aligned}\mathrm{var}[c(z,t)] &= \int_0^\infty\int_0^\infty [c(z,t) - < c(z,t) >]^2 \, f(v,D)\,dv\,dD \\ &= < c^2(z,t) > - < c(z,t) >^2 \end{aligned} \tag{3.21}$$

All parameters are assumed as constant within each stream tube, but v and D are allowed to vary with a known distribution across the stream tubes defining the field domain.

3.2.5 Breakthrough Curves

It is not difficult to compute the breakthrough time, defined as the time at which the concentration equals 0.5 times its maximum value at a particular depth, and the spreading of the concentration at that depth from analytical solutions of Equation (3.10), such as Equation (3.11). However, in the stream tube model, one is more interested in the mean breakthrough time and the mean degree of spreading, which can be characterize through the first (M_1) and the second (M_2) time moments (Toride and Leij, 1996a) given by

$$\begin{aligned} M_1 &= \frac{D}{v^2} + \frac{z}{v} \\ M_2 &= \frac{4D^2}{v^4} + \frac{4Dz}{v^3} + \frac{z^2}{v^2} \end{aligned} \tag{3.22}$$

for a conservative tracer such as bromide with the distribution coefficient $K_d = 0$ and retardation factor $R = 1$.

These equations assume in the stream tube model, in which only v is a random parameter ($\sigma_D = 0$), respectively the forms (Toride and Leij, 1996a)

$$\begin{aligned} M_1 &= \frac{D}{< v >^2}\exp(3\sigma_v^2) + \frac{z}{< v >}\exp(\sigma_v^2) \\ M_2 &= \frac{D^2}{< v >^4}\left[4\exp(10\sigma_v^2) - \exp(6\sigma_v^2)\right] \\ &+ \frac{2Dz}{< v >^3}\left[2\exp(6\sigma_v^2) - \exp(4\sigma_v^2)\right] + \frac{z^2}{< v >^2}\left[\exp(3\sigma_v^2) - \exp(2\sigma_v^2)\right] \end{aligned} \tag{3.23}$$

Equations (3.22) and (3.23) were used in this study to determine the mean breakthrough time and the variance.

3.3 FIELD INVESTIGATIONS

3.3.1 Tracer Studies

Studies on the movement of water and solutes in laboratory and field soils are conventionally conducted with tracers—chemical compounds that dissolve easily in water. In studies of groundwater pollution, the tracer is automatically provided by the dissolved pollutant, but in other studies the investigator has the freedom to choose a suitable tracer, unless one is interested in the sorptive or reactive properties of a specific tracer. Tracers used in studies of the solute transport properties of soils are therefore usually selected with the following properties in mind (Bowman, 1984).

(a) The tracer should be conservative (chemically or biologically).

(b) The tracer should be detectable at very low concentrations.

(c) The tracer should have no adverse effect on the environment.

A tracer that satisfies these constraints is bromide (Smith and Davis, 1974; Onken *et al*., 1977; Rice *et al*., 1986; Jaynes *et al*., 1988; Kung *et al*., 1990; Silvertooth *et al*., 1992; Ashraf *et al*., 1997; Bandaranayake *et al*., 1999; Nachabe *et al*., 1999). Since this tracer has the additional advantage that it can be analysed by several methods, it was also used in this study.

Many of the field tracer studies are carried out with ponded water, because of difficulties experienced with the interpretation of the observations with non-ponding conditions, due to the non-uniformity in the application of water. Nevertheless, there are a number of studies (Wild and Babiker, 1976; van de Pol *et al*., 1977; Butters *et al*., 1989; Ellsworth *et al*., 1991) where sprinkler and trickle irrigation have been used. Following Myers *et al*. (1995), the present study was performed with the rainfall simulator discussed in Chapter 2. This simulator with its controllable intensity applied the water fairly uniform across the test patch.

3.3.2 Experimental Procedures

Two sets of field experiments with rainfall intensities of 5.41 and 3.27 mm h^{-1} were conducted with the rainfall simulator on a (100 x 100) cm^2 patch of soil at the experimental site of the Department of Soil, Climate and Crop Sciences at the University of the Free State. The layout and instrumentation of the patch, discussed in Chapter 2 are shown in Figure 3-2 together with the sampling locations used in the experiments.

A solution of 20 g KBr (equivalent to 13.5 g Br^-) dissolved in 500 ml of distilled

deionised water was applied to the surface of the 1 m^2 patch to give a bromide concentration of 27 g L^{-1} (equivalent to 13.5 g m^{-2} or 135 kg ha^{-1}). Similar concentrations of Br^- have been used in other studies (Baker and Laftlen, 1982; Owens *et al*., 1985; Rice *et al*., 1986; Bicki and Guo, 1991; Nachabe *et al*., 1999). The solution was applied in perpendicular spray patterns in two traverses. Uniform application was ensured by practicing with the sprayer before the start of the actual experiment. After application of the bromide solution, water was applied to the experimental patch through the rainfall simulator at the required intensity.

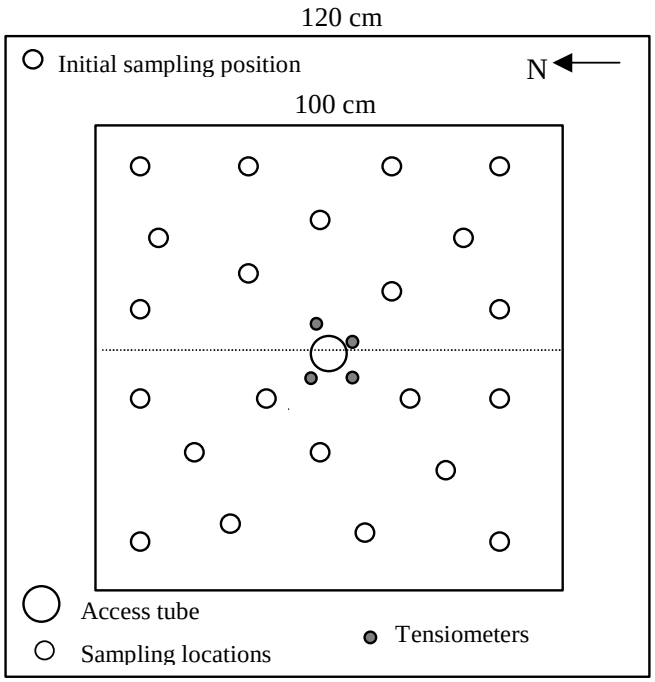

Figure 3-2 The layout of instruments and soil core sampling locations on the patch of soil used in this investigation.

The rainfall simulator used for the experiment was manufactured according to the design of Claassens and van der Watt. (1993). The uniformity of application was checked repeatedly before the start of each experiment and the coefficient of uniformity was found to be greater than 90% in all the cases.

There are a number of methods to acquire data in solute transport studies, of which the most common are: soil coring, solution sampling and time domain reflectrometry. The removal of soil cores for subsequent extraction and analysis of solutes is perhaps the most intuitive approach to evaluate the spatial distribution of solutes within the soil profile (Rhoades, 1982). Solute concentrations determined in this fashion are interpreted as

resident concentrations (i.e., the amount of solute per unit volume of fluid in the system). Although soil cores have the advantage of yielding a 'snapshot' of the distribution of solutes at a particular instant, the method has distinct disadvantages, in that it is labour intensive, destructive, and not well suited for continuous monitoring. The present study was, nevertheless, based on soil coring, since this was the only method available.

The (100 x 100) cm^2 test patch was divided into two equal halves, which was further divided into smaller subunits (17 x 17) cm^2 (not shown in Figure 3-2) for sampling purposes. The central subunits were not sampled to avoid interference with the tensiometers and neutron probe measurements. Soil samples were taken from two subunits, one from each half of the plot, during each sampling time and the samples taken from the same depth mixed to give a composite sample. To avoid soil disturbance and compaction, the plots were accessed via a wooden beam placed on the metal frame surrounding the plot.

The samples for the bromide concentration determinations were taken at predetermined randomised positions as shown in Figure 3-2, at intervals of 20 cm to a maximum depth of 160 cm with an auger type coring tube 20 cm long and 4.2 cm in diameter. Since the core length was small and the diameter large enough, compaction of the soil sample was negligible. After each sampling, the core sampler was cleaned with tap water and rinsed in distilled water before taking the sample at the next depth. After retrieving all the cores, the holes were backfilled with soil from outside of the plot and the position marked with a metal pin to avoid sampling again from the same position. A sub-sample of approximately 100 g of soil was taken from each core sample and placed in paper bags to determine the water content of the soil with the conventional gravimetric method (dry the sample for 24 h at 105 °C). The balances of the soil samples were stored in polyethylene bags for bromide analysis.

The soil samples for Br^- analysis were oven dried and crushed to pass through a 2 mm sieve. A mixture consisting of 50 g of the dried soil sample and 50 ml of distilled deionised water was then prepared in a 250 ml plastic bottle for each soil sample and shaken with a laboratory shaker for about one hour and then filtrated using filter paper. The filtrates were all stored in a refrigerator at 4 °C before they were analysed with an Ion Chromatograph (Dionex 2200I spectrograph) of the Institute for Groundwater Studies at the University of the Free State. The bromide concentration of the field soil solution was then calculated from the filtrate concentration, taking into account the mass of soil extracted and the volume of water used for the extraction (1:1 ratio) and the gravimetric water content of the soil sample. The detection limit attainable with this procedure was approximately 0.01 mg L^{-1}.

3.4 RESULTS AND DISCUSSION

3.4.1 The Soil Water Distribution

The average soil water contents and matric heads along the soil profile during the experiment are given in Figures 3-3 and 3-4 respectively. The observed average standard deviation of 0.25% in the volumetric water content at the different depths indicates that the water distribution in the soil profile was at a steady state during the experiment.

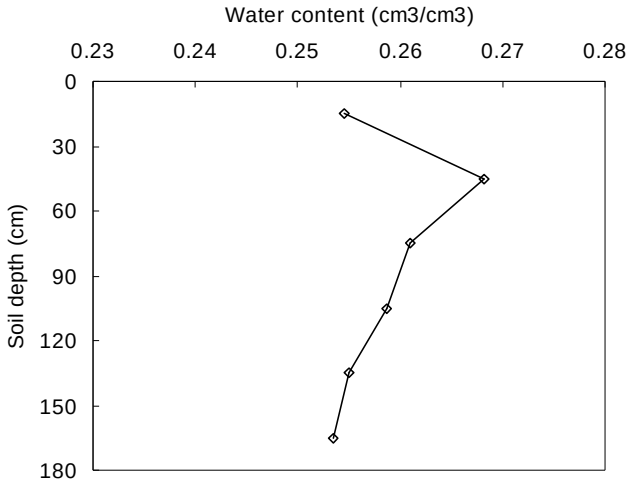

Figure 3-3 Average water content of the soil profile during the experimental period.

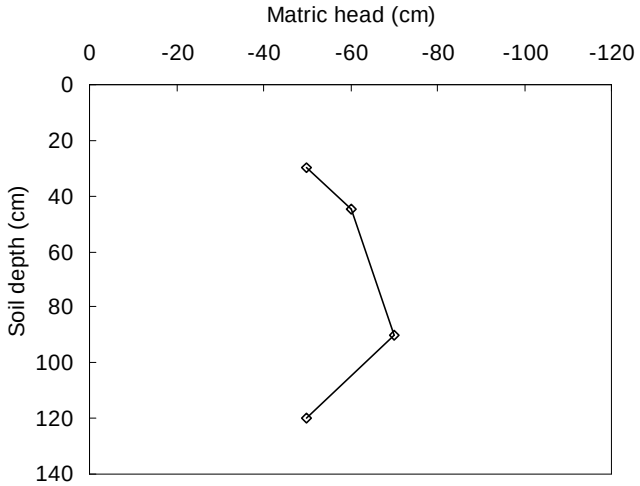

Figure 3-4 Average matric head of the soil profile during the experimental period.

The water content was the highest at the depth with the highest bulk density, see Table 2-1, and decreased consistently with depth. The relatively low water content of the top sandy layer can be ascribed to its lower water holding capacity. The matric head, on the

other hand, decreased with depth to a depth of approximately 90 cm, but then increased over the rest of the sample depth. This behaviour suggests that the hydraulic conductivity of the soil changed dramatically between the depths of the tensiometers 3 and 4, a conclusion confirmed by the discussion of the hydraulic conductivities in Chapter 2.

3.4.2 Bromide Recovery

It is imperative that every effort should be made to ensure that mass is conserved in all studies pertaining to the movement of soil water and solutes in laboratory and field studies. The method used in the present study for this purpose was to compare the mass of Br recovered from the core samples with the mass of the applied solute. The recovered mass of Br^- associated with a core sample, m_i, was calculated as:

$$m_{i,j} = c(z_i, t_i)\theta(z_i, t_i)A\,\Delta z_i \tag{3.24}$$

where $c(z_i, t_j)$ is the bromide concentration at depth z_i and sampling time t_j, $\theta(z_i, t_j)$ the volumetric soil water content, A the cross-sectional area of the core sampler (= 13.85 cm^2), and Δz the thickness of the sample (= 20 cm). The total mass, m_k, of Br^- recovered from the soil profile over a depth Z at a given horizontal position (x_k, y_k) is then simply the sum of the m_{ij} at (x_k, y_k).

$$m_k = \sum_i m_{ij} \quad (z_i \le Z) \tag{3.25}$$

The sum of the recovered bromide masses for the soil profile, during each sampling event, again expressed as a percentage of the applied bromide mass is given Table 3-1. According to this table, the average mass recovered was more than 100%for three of the first four sampling times. This behaviour may be ascribed to the concentration of 0.07 mg/l Br^- in the water used for the experiment and the background concentration of bromide in the soil profile, 1.06 mg/l on average, which was neglected in the computation of the values. However, approximation and experimental errors in computing the percentages and the inhomogeneous application of the KBr solution could also have contributed to the results. Higher or lower than full recovery is common in field-scale solute transport experiments (Butters *et al.*, 1989; Izadi *et al.*, 1993). Rice *et al.* (1986) found an average recovery of about 14% greater than the amount added. Nachabe *et al.* (1999) recovered about 78% of the applied bromide under sprinkler irrigation. Ashraf *et al.* (1997) found average bromide recoveries of 113% at 30 cm depth and 45% at 60 cm depth under ponding condition. These authors attributed the variation to a number of reasons: incorrect sample volume, incomplete bromide extraction, nonuniform water and chemical application, and lateral divergence outside of the subject area due to water content and concentration gradients.

Table 3-1 Percent bromide recovered (*r*) from the soil profile at different times of sampling after bromide application

Time (h)	2.0	4.8	9.8	17.8	27.5	37.0	46.5	56.0	66.0	77.0	96.0
***r* (%)**	99.0	100.0	114.4	131.0	91.4	65.5	45.6	55.6	41.6	39.1	12.3

Figure 3-5 shows the observed bromide concentration profiles at a number of sampling periods after the start of the experiment. Notice how the peak concentration decreased and moved deeper into the soil with time, ultimately, beyond the maximum sampling depth, while the concentration profile becomes flatter and wider as time increases.

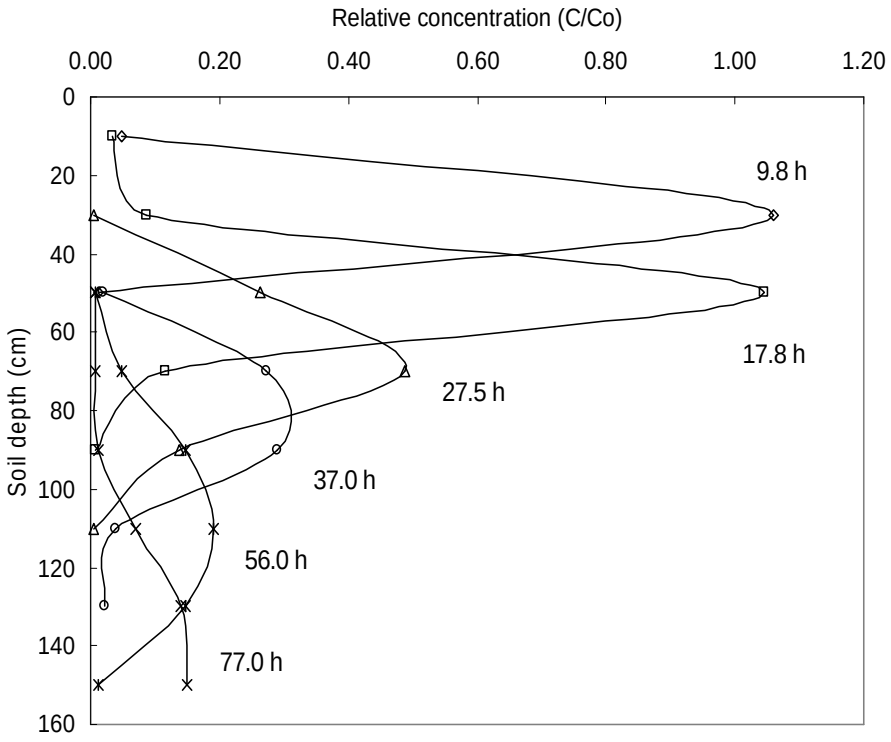

Figure 3-5 Observed concentration profiles at different times after bromide application.

A rather unexpected property of the data in Table 3-1 is the rapid decrease in the percentage bromide recovered from the sixth sampling time onwards. In the absence of plant uptake, as was the case during this experiment, this behaviour can often be ascribed to leaching of the solute below the depth of sampling, as indicated by open-ended distributions in concentration versus depth data (Fleming, 1995). However, this behaviour is not present in the graphs of Figure 3-5 for the first eight sampling periods (56 h). One possible explanation for this is that the leaching of the bromide was significantly affected

by lateral dispersion at late sampling times. There is though a second mechanism that could have a significant effect, especially when using small patches of soils and taking samples near the periphery of the site—*molecular diffusion*. As mentioned above, an attempt was made to limit lateral effects in the present study, by using two samples, one near the centre and one further away, in deriving the concentration profiles for the different sampling times. While this procedure may reduce the influence of lateral dispersion, it cannot account for molecular diffusion from the periphery of the site, which may be implied by the low recovery of bromide for the seventh sampling time (46.5 h) compared to that of the eighth sampling time (56 h) in Table 3-1. The results of the experiment under discussion may therefore not be perfect, but it is felt that they are reliable, especially for the first five sampling times.

The ideal would have been to repeat the present experiment with the remarks above in mind, but this was, unfortunately, not possible because of a lack of funds. Nevertheless, it is felt that it will be worthwhile to investigate the role of molecular diffusion in future experiments of this type in more detail.

3.4.3 Parameter Estimation

The solute transport parameters were estimated by fitting the bromide concentration data to the convective-dispersive equation and stochastic stream tube model, discussed previously in Section 3.2, with the computer package CXTFIT of Toride *et al*. (1995). The first case considered was where both the velocity and dispersion coefficients were assumed to be stochastic in the stream tube model. As shown by the observed and fitted curves for the two models, in Figures 3-6 and 3-7 respectively, both models fit the observed data excellently considering an *in situ* experiment where many factors interact and affect the transport process.

From Table 3-2, it can be seen that both models gave very similar transport velocities with an average of 2.24 cm h^{-1} for the CDE and 2.20 cm h^{-1} for the STM respectively. The average dispersion coefficient values were 3.48 cm^2 h^{-1} and 3.29 cm^2 h^{-1} respectively. As indicated by the coefficients of determination (r^2), the fitting was relatively better for the earlier sampling times compared with the later times, probably because of the mass balance effect discussed above.

The fits discussed above were determined by fitting the concentration data observed at the various depths at every time of sampling with results displayed in Table 3-2. The relatively high values of the correlation coefficient in the table can probably be ascribed to the small number of sampling depths.

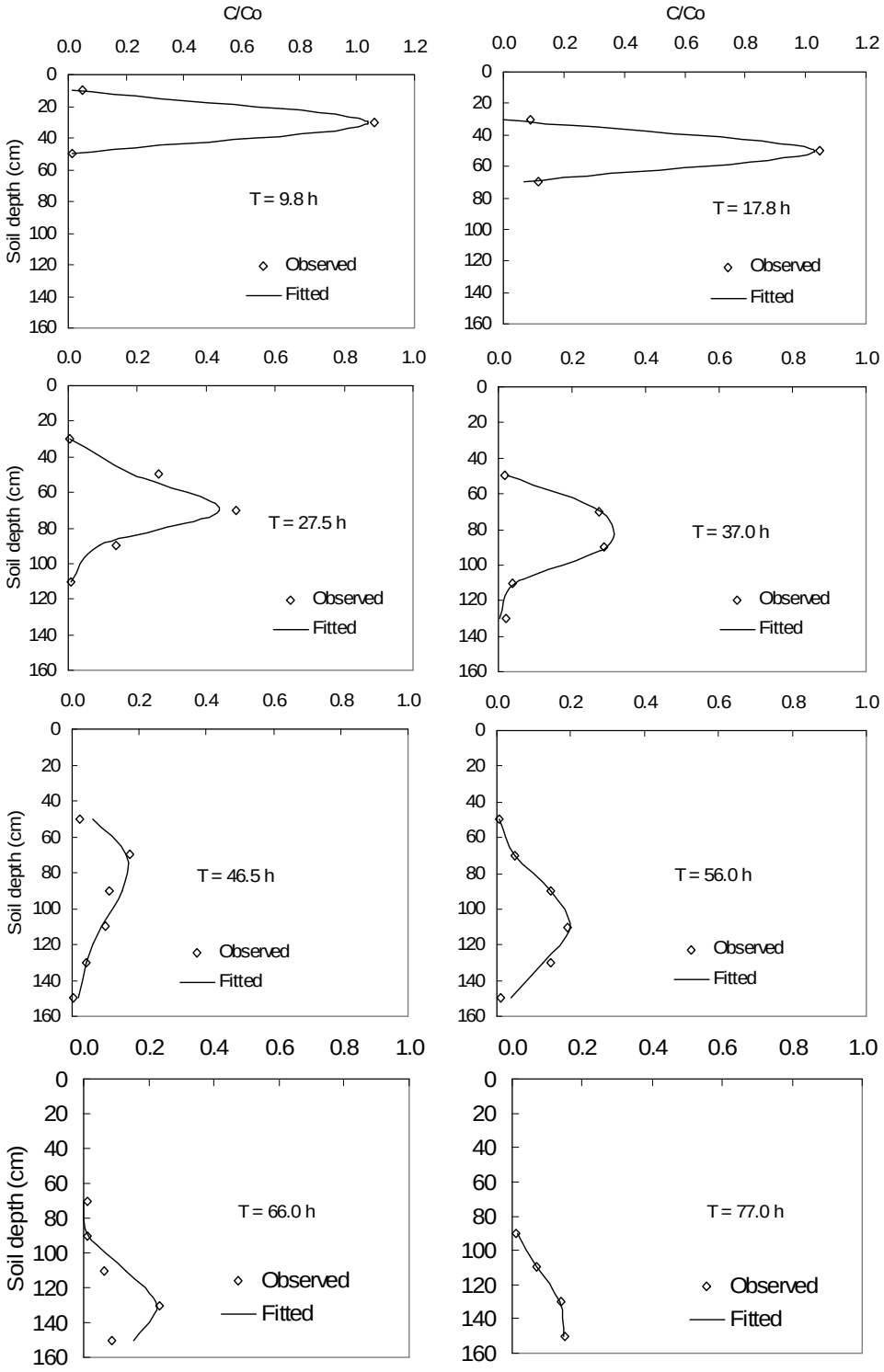

Figure 3-6 Observed and convective-dispersive model fitted concentration profiles at different times after bromide application.

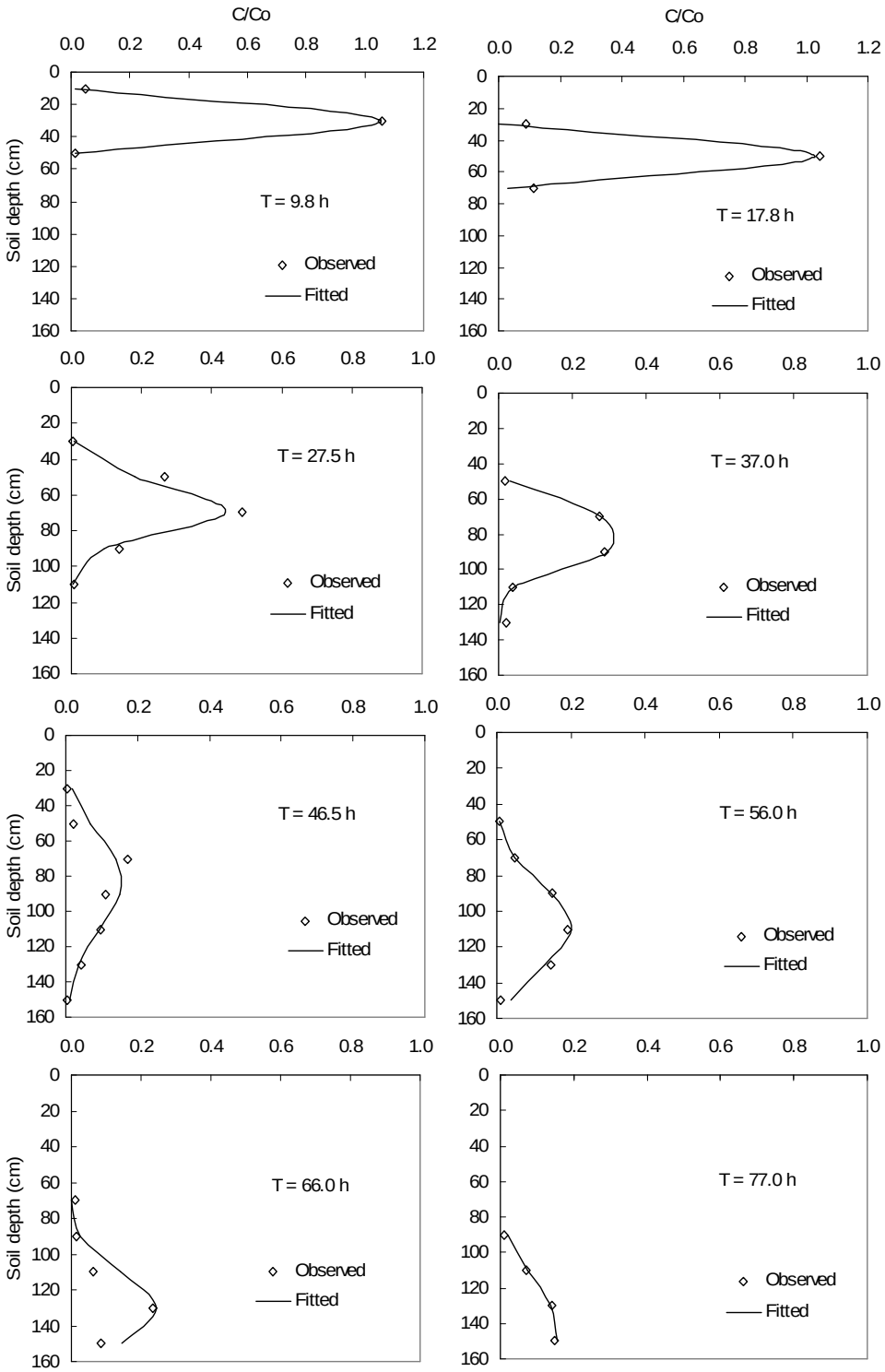

Figure 3-7 Observed and stochastic stream tube model fitted concentration profiles at different times after bromide application.

Table 3-2 The deterministic (v, D, α) and stochastic ($\langle v \rangle$, $\langle D \rangle$, α) transport parameters determined from the concentration profiles in Figures 3-6 and 3-7 ($\rho_{vD} = 1$)

Time	Convective-dispersive model				Stream tube model				
	v	D	α	r^2	$\langle v \rangle$	$\langle D \rangle$	α	σ_v	r^2
(h)	(cm h^{-1})	(cm^2 h^{-1})	(cm)		(cm h^{-1})	(cm^2 h^{-1})	(cm)		
4.8	2.75	3.15	1.15	1.000	2.10	2.31	1.10	0.27	1.000
9.8	2.94	2.31	0.79	0.999	2.94	2.40	0.82	0.01	0.998
17.8	2.95	1.12	0.38	0.982	3.00	1.02	0.34	0.05	0.982
27.5	2.40	3.01	1.25	0.950	2.40	2.87	1.20	0.15	0.950
37.0	2.15	2.60	1.21	0.995	2.16	2.03	0.94	0.08	0.996
46.5	1.70	7.96	4.68	0.804	1.74	7.83	4.50	0.12	0.808
56.0	1.89	4.61	2.44	0.971	1.89	4.74	2.51	0.01	0.971
66.0	1.96	2.79	1.42	0.778	2.00	2.67	1.34	0.04	0.778
77.0	1.85	5.27	2.85	0.989	1.88	5.13	2.72	0.05	0.989
96.0	1.84	1.96	1.07	0.961	1.84	1.94	1.05	0.02	0.961

The dispersivitiy values obtained in this experiment are relatively small when compared with the results from similar field studies. For example, Biggar and Nielsen (1976) obtained a dispersivity of 4.81 cm (dispersion coefficient of 8.776 cm^2 h^{-1} and mean pore-water velocity of 1.826 cm h^{-1}) from chloride tracer experiments on 20 patches distributed over 150 ha, while van de Pol *et al*. (1977) obtained a dispersivity of 9.39 cm (dispersion coefficient of 1.531 cm^2 h^{-1} and pore water velocity of 0.163 cm h^{-1}) from a chloride and tritium tracer experiment on an (8 x 8) m^2 plot continuously irrigated by trickle lines. Jaynes (1991) reported a dispersivity of 31.49 cm (dispersion coefficient of 149.6 cm^2 h^{-1} and a velocity of 4.75 cm h^{-1}) from a bromide tracing experiment carried out on a (6.1 x 6.1) m^2 plot of a clay loam soil. Jaynes *et al*. (1988) from a study under flooded conditions on a 37 m^2 plot reported a dispersivity of 17.78 cm (dispersion coefficient of 88.92 cm^2 h^{-1} and velocity of 5.00 cm h^{-1}). However, such differences are most likely caused by differences in the properties of the soils used in the investigations.

As can be seen in Table 3-2, dispersivity (α) changes with time. This might due to the vertical and horizontal soil heterogeneity. The solute is at different depths at different times of sampling. The soil cores were taken from different positions at different times which can result in different transport parameters because of spatial soil heterogeneity. The high dispersion coefficient at the 46.5th hour might be caused by the change in soil texture at the depth reached by the solute plume at this time. Several studies have shown that dispersion coefficient increases with time in the saturated zone. In the unsaturated zone, it is less clear whether dispersion increases with travel time (Persson and Berndtsson, 1999). The variation in dispersivity here shows the effect of spatial variation.

The standard deviation for the velocities shown in Table 3-2 were relatively small when compared, for example, with the values of σ_v = 1.25 obtained by Biggar and Nielsen (1976) for ponded infiltration condition. This behaviour and the small dispersion coefficients can be taken as an indication that dispersion is limited during this experiment and that the transport could be described adequately with the convection-dispersion model.

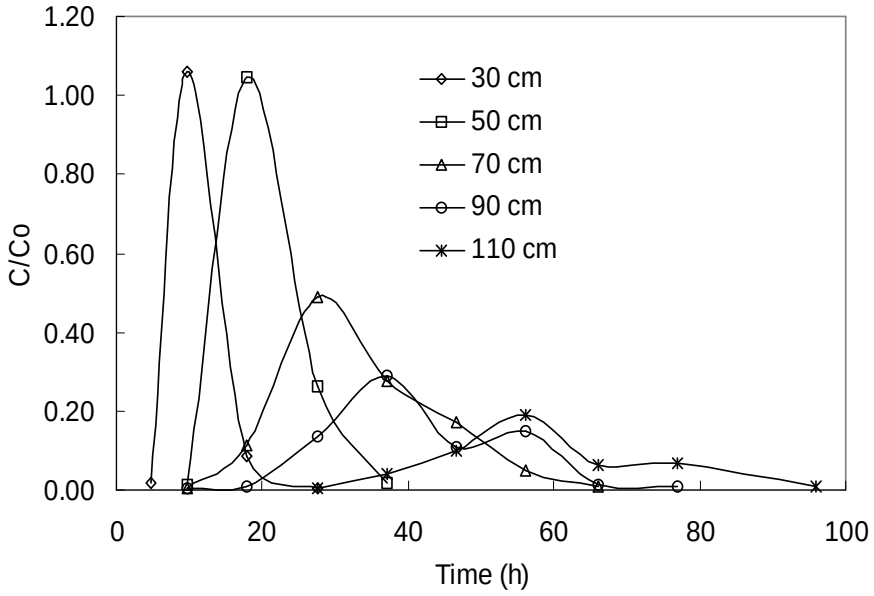

Figure 3-8 Observed breakthrough curves at different depths of the soil profile.

The observed breakthrough curves are presented in Figure 3-8. The peak breakthrough concentration was attenuated as the depth increases and the curve became wider and less peaked. Bromide transport parameters were also determined by fitting the breakthrough curves to the convective-dispersive and stream tube models. The breakthrough curves at 30, 50, 70, 90, and 110 cm depths and their associated fits to the convective-dispersive and stream tube models are presented in Figures 3-9 and 3-10. As in the case of the concentration profiles, the curves became less peaked and wider with depth. The convective-dispersive and stream tube models fitted the data equally well.

Transport parameters that were determined from the breakthrough curves at specific sampling depths are presented in Table 3-3. Solute concentration in core sampling is of resident (volume-averaged) type while a sample obtained with soil solution sampler or suction cup at a given depth is often considered as flux concentration. Core sampling provides a “snapshot” of the solute concentration profile at a particular instant. Therefore, the concentration data in this study is, normally, best expressed as a concentration profile

than as breakthrough concentration. This might be the reason why the coefficients of determination in Table 3-3 were lower than the coefficients of determination of the concentration profile given in Table 3-2.

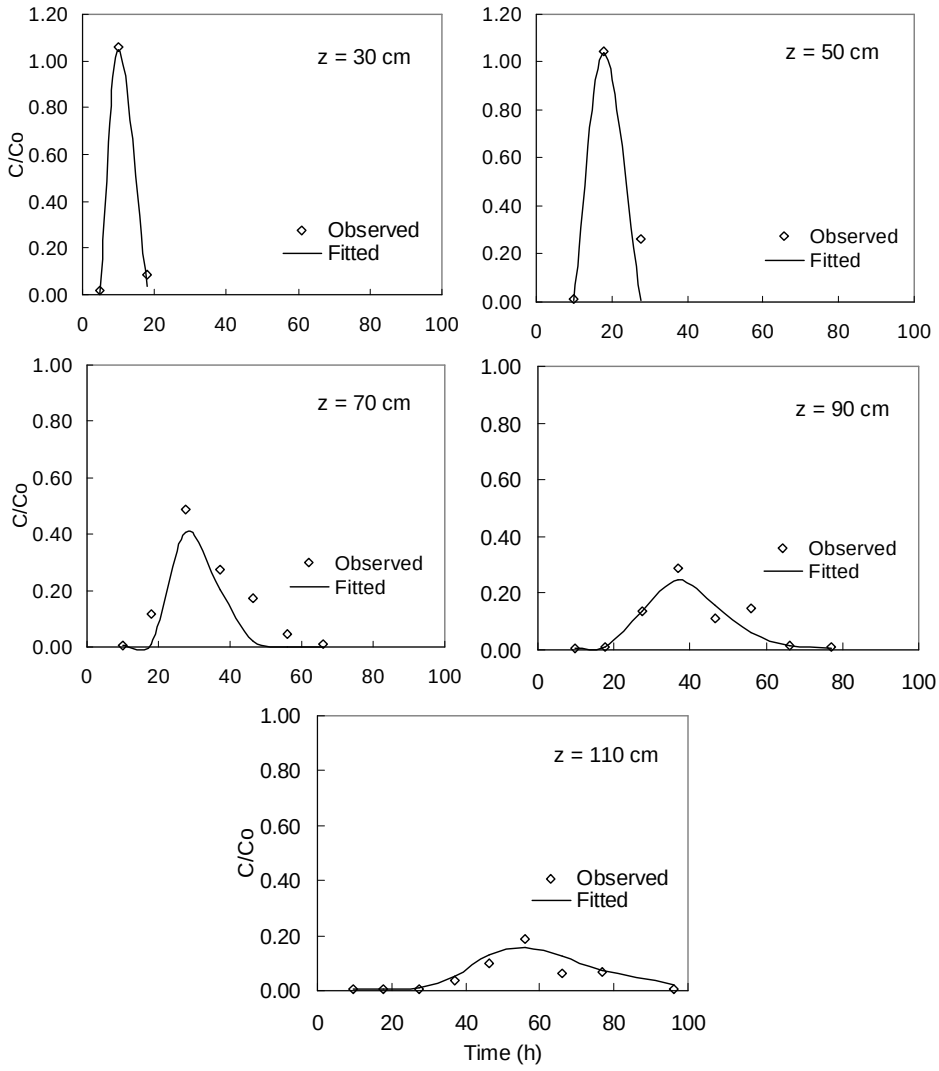

Figure 3-9 Observed and convective-dispersive fitted breakthrough curves at different depths of the soil profile.

Average coefficient of determination (r^2) was 0.880 for both the CDE and STM fitted to the breakthrough concentration data. Both models gave very similar transport velocities that tend to decrease with depth as the more clayey soil started to control the flux. The average pore-water velocity estimated by fitting the convective-dispersive equation to the breakthrough data was 2.41 cm h^{-1} and the stream tube model resulted in the average velocity of 2.42 cm h^{-1}.

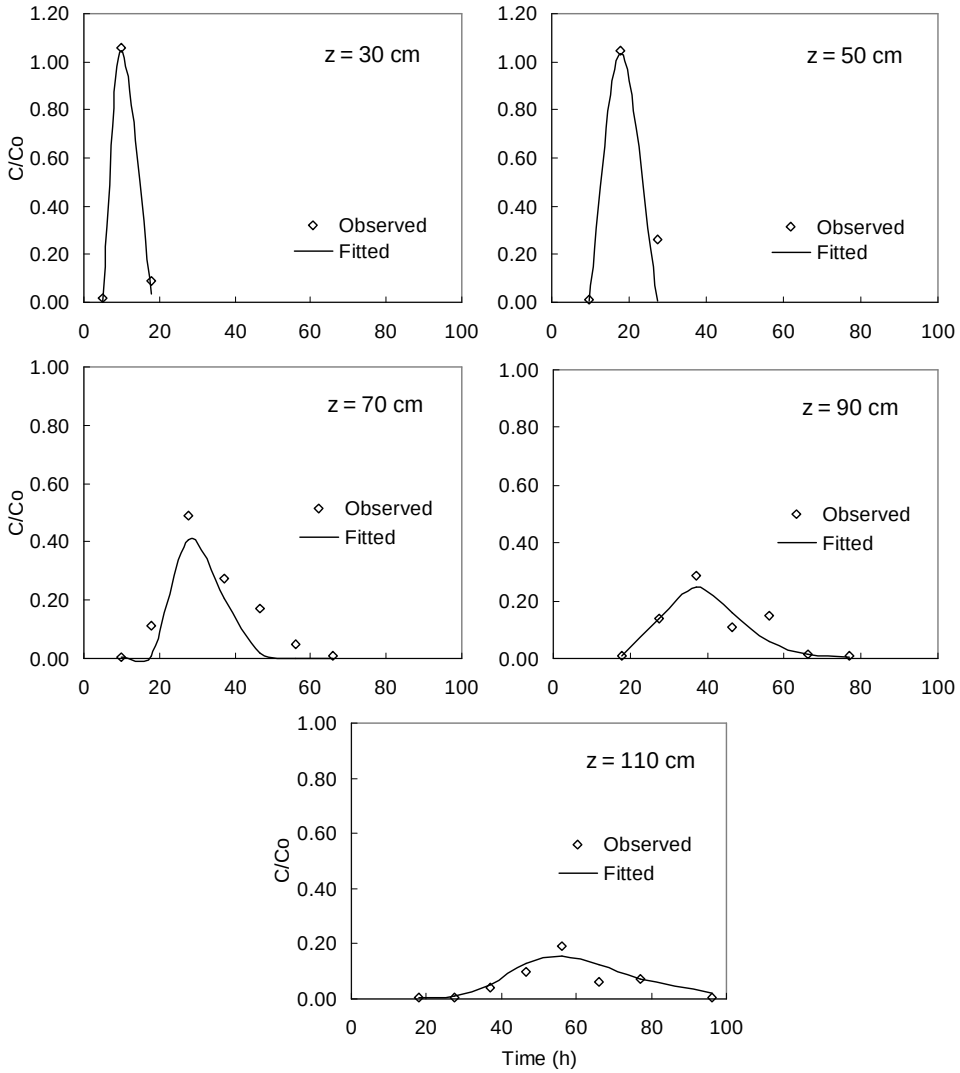

Figure 3-10 Observed and stream tube model fitted breakthrough curves at different depths of the soil profile.

From Table 3-3 it can be observed that the velocity decreased with depth. This trend can be attributed to the increase in clay content at deeper parts of the soil profile. Dispersion coefficient also increased with depth. Since both velocity and dispersion coefficients are increasing with depth, dispersivity also increases. Several studies have shown that dispersivity (dispersivity) increases with the depth of soil or travel time (Sposito *et al*., 1986). However, some studies have also shown that the correlation between the dispersion coefficient and velocity (i.e., dispersivity) can be highly variable (van Ommen *et al*., 1989).

Table 3-3 The deterministic (v, D, α) and stochastic ($\langle v \rangle$, $\langle D \rangle$, α) transport parameters determined from the breakthrough curves in Figures 3-9 and 3-10 ($\rho_{vD} = 1$)

Depth	Convective-dispersive model				Stream tube model				
	v	D	α	r^2	$\langle v \rangle$	$\langle D \rangle$	α	σ_v	r^2
(cm)	(cm h^{-1})	(cm^2 h^{-1})	(cm)		(cm h^{-1})	(cm^2 h^{-1})	(cm)		
30	2.84	2.01	0.71	0.997	2.85	1.84	0.65	0.07	0.997
50	2.72	1.05	0.39	0.930	2.75	1.24	0.45	0.03	0.930
70	2.30	2.64	1.15	0.798	2.33	2.74	1.17	0.04	0.799
90	2.32	7.05	3.04	0.867	2.32	6.79	2.93	0.05	0.867
110	1.86	7.72	4.15	0.810	1.87	7.62	4.07	0.17	0.811

In the previous discussions, both v and D were considered as stochastic variables, albeit perfectly correlated parameters ($\rho_{vD} = 1$). However, there are indications that this may not always be the case. Biggar and Nielsen (1976), for example, studied the spatial variability of v and D for a field soil and found that $\rho_{vD} = 0.795$, $\langle v \rangle = 44.2$ cm d^{-1} with $\sigma_v = 1.25$, and $\langle D \rangle = 367.6$ cm^2 d^{-1} with $\sigma_D = 1.74$. In this study, it was therefore thought worthwhile to see what effect would keeping only one parameter (velocity v) stochastic and the other (dispersion coefficient D) deterministic will have on the fitted transport parameters.

The package CXTFIT was therefore again used to determine values of the velocities and dispersion coefficients, but this time assuming that D is a deterministic variable. The results of these fits are summarized in Tables 3-4 and 3-5. The average velocity and dispersion coefficients were similar to the ones estimated with both the velocity and dispersion coefficients as stochastic parameters. In Figure 3-11, fitted breakthrough curves assuming both v and D and only v as stochastic variable were shown together. It can be seen that the simulation gave similar results.

Table 3-4 Transport parameters determined from the concentration profile data using the stochastic stream tube model with only velocity v as a stochastic variable

Time (h)	$\langle v \rangle$ (cm h^{-1})	$\langle D \rangle$ (cm^2 h^{-1})	α	σ_v	r^2
4.8	1.35	2.37	1.00	0.26	1.000
9.8	2.94	2.30	0.78	0.01	0.999
17.8	2.95	1.12	0.38	0.01	0.982
27.5	2.41	3.45	1.43	0.01	0.945
37.0	2.15	1.31	0.61	0.12	0.996
46.5	1.70	7.23	4.25	0.12	0.806
56.0	1.89	4.51	2.39	0.03	0.971
66.0	1.96	2.87	1.46	0.25	0.777
77.0	1.86	4.83	2.60	0.07	0.988
96.0	1.84	1.95	1.06	0.01	0.961

Table 3-5 Transport parameters determined from the breakthrough curves using the STM taking *v* as a stochastic variable and *D* as a deterministic variable

Depth (cm)	$\langle v \rangle$ (cm h^{-1})	$\langle D \rangle$ (cm^2 h^{-1})	α	σ_v	r^2
30	2.88	1.92	0.67	0.08	0.997
50	2.78	1.17	0.42	0.01	0.929
70	2.30	2.69	1.17	0.07	0.799
90	2.31	7.13	3.09	0.07	0.867
110	1.83	7.51	4.10	0.17	0.795

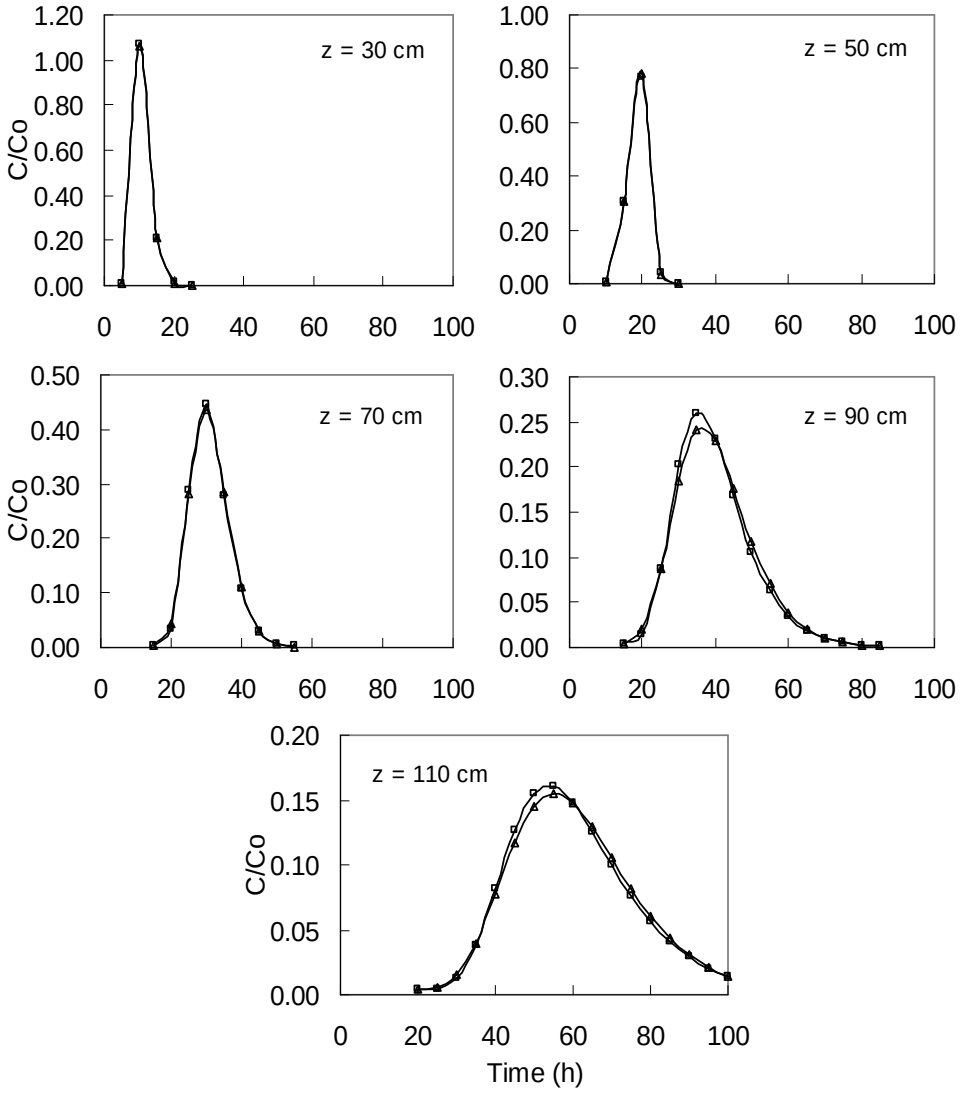

Figure 3-11 Fitted breakthrough curves at different depths of the soil profile when both *v* and *D* are stochastic (▲) and when only *v* is stochastic (□).

3.4.4 Water and Bromide Velocities

One of the objectives of this study was to investigate the nature of the solute transport in the Bainsvlei sandy loam soil. If a conservative tracer, such as bromide is transported continuously throughout the soil profile (often referred to as piston-type flow) one would expect that solute would move at the same rate as the pore-water velocity, v_w (Jury *et al*., 1991; Nachabe and Morel-Seytoux, 1995). Otherwise, it is said that the solute experiences preferential flow, indicated by either a shorter or longer time of arrival at a given depth than indicated by the pore-water velocity.

The average downward movement of the solute front was computed by the pore water velocity (provided that all of the water is participating in the transport) with Equation (3.26).

$$v_w = \frac{q}{\theta} \tag{3.26}$$

where q is the Darcian flux and θ is the average volumetric water content from the soil surface to the maximum depth of detected solute at a given sampling time. The Darcian flux was calculated as the net water applied divided by the duration of application. The amount of water applied during the experimental period of 4 days (96 hours) was 519.4 mm which gives q = 5.41 mm h^{-1}. The average volumetric water content of the soil profile was 0.259. The pore-water velocity or pore-water velocity, calculated using Equation (3.26) is 2.08 cm h^{-1}.

The pore-water velocity was also determined using the least-square inversion program CXTFIT (Toride *et al*., 1995). Using this approach, the average pore-water velocities for the convective-dispersive and stream tube models were 2.24 cm h^{-1} and 2.20 cm h^{-1} respectively (Table 3-2). Therefore, the average pore-water velocity v_w (from water balance, CDE, and STM) is 2.17 cm h^{-1}.

To characterize the bromide transport, the average pore-water velocity v_w was compared with the solute velocity v_s. The solute velocity v_s was determined (a) as the ratio between the depth of observation and the arrival time of the concentration peak (Butter *et al*., 1989), and (b) the location of the centre of mass of the solute plume (Ellsworth *et al*., 1991).

The velocity of the concentration peak of the solute pulse was calculated as the depth increase by the concentration peak between two consecutive sampling events divided by the time interval between the two sampling events, Equation (3.27).

$$v_s = \frac{(z_p)_i - (z_p)_{i-1}}{t_i - t_{i-1}} = \frac{\Delta z_p}{\Delta t} \tag{3.27}$$

where Δz_p is the change in depth of concentration peak of the solute pulse and Δt is the corresponding change in time between the two peaks.

The solute velocity calculated from the arrival times of the concentration peaks of the bromide pulse at various depths in the soil profile (Equation (3.27)) is presented in Table 3-6. It is clear that the mean measured solute velocity of 2.05 cm h^{-1} is very similar to the theoretical pore-water velocity of 2.08 cm h^{-1}.

Table 3-6 Bromide concentration peak velocity calculated using Equation (3.27)

Depth, *z*	**Time, *t***	**Difference**		**Velocity, v_s**	v_s/v_w
(cm)	**(h)**	z_i-z_{i-1} **(cm)**	t_i-t_{i-1} **(h)**	**(cm h^{-1})**	
10	2.0				
30	9.8	20	7.8	2.56	1.2
50	17.8	20	8.0	2.50	1.2
70	27.5	20	9.7	2.06	1.0
90	37.0	20	9.5	2.11	1.0
110	56.0	20	19.0	1.05	0.5
130	66.0	20	10.0	2.00	0.9
			Average	2.05	0.97

The depth to the centre of mass of the bromide profiles was calculated as

$$\overline{z_i} = \frac{1}{m_i} \sum_{z=0}^{z=Z} z\theta(z,t)c(z,t_i)A\Delta z \tag{3.28}$$

where $\overline{z_i}$ is the depth to the centre of mass at the sampling time t_i.

The velocity of the centre of mass of the solute between two samplings was calculated as

$$v_s = \frac{\overline{z_i} - \overline{z_{i-1}}}{t_i - t_{i-1}} = \frac{\Delta \overline{z}}{\Delta t} \tag{3.29}$$

where $\overline{z_i}$ and $\overline{z_{i-1}}$ are the depth to the centre of mass of Br at sampling times t_i and t_{i-1}.

The velocity of the solute centre of mass though the soil profile, calculated using Equation (3.29) is presented in Table 3-7 where $\overline{z}$ is the depth of the centre of mass of bromide concentration profile. The average centre of mass velocity of the concentration profile is 2.02 cm h^{-1} which is again very similar to the theoretical pore-water velocity calculated using Equation (3.26).

Table 3-7 Bromide centre-of-mass velocity calculated using Equation (3.29)

Time *t* (h)	4.8	9.8	17.8	27.5	37.0	46.5	56.0	66.0
$\bar{Z}$	11.5	31.0	50.7	67.9	82.8	88.8	106.0	126.2
$\Delta\bar{Z} = \bar{Z}(t_i) - \bar{Z}(t_{i-1})$		19.5	19.7	17.2	14.9	6.1	17.2	20.1
$\Delta t = t_i - t_{i-1}$		5.0	8.0	9.7	9.5	9.5	9.5	10.0
$v_s = \Delta\bar{Z} / \Delta t$		3.90	2.46	1.77	1.57	0.64	1.81	2.01

Depending on the method with which solute velocity is determined, different and sometimes contradicting results can be obtained when describing field solute transport by simple piston flow models (Biggar and Nielsen, 1976; Star *et al*., 1978; Rice *et al*., 1988; Butters *et al*., 1989; Ellsworth *et al*., 1991). Biggar and Nielsen (1976) obtained a good agreement between the pore-water velocity and the solute velocities (v_s/v_w =1.0), under steady ponding conditions in a clay loam soil. Rice *et al*. (1988) found under intermittent ponding conditions, that the solute velocity was almost five times larger than the pore-water velocity in a sandy loam soil. Starr *et al*. (1978) conducted a study in a layered sandy loam soil and found that the solute velocity calculated from the arrival times of the concentration peak was only about half of the pore-water velocity under ponded conditions. Butters *et al*. (1989) studied the leaching of bromide in a loamy sand soil using bidaily sprinkler irrigation. He found the solute velocity, calculated as the ratio of the depth of observation to the mean solute pulse arrival time, to be substantially less than the pore-water velocity in the top 1.8m. Deeper down the agreement was better. Ellsworth *et al*. (1991) leached solutes using trickle irrigation in a loamy sand soil and the solute velocity, estimated by the position of the centre of mass of the solute plume, agreed almost perfectly with the pore-water velocities. These research studies illustrate the complexity of the field regime.

In this study, the ratios of v_s to v_w were 0.98 and 0.93 when the bromide velocity v_s was determined from the movement of bromide concentration peak and centre of mass respectively. As can be seen, these ratios (average = 0.96) indicate that there was no preferential transport of Br^- in this soil during this steady state experiment. The soil was relatively homogeneous and of a low clay content. It can be classified as weakly structured soil and there is less possibility of preferential flow in such soils.

3.4.5 Estimation of Breakthrough Time using Moment Analysis

The mean breakthrough time of bromide and its variance was calculated using Equation (3.22) for convective-dispersive equation and Equation (3.23) for stochastic stream tube model. The results are presented in Tables 3-8 and 3-9 at different depths of the soil profile.

Table 3-8 Mean breakthrough time (M1) and variance (M2) of breakthrough concentration using the CDE parameters at different depths

Depth (cm)	v (cm h^{-1})	D (cm^2 h^{-1})	M1 (h)	M2 (h^2)
30	2.84	2.01	10.8	122.4
50	2.72	1.05	18.5	348.4
70	2.30	2.64	30.9	988.0
90	2.32	7.05	40.1	1715.0
110	1.86	7.72	61.4	4045.3

Table 3-9 Mean breakthrough time (M1) and variance (M2) of breakthrough concentration using the STM parameters at different depths

Depth (cm)	$\langle v \rangle$ (cm h^{-1})	D (cm^2 h^{-1})	σ_v	M1 (h)	M2 (h^2)
30	2.88	1.91	0.08	10.7	5.9
50	2.78	1.17	0.01	18.2	5.5
70	2.30	2.69	0.07	30.6	37.4
90	2.31	7.13	0.07	40.5	121.2
110	1.83	7.51	0.17	64.3	470.9

The breakthrough times for the convective-dispersive equation and stochastic stream tube model (when only v is stochastic) were very similar. However, the variance determined using the stochastic stream tube model parameters was lower than the one determined using the convective-dispersive equation parameters. As can be seen from Table 3-8, the breakthrough times correspond well with the times at which the bromide peaks reached these depths (Figure 3-5). This indicates that Br^- movement can be described by pore-water velocity in this experiment. The variance increased with depth because the breakthrough curves became more dispersed at deeper depths (Figure 3-10).

Both the mean breakthrough time and variance are directly proportional to the dispersion coefficient at the depth of observation and are inversely proportional to velocity. The higher the velocity at shallow depths, the less the dispersion of the solute occurred and deeper in the profile the dispersion coefficient increased because of the lower velocity of bromide displacement.

3.4.6 Sensitivity Analysis

One of the usefulness of analytical solutions of subsurface transport problems is for sensitivity analyses to investigate the effect of various transport parameters (Leij and Bradford, 1994). Sensitivity analysis helps identify the parameters whose value it is critical to determine accurately and thus helps the user to focus parameterisation effort where it is needed most. This is achieved by assessing the effects on output of variability

in input parameters. In this section, the effect of variation in velocity and dispersion coefficient on the transport process will be studied.

The analysis was done using the convective-dispersive equation at 9.8, 37.0, and 56.0 h after bromide application. The actual measured velocities were increased and decreased by 25% and 50% keeping the actual dispersion coefficient constant for a specific time (Table 3-10). Figure 3-12 presents the sensitivity of bromide transport due to a variation in transport velocities. It can be observed that the solute plume moves deeper as the velocity increases while the width of the plume remains the same. This illustrates that velocity determined the position of the concentration peak and the centre of mass.

Table 3-10 Velocity and dispersion coefficient values at different times after bromide application used in the sensitivity analysis of velocity using the CDE and STM

Time (h)	Convective-dispersive model		Stream tube model	
	v	***D***	**<*v*>**	**<*D*>**
9.8	1.47	2.31	1.47	2.40
	2.21	2.31	2.21	2.40
	2.94	2.31	2.94	2.40
	3.68	2.31	3.68	2.40
	4.41	2.31	4.41	2.40
37.0	1.08	2.60	1.08	2.03
	1.61	2.60	1.62	2.03
	2.15	2.60	2.16	2.03
	2.69	2.60	2.70	2.03
	3.23	2.60	3.24	2.03
56.0	0.95	4.61	0.95	4.74
	1.42	4.61	1.42	4.74
	1.89	4.61	1.89	4.74
	2.36	4.61	2.36	4.74
	2.84	4.61	2.84	4.74

From the curve at 37.0 h, for example, it can be observed that a 50% increase in velocity moved the concentration peak 40 cm deeper from 80 cm to 120 cm. The variation in velocity did not affect the width of the concentration curves because dispersion coefficient was kept the same. At the 56.0 h, a 50% increase in velocity moved the concentration peak from 110 cm to out of the soil profile (160 cm). Similar analysis conducted with the stream tube model gave the same results as with the CDE model (Figure 3-13).

From Figures 3-12 and 3-13, it can be seen that the shapes of the curves are the same for both models. The change in velocity only shifted the plume and do not change the size or shape of the plume as long as the simulation is done for the same applied mass.

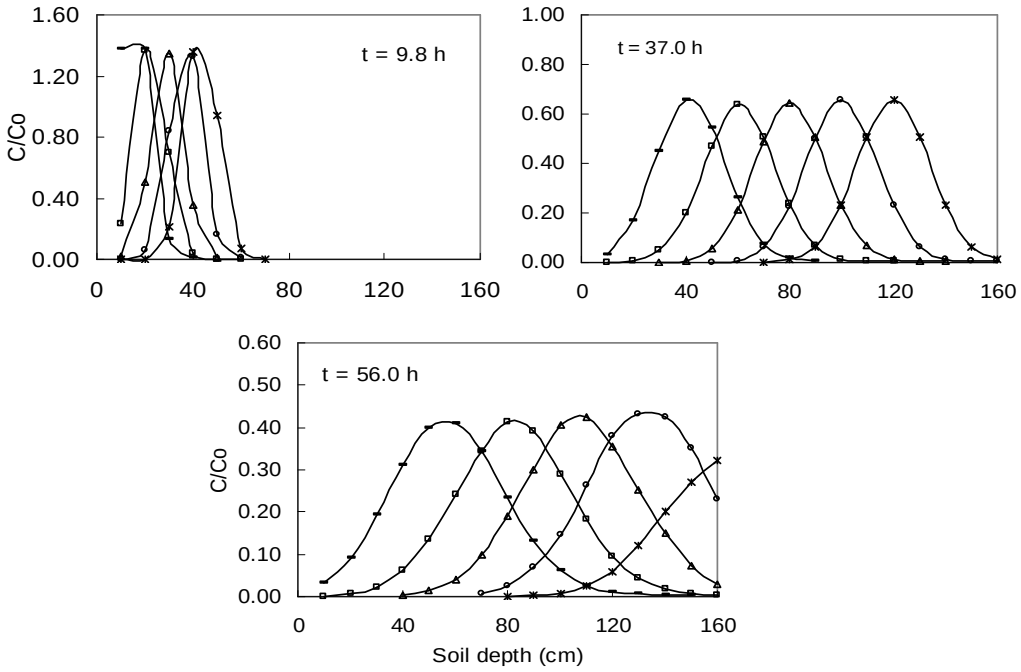

Figure 3-12 Sensitivity of bromide transport for the variation in velocities analysed using the CDE (- = 0.50*v*, □ = 0.75*v*, △ = *v*, ▯ = 1.25*v*, ∗ = 1.50*v*).

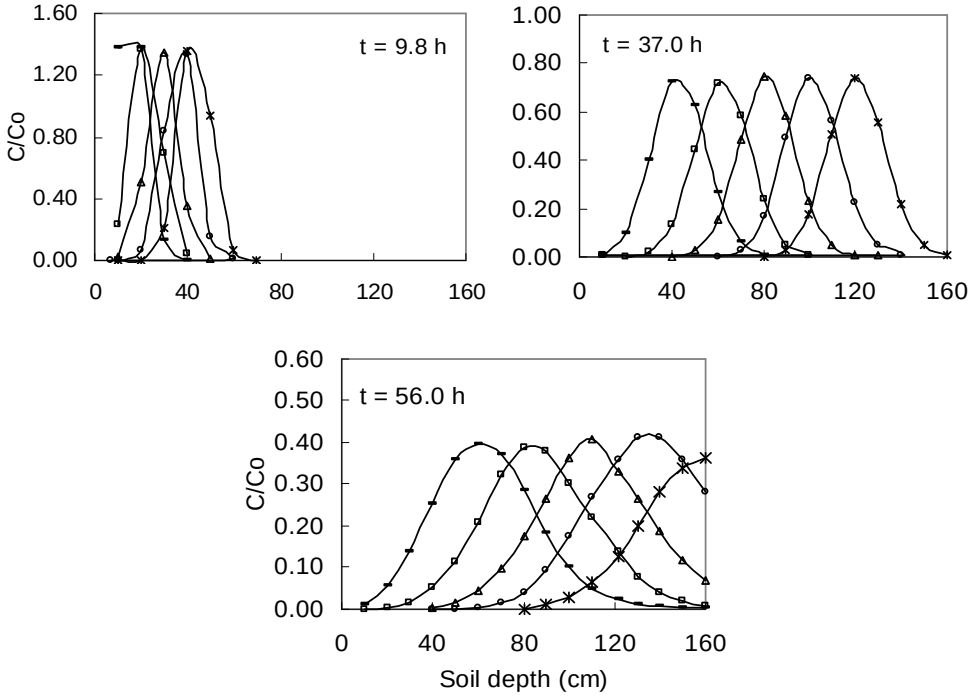

Figure 3-13 Sensitivity of bromide transport for the variation in velocity analysed using STM (- = 0.50*v*, □ = 0.75*v*, △ = *v*, ▯ = 1.25*v*, ∗ = 1.50*v*).

To illustrate the effect of a variation in the dispersion coefficient, between 0.5*D* and 1.5*D*, the velocity for each time was kept constant (Table 3.11) and the results are presented in Figures 3-14 and 3-15 for the convective-dispersive and stochastic stream tube models.

Table 3-11 Velocity and dispersion coefficient values used in the sensitivity analysis of dispersion coefficients

Time (h)	Convective-dispersive model		Stream tube model	
	v	***D***	**<*v*>**	**<*D*>**
9.8	2.94	1.16	2.94	1.20
	2.94	1.73	2.94	1.80
	2.94	2.31	2.94	2.40
	2.94	2.89	2.94	3.00
	2.94	3.47	2.94	3.60
37.0	2.15	1.30	2.16	1.02
	2.15	1.95	2.16	1.52
	2.15	2.60	2.16	2.03
	2.15	3.25	2.16	2.54
	2.15	3.90	2.16	3.05
56.0	1.89	2.31	1.89	2.37
	1.89	3.46	1.89	3.56
	1.89	4.61	1.89	4.74
	1.89	5.76	1.89	5.93
	1.89	6.90	1.89	7.11

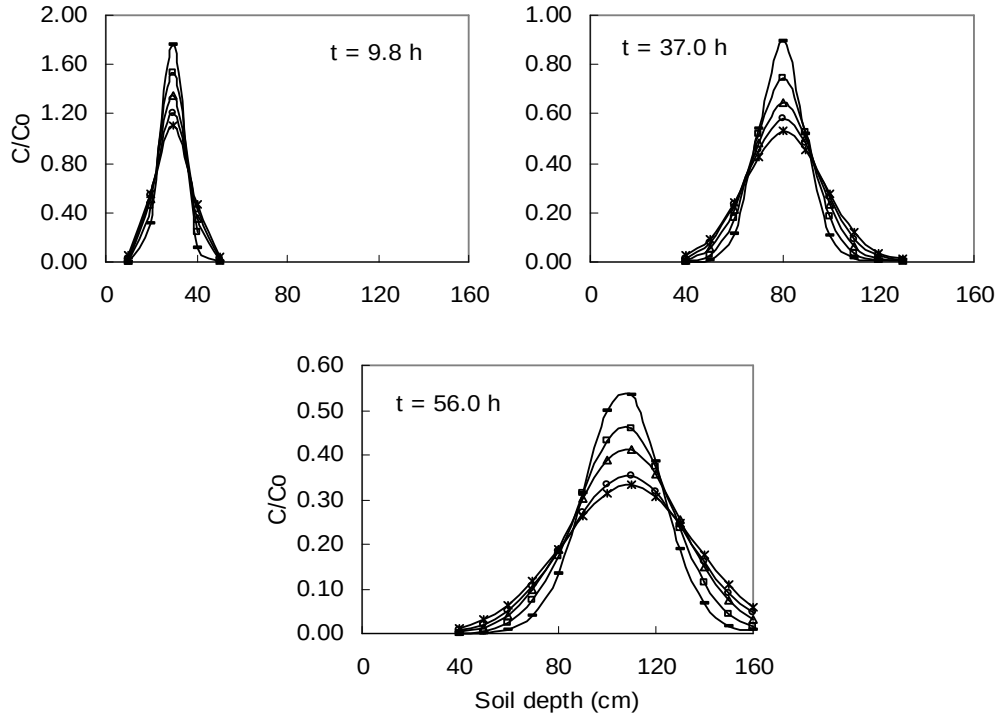

Figure 3-14 Sensitivity of bromide transport for variation in dispersion coefficient using CDE (- = 0.50*D*, □ = 0.75*D*, △ = *D*, ▯ = 1.25*D*, ∗ = 1.50*D*).

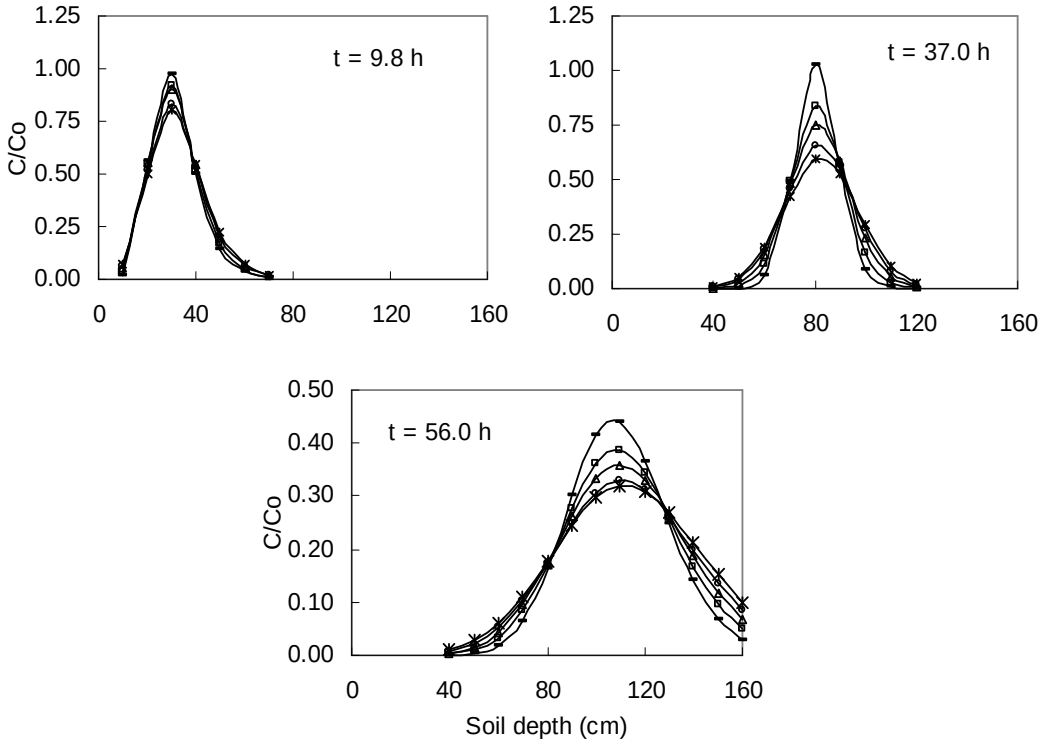

Figure 3-15 Sensitivity of bromide transport for the variation in dispersion coefficient analysed using STM (- = 0.50*D*, □ = 0.75*D*, △ = *D*, ▯ = 1.25*D*, ∗ = 1.50*D*).

As the dispersion coefficient is increased, the peak concentration is lowered in magnitude and the concentration profile curve gets wider. Variation in the dispersion coefficient does not significantly affect the bromide transport processes. The dispersion coefficient does, however, affect the width of the solute pulse as it moves through the soil, but not the depth of the peak (Porro *et at.*, 1993). Previous studies have also shown that the contribution of *D* to the dispersion processes may be minimal, compared with the variations in the pore-water velocities (Amoozegard-Fard *et al.*, 1982; Jaynes *et al.*, 1988). Generally, it can be stated that dispersion has only small effect on bromide transport when compared with the convection rate (velocity) and convection component of the transport processes is the dominant mechanism in the soil solute transport.

3.4.7 Comparison of Bromide Transport under 5.41 mm h^{-1} and 3.27 mm h^{-1} Fluxes

The analyses in the previous sections of this Chapter were done from the data of the experiment with a flux of 5.41 mm h^{-1}. Another similar experiment was conducted using a lower simulated rainfall intensity of 3.27 mm h^{-1}. The analysis of bromide transport

under the 5.41 mm h^{-1} flux was presented in the previous Sections of this Chapter. In this Section the Br^- transport at a 3.27 mm h^{-1} flux will be analysed and compared with the 5.41 mm h^{-1} flux.

Table 3-12 Relative bromide concentrations at different depths and times after the application of potassium bromide (Darcian flux = 5.41 mm h^{-1})

Depth	Time (h)										
(cm)	2.0	4.8	9.8	17.8	27.5	37.0	46.5	56.0	66.0	77.0	96.0
	Relative concentration (C/Co)										
10	0.968	0.968	0.048	0.035	0.003	0.002	0.000	0.000	0.000	0.000	0.000
30	0.013	0.016	1.059	0.088	0.005	0.005	0.003	0.004	0.003	0.004	0.003
50	0.006	0.004	0.013	1.046	0.264	0.019	0.023	0.007	0.008	0.008	0.007
70	0.003	0.004	0.006	0.115	0.488	0.274	0.173	0.048	0.010	0.008	0.008
90	0.004	0.005	0.004	0.008	0.138	0.289	0.110	0.148	0.013	0.011	0.006
110	0.003	0.004	0.005	0.006	0.006	0.039	0.098	0.190	0.062	0.070	0.007
130	0.003	0.003	0.005	0.006	0.005	0.022	0.044	0.147	0.235	0.141	0.010
150	0.003	0.003	0.004	0.006	0.005	0.005	0.005	0.012	0.085	0.149	0.082
Sum	**1.003**	**1.007**	**1.144**	**1.310**	**0.914**	**0.655**	**0.456**	**0.556**	**0.416**	**0.391**	**0.123**

Table 3-13 Relative bromide concentrations at different depths and times after the application of potassium bromide (Darcian flux = 3.27 mm h^{-1})

Depth (cm)	Time (h)								
	6.1	23.1	29.9	47.2	54.2	70.8	97.1	102.0	124.3
	Relative concentration (C/Co)								
10	0.865	0.489	0.375	0.089	0.066	0.095	0.063	0.064	0.067
30	0.435	0.232	0.393	0.221	0.194	0.128	0.158	0.131	0.086
50	0.159	0.087	0.095	0.144	0.223	0.182	0.238	0.155	0.079
70	0.005	0.071	0.082	0.085	0.078	0.199	0.150	0.152	0.168
90	0.003	0.069	0.076	0.073	0.072	0.073	0.082	0.208	0.214
110	0.004	0.005	0.006	0.074	0.012	0.074	0.073	0.195	0.080
130	0.003	0.002	0.004	0.074	0.075	0.075	0.073	0.081	0.070
150	0.004	0.004	0.004	0.006	0.071	0.072	0.072	0.092	0.069
Sum	**1.478**	**0.959**	**1.035**	**0.766**	**0.790**	**0.898**	**0.909**	**1.078**	**0.833**

The total amount of water applied during the 124.3 h experimental period was 406.3 mm. There was no evaporation or runoff. Hence, the Darcian flux, q was 3.27 mm h^{-1}. The average volumetric water content during the experimental period at different depth intervals was 0.260 (0–30 cm), 0.243 (30–60 cm), 0.209 (60–90 cm), 0.244 (90–120 cm), 0.254 (120–150 cm), and 0.266 (150–180 cm). The average soil profile water content (θ) was 0.246. The average pore water velocity or pore-water velocity (q/θ) was 13.3 mm h^{-1} or 1.33 cm h^{-1}. The average matric potential head as measured by the tensiometers

installed at 30, 45, 90 and 120 cm depths was -20, -60, -80, and -40 cm of water. The relative bromide concentrations of the soil profile at different times after the application of Br^- are presented in Tables 3-12 and 3-13 for both the fluxes of 5.41 and 3.41 mm h^{-1}. The underlined numbers indicate the concentration peaks at the times of sampling.

The Br^- velocities under the 3.27 mm h^{-1} flux determined from the rate of the concentration peak movement were 1.31 (10–30), 0.82 (30–50), 1.21 (50–70), and 0.64 cm h^{-1} (70–90) between the depth intervals indicated in parenthesis. The average bromide velocity according to the concentration peak velocity was, therefore, 0.99 cm h^{-1}. The concentration peak did not pass the 90 cm depth. The bromide velocity was also determined from the velocity of the centre of mass. The changes in the centre of mass depths of bromide were 8.7 (17.0), 4.5 (6.8), 26.4 (17.3), 5.1 (7.0), 5.3 (16.6), and 11.4 cm (4.96 h) with the corresponding times elapsed for the displacement indicated in parenthesis. The respective bromide velocities determined from the centre of mass transport were, therefore 0.51, 0.67, 1.52, 0.72, 0.32, and 2.31 cm h^{-1}. The average centre of mass velocity was therefore 1.01 cm h^{-1}.

The average Br^- velocity (1.00 cm h^{-1}) under the 3.27 mm h^{-1} flux was lower than the average Br^- velocity (2.20 cm h^{-1}) under the 5.41 mm h^{-1} flux. Generally, transport of a conservative tracer such as Br^- is affected by the amount of applied water and the soil water content. The chemical is transported deeper as the amount of applied water is increased and the velocity is also higher at lower soil water contents. Comparing the two flux rates at equal amounts of water applied, the Br^- peak was moved deeper into the soil profile in the 5.41 mm h^{-1} flux. For example, at the end of the experiment with the 3.27 mm h^{-1} flux, the cumulative amount of water applied was 406.3 mm and the Br^- peak reached 90 cm depth. After 416.8 mm of water was applied in the 5.41 mm h^{-1} flux experiment, the Br^- peak has already passed the deepest sampling depth of 160 cm. The average soil profile water content (0.246) during the 3.27 mm h^{-1} flux experiment was lower than the water content (0.259) during the 5.41 mm h^{-1} flux experiment. This indicates that Br^- transport in this soil is influenced by the water application rate, the cumulative amount of water applied and the soil water content.

3.5 CONCLUSIONS

The rainfall simulator provided an excellent facility for studying non-ponding solute transport in the field. The solute velocities determined from the concentration peak movement and the movement of the solute centre of mass were in good agreement with the average pore-water velocity determined from soil water balance and fitting concentration data to theoretical models, indicating that piston flow can describe the

transport process. The Bainsvlei soil is a weakly structured fine sandy loam and preferential flow paths are less likely to develop under this steady state condition.

The CXTFIT computer package provided a convenient tool for analysing the data. The deterministic convective-dispersive model and the stochastic stream tube model performed almost equally well in estimating the transport parameters and predicting the solute concentrations as functions of time and space. No significant differences were observed between the results obtained by these methods. The CDE and STM models produced similar estimates of about 2.2 cm/h for the pore-water velocity.

It is important to note that the leaching of bromide increased in direct relation to an increase in the irrigation rate and associated percolation rate. It is therefore important to adjust the irrigation rate to retain as much water as possible in the root zone of crops on a per event basis, since water lossed through deep percolation is unavailable to crops. Such a practice will also reduce the rate at which a fertilizer will leach from the root zone, thereby minimizing the potential for groundwater contamination. One approach to achieve these objectives is to regularly measure or estimate crop evapotranspiration.

The effects of simulated rainfall intensity on the downward movement of water and chemicals in macropores appear to be similar to the well-established relations between rainfall and surface runoff transport, that is the deep percolation and leaching increases with the rainfall intensity. However, the transport of solutes is dominated more by the deep percolation rate than the rainfall intensity.

From sensitivity analyses of the convective (velocity) and dispersive (dispersion coefficient) components of the solute transport equations, it has been observed that the depth to which the peak concentration of the tracer pulse will be moved is determined by the convection (velocity) while dispersion affects only the spreading. The effect of velocity is more significant in determining the location of the solute plume.

The uniform manner in which the water and solute was applied and subsequently leached, the consistency of sampling technique, and the near 100% average recovery of solutes contributed towards compiling a comprehensive data set for model development and verification.

CHAPTER 4

TRANSIENT STATE TRANPORT OF BROMIDE AND NITRATE IN THE FIELD

4.1 INTRODUCTION

Maintaining a constant infiltration rate for a long time to create steady state solute fluxes in the soil profile occurs seldom in practice since intermittent rainfall or irrigation creates transient state solute fluxes through the profile. To interpret concentration measurements that were obtained during leaching experiments, it is necessary to compare the measured concentration data with model predictions. For steady-state conditions, analytical solutions of the transport equation are available and least-squares optimisation procedures (e.g., the CXTFIT program of Toride *et al.*, 1995) can readily be used to estimate transport parameters (Chapter 3). In many studies, steady state flow approximations of transport models were used to interpret the measured concentrations and to estimate transport model parameters for transient conditions (Jury *et al.*, 1982; Bowman and Rice, 1986; Butters and Jury, 1989; Jarvis *et al*., 1991; Roth *et al*., 1991; Jaynes and Rice, 1993;Ward *et al*., 1995). This is because transient models are more difficult to apply and there is evidence to suggest that, under many conditions, the two types of models give similar results (Sharma and Taniguchi, 1991). From numerical simulation results, based on the solution of an equation describing simultaneous movement of water and solutes, Wierenga *et al*. (1975) concluded that both analytical and numerical models yield comparable results when solute concentrations are expressed as a function of cumulative drainage.

A technique commonly used to transform a time series of concentrations measurements taken during a transient flow leaching experiment at a certain depth in the soil profile is to replace the time variable with cumulative drainage. When time is transformed to cumulative drainage, the simulated breakthrough curves are smoothed out. Studies of transient flow convective-dispersive solute transport by Wierenga (1977), Beese and Wierenga (1980) and Russo *et al*. (1989) illustrated that breakthrough curves as a function of cumulative drainage have shapes similar to the solute breakthrough curves obtained during steady-state leaching experiments. It is assumed that solute distribution simulated with steady-state models will be practically the same as for transient conditions. Despite the obvious advantage of using steady state models for describing transient state data, there has generally been a lack of adequate supportive field

experimental evidence, with the exception of a few studies conducted under field conditions (e.g. Wild and Babiker, 1976; Jury *et al*., 1982; Rose *et al*., 1982; Sharma *et al*., 1985; Bowman and Rice, 1986).

Meyer-Windel *et al*. (1999) created steady state and transient state conditions in "undisturbed" soil columns by applying water at different frequencies and concluded that for an equal cumulative drainage a larger percentage of Br^- was leached under the steady state flow than under transient flow. Sharma and Taniguchi (1991) conducted a similar experiment using different repacked laboratory soil columns by applying water as rainfall either at a steady state or intermittently. From the range of steady and intermittent leaching used, they observed that for the same amount of water applied, the solute peak moved faster under the steady state than under intermittent applications. From simulation studies, Watson *et al*. (1987) showed that the duration of the infiltration event is a significant factor in determining the position and shape of the solute peak in the profile. Wierenga (1977), on the other hand, concluded that the use of steady or intermittent leaching had little or no effect on the location of the peak. Wild and Babiker (1976) from a field experiment with four water application treatments also found no significant differences between the mean depths of tracer movement. McLay *et al*. (1991) from a study in soil lysimeters, found that continuous rather than intermittent water application results in efficient leaching.

Solute transport processes in laboratory columns can be different from those in the field where the effects of soil structure and natural macropores may dominate water flow and the solute transport mechanism. Studies conducted *in situ* on the effect of intermittency of water application on solute leaching are very rare. In this study, a field tracer experiment with intermittent water application was conducted and the measured concentration data was fitted to the steady state analytical models. The experiment ran for one month. Water was applied four times, at weekly intervals, using sprinkler irrigation. A comparison was also made between the steady state and intermittent leaching with bromide as an indicator.

In many instances, the leaching of nitrate is the largest cause of nitrogen loss from the soil-plant system (Cameron and Hyanes *et al*., 1986). Nitrate leaching from agricultural soils represents an economic loss to the farmer and acts as a source for polluting groundwater resources. Since nitrogen undergoes complex biochemical transformations in the soil-pant system, it is often difficult to quantify the fraction of N that the crop derives from fertilizer and the fraction that it derives from other sources. It is also difficult to determine the movement and fate of fertilizer N through the soil. Isotopically labelled N fertilizer (using ^{15}N) can be used with a high degree of accuracy to distinguish

between fertilizer N and N from other sources. However, these techniques are very costly (Silvertooth *et al*., 1992). Therefore, anions that are biologically and chemically conserved, similarly charged, and with low background concentrations are often used to simulate the movement of NO_3^--N through the soil profile. Chloride (Cl^-) and bromide (Br^-) ions are the two tracers often used to quantify the mobility of anions such as NO_3^--N in the soil. The Br^- ion is the most commonly used tracer of the two anions (Rice *et al*., 1986; Jaynes *et al*., 1988; Jardin *et al*., 1990; Silvertooth *et al*., 1992; Nachabe *et al*., 1999). The reasons being that Br^- generally has very low background concentrations in soils. In addition, it has no known adverse effects on human health, provided it is applied in small quantities (Flury and Papritz, 1993). Tracer studies can also be used as an independent method to predict the rate of water movement in the vadose zone (Rice *et al*., 1986).

In this thesis, a field experiment was conducted in a Bainsvlei soil of South Africa to evaluate the leaching behaviour of Br^- ions in comparison with that of nitrate under natural rainfall conditions.

Section 4.2 of this Chapter presents the field experiments conducted (*i*) under sprinkler irrigation to study transient bromide movement, and (*ii*) under natural rainfall conditions to compare the movement of bromide and nitrate. The solute transport was modelled and the results analysed and discussed in Section 4.3. Transient state movement of bromide was also compared with its movement under steady state condition discussed in Chapter 3.

4.2 MATERIALS AND METHODS

Two separate experiments were conducted in the field to create transient soil water flux conditions. In the first experiment, water was applied with sprinkler irrigation at weekly intervals for a period of one month. The second experiment ran over seven months to compare Br^- and NO_3^--N transport with natural rainfall being the mode of water application.

In both experiments, the mass of Br^- recovered from a given core sample was calculated using Equations (3.24) and (3.25). The pore-water velocities, the solute peak, and centre of mass velocities were determined using Equations (3.26), (3.27) and (3.29). Solute transport parameters were also determined using the CXTFIT program of Toride *et al*. (1995).

4.2.1 Transient State Bromide Transport with Intermittent Sprinkler Irrigation

This experiment was conducted at the field experimental station of the Department of Soil, Climate and Crop Sciences of the University of the Free State, South Africa. A general description of the experimental site was given in Chapter 2. The details of the procedures for soil water content measurement, soil sampling technique, and bromide analysis were the same as given in Chapter 3. The experiment was conducted from 14 January–14 February 2002. Galvanized sheet metal frame of 200 x 200 x 25 cm was used to isolate a (200 x 200) cm^2 plot area. The metal frame was inserted 15 cm into the soil and 10 cm left above ground to isolate the plot. Water was applied using two sprinklers. Rain gauges were placed at the centre and corners of the plot to record the amount of water applied. The uniformity of distribution of the sprinkler application rate was found to be more than 95 percent. The drainage curve of the soil was determined in a previous experiment (Chapter 2). The soil water status was brought to field capacity before starting the experiment by applying water with the sprinkler. From the drainage curve, it was determined that about 75 mm of water drains from the soil profile in one week when wetted above field capacity. Water was therefore applied four times at the beginning of each week. At the beginning of the experiment (first week), 71 mm of water was applied and at the beginning of the three remaining consecutive weeks 72, 65 and 71 mm of water was applied respectively. Soil sampling was done to depth of 160 cm before each irrigation. The measured bromide concentration data was fitted to analytical models using the CXTFIT program. The depths of bromide concentration peaks of the intermittent leaching experiment were compared with the steady state experimental data presented in Chapter 3.

4.2.2 Bromide and Nitrate Transport under Natural Rainfall

From October 2000 to May 2001, which includes the rainy season of the region, a tracer study field experiment was conducted at the experimental station of the Department of Soil, Climate, and Crop Sciences at the University of the Free State, South Africa. A square plot (245 x 245) cm^2 of bare soil was prepared for the experiment. The plot was kept bare, weed free and without growing any crops. To prevent run-off and erosion from one part of the plot to another, the plot was levelled. In order to prevent surface and shallow subsurface flows into and out of the plot, the plot was isolated from the surrounding area by a galvanized sheet metal. The sheet metal was driven into the soil to a depth of 20 cm, while a 20 cm high section was left protruding above the ground level.

Potassium bromide and potassium nitrate were used as sources of bromide and nitrate ions respectively in the experiment. Potassium bromide was applied at a rate of 200 kg

KBr ha^{-1} (13.5 g Br^{-} m^{-2}). Potassium nitrate was applied at a rate of 145 kg KNO_3 ha^{-1} (20 g N m^{-2}). This is the fertilizer rate commonly used by the farmers in this area. In order to apply the solute evenly, the plot was divided into six subplots of each one square meter. For each subplot 20 g KBr and 145 g KNO_3 were mixed with a 500 ml of distilled deionised water. The solution was applied uniformly with a hand held sprayer on 13 October 2000.

Soil samples were taken five times during the season. The procedures for soil sampling, soil water content measurement, and Br^{-} and nitrate analysis were the same as discussed in Chapter 3. Rainfall was measured using two rain gauges next to the experimental plot. A water sample was taken from a borehole used by the experimental site to determine the NO_3^{-}-N concentration of the groundwater.

Rainfall, evaporation, deep percolation, and change in water content of the soil profile were the major components of the water balance for the experimental plot. Of particular interest to the study was the quantitification of deep percolation, D_p. The deep percolation over a given period can be given as

$$D_p = P - E_v - \Delta S \tag{4.1}$$

where D_p = deep percolation, P = rain, E_v = evaporation, and ΔS = change in storage. The change in storage, ΔS, was calculated from water contents measured with a neutron probe. Evaporation from the bare soil was calculated using Ritchie's equation (Ritchie, 1972), Equation (4. 2). This equation has been studied in the area used for this experiment by Bennie *et al*. (1998). The results of this study indicated that cumulative evaporation from this bare soil is limited more by soil properties than climatic factors. The Ritchie's equation reads as follows

$$E_v = Ct^{1/2} \tag{4.2}$$

where C = 26.35 (θ_i - θ_a), t is time, θ_i is the initial volumetric water content of the top soil and θ_a is the air-dry volumetric water content of the top soil. The coefficient C is experimentally determined for the local Bainsvlei soil (Bennie *et al*., 1998).

Changes in the soil water content of the soil profile over the experimental period were determined using two approaches. The first approach involves calculation of the seasonal change in soil water content as the difference of the soil water contents at the beginning and at the end of the experiment. In the second approach, the total seasonal change in soil water content was calculated as the sum of the differences in soil water contents measured at consecutive sampling events.

4.3 RESULTS AND DISCUSSION

4.3.1 Transient State Bromide Transport

The relevant water balance components of the experimental plot were: water applied, change in storage and the deep percolation. Since the plot was covered with plastic sheeting between irrigations there was no rainfall or evaporation. The variation in soil water contents as measured at different times of the experiment is presented in Figure 4-1. It can be seen from the figure that the fluctuation in soil water content over the one-month period was small. The soil water content was the lowest at the beginning of the experiment and the highest gain in water content was on 23 Jan. During the rest of the experimental period the soil water content stayed between these two limits.

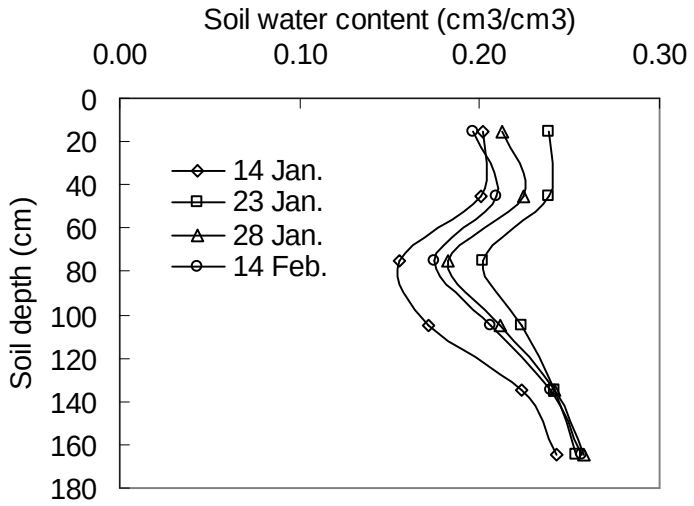

Figure 4-1 Soil water content profiles at different times of the experiment.

The total amount of water applied during the experimental period was 279 mm. The increase in soil profile water storage was 27 mm. The remaining 252 mm of the applied water was drained beyond the maximum soil sampling depth of 160 cm. The cumulative amounts of water that percolated past different depths of the soil profile are presented in Figure 4-2. As can be seen from the figure, water drained similarly at different depths of the soil profile. However, there was a slight decrease in drainage with depth as some amount of the applied water was stored in the soil profile.

The mass of Br^- recovered at different sampling times of the experiment is presented in Table 4-1. Since the Br^- was not leached beyond the maximum sampling depth, the average recovery of 103.2 percent was close to 100 percent.

Table 4-1 Mass of Br^- recovered at different times of the experiment expressed as percentage of the applied mass, Equation (3.25)

Sampling dates	17/01	22/01	23/01	28/01	30/01	4/02	7/02	14/02
Recovery (%)	94.2	108.6	94.5	105.6	96.8	86.7	107.3	132.0

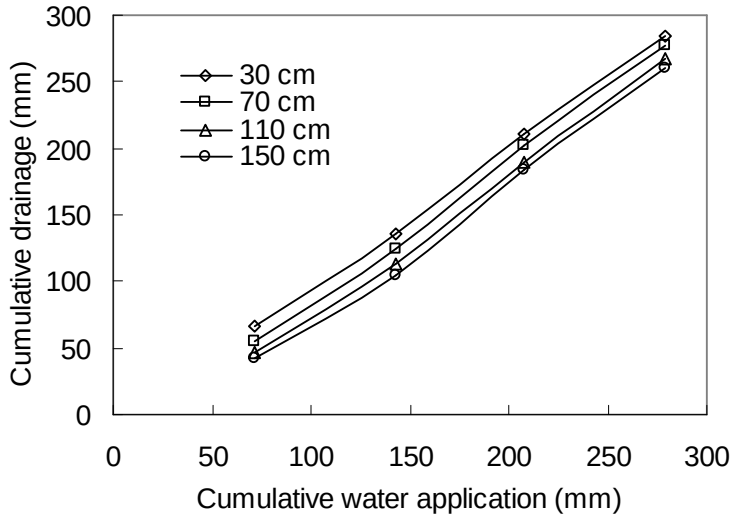

Figure 4-2 Cumulative drainage at different depths of the soil profile after a given amount of water is applied.

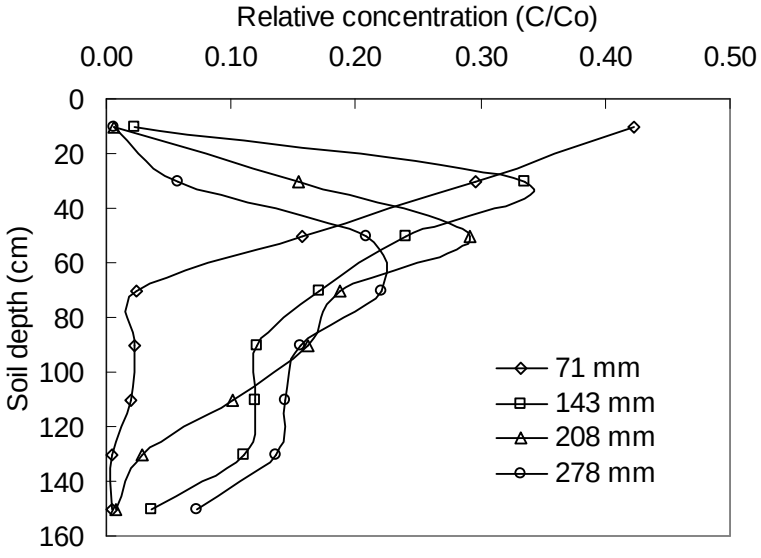

Figure 4-3 Bromide concentration profiles as a function of the amount of water applied.

Figure 4-3 shows the observed bromide concentration profiles after a given cumulative amount of water was applied. It can be seen that the concentration peak was attenuated and the concentration profile became wider with the increase in the amount of water.

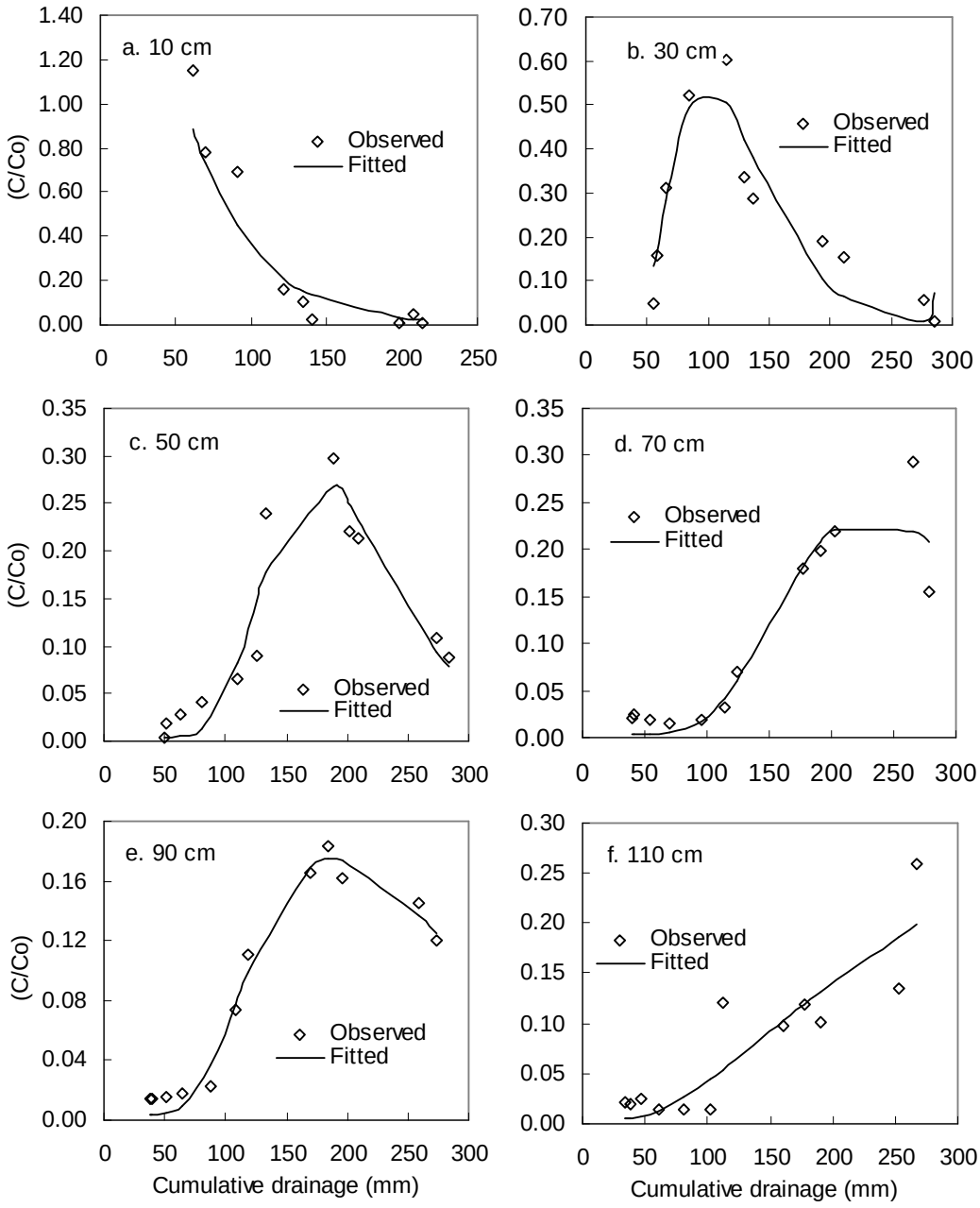

Figure 4-4 Observed and stream tube fitted Br^- concentration breakthrough curves as a function of cumulative drainage.

Figure 4-4 shows the observed relative concentration data and the steady-state stream tube model fitted curves. The breakthrough curves determined using the deterministic

convective-dispersive model were similar to the ones obtained using the stream tube models; hence only the stream tube model graphs were presented here. The breakthrough curve at the 30 cm depth started and ended at the background relative concentration values with a prominent peak at 100 mm cumulative drainage. The breakthrough curves at the 50, 70, 90 and 110 cm depths were open ended especially the one at the 110 cm depth, with prominent peaks occurring after approximately 200 mm of cumulative drainage.

The Br^- transport parameters obtained by fitting the analytical models to the observed Br^- breakthrough concentration data points are presented in Table 4-2. For the convection-disperision transport model, the Br^- transport in cm per cm of cumulative drainage at the different depths indicated in parenthesis, were 1.5 cm (10 cm), 2.7 cm (30 cm), 2.6 cm (50 cm), 2.6 cm (70 cm), 3.9 cm (90 cm), and 1.5 cm (110 cm). For the stream tube model, these velocities were 1.9 cm (10 cm), 2.7cm (30 cm), 2.7 cm (50 cm), 2.8 cm (70 cm), 3.9 cm (90 cm), and 1.0 cm (110 cm) at the depths indicated in parenthesis. The transport parameters presented in Table 4-2 were obtained by using cumulative drainage, instead of time, in the CXTFIT program.

The average velocities of bromide obtained from the CDE and STM were 2.22 and 2.32 cm d^{-1} respectively. The corresponding average dispersion coefficients were 20.67 and 18.02 cm^2 d^{-1}. The coefficients of determination (r^2) were smaller when compared with the ones for the steady state using time as an independent variable (Chapter 3), because of the more irregular shape of the breakthrough curves. The application of a steady-state model for the prediction of transient solute transport seems justified as have been suggested also by Wierenga (1977), Russo *et al*. (1989) and Meyer-Windel *et al*. (1999) among others.

Table 4-2 The deterministic (v, D, α) and stochastic ($<v>$, $<D>$, α) transport parameters determined from the breakthrough curves presented in Figure 4-4 ($\rho_{vD} = 1$)

Soil	Convective-dispersive model				Stream tube model				
depth	V	D	α	r^2	$<v>$	$<D>$	α	σ_v	r^2
(cm)	(cm d^{-1})	(cm^2 d^{-1})	(cm)		(cm d^{-1})	(cm^2 d^{-1})	(cm)		
10	1.38	1.61	1.17	0.815	1.28	1.06	0.83	0.17	0.811
30	2.45	5.14	2.10	0.856	2.47	4.45	1.80	0.13	0.856
50	2.38	5.62	2.36	0.891	2.40	4.87	2.03	0.11	0.891
70	2.36	12.03	5.10	0.914	2.38	11.94	5.02	0.23	0.889
90	3.45	32.80	9.51	0.979	3.46	30.20	8.73	0.12	0.979
110	1.30	66.80	51.38	0.752	1.93	55.60	28.80	0.26	0.743

4.3.2 Comparison of Intermittent vs. Steady State Bromide Transport

In this Section, Br^- transport under steady state conditions presented in Chapter 3 is compared with the transient state results presented in Section 4.3.1. Both data sets were obtained from experiments conducted on the same soil with the plots being only a few meters apart.

The relative concentration of Br^- measured at different depths in the soil profile under the steady and intermittent modes of water application is presented in Table 4-3. For ease of tracking the movement of the Br^-, the concentration peak values are underlined. The Br^- relative concentration peaks are also presented graphically in Figure 4-5 as a function cumulative water applied.

Table 4-3 Bromide movement as a function of cumulative water applied under steady state and intermittent irrigations

Steady state					
Soil	**Water applied (mm)**				
depth	**28**	**57**	**101**	**157**	**215**
(cm)	**Relative concentration (C/Co)**				
10	0.968	0.048	0.035	0.003	0.002
30	0.016	1.059	0.088	0.005	0.005
50	0.004	0.013	1.046	0.264	0.019
70	0.004	0.006	0.115	0.488	0.274
90	0.005	0.004	0.008	0.138	0.289
110	0.004	0.005	0.006	0.006	0.039
130	0.003	0.005	0.006	0.005	0.022
150	0.003	0.004	0.006	0.005	0.005
Total	1.007	1.144	1.310	0.914	0.655
Transient state					
Soil	**Water applied (mm)**				
depth	**71**	**143**	**208**	**279**	
(cm)	**Relative concentration (C/Co)**				
10	0.423	0.023	0.006	0.006	
30	0.296	0.336	0.154	0.057	
50	0.157	0.240	0.292	0.208	
70	0.024	0.170	0.188	0.221	
90	0.022	0.121	0.162	0.156	
110	0.019	0.119	0.101	0.145	
130	0.004	0.111	0.028	0.136	
150	0.005	0.036	0.007	0.073	
Total	0.950	1.156	0.938	1.002	

It is clear from Table 4-3 and Figure 4-5 that less water was required to move Br^- peak to a given depth under continuous water application than under intermittent application. These experimental results demonstrate that for the same amount of water applied, the solute peak moves faster under steady state than under transient soil water conditions. Studies comparing intermittent with continuous leaching have revealed similar results for both non-reactive tracers and herbicides (e.g., Rawitz *et al*. (1980); White *et al*., 1986; McLay *et al*., 1991; Clothier and Green, 1994; Meyer-Windel *et al*., 1999).

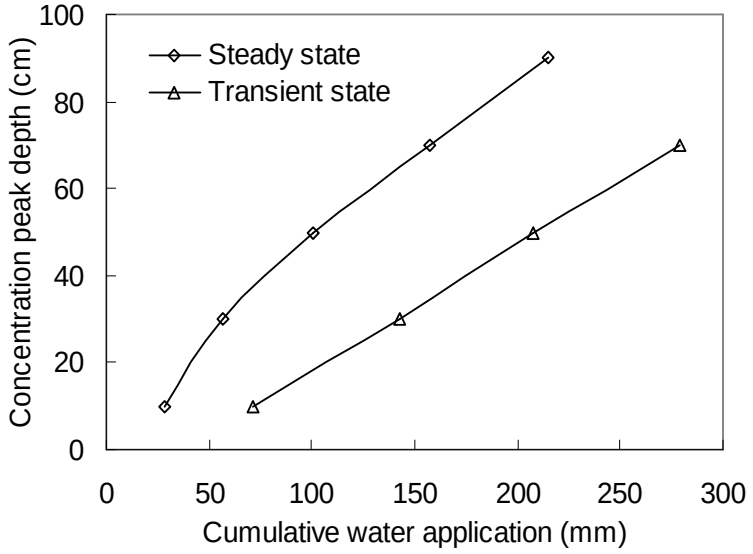

Figure 4-5 Movement of concentration peaks of Br^- as functions of cumulative water applied under steady and intermittent water application conditions.

These different patterns of Br^- movement may be caused by (*i*) differences in water contents, and/or (*ii*) the intermittency of water input. The average soil profile volumetric water content during the steady and the intermittent leaching experiments were 0.259 and 0.224 respectively. The lower soil water content of the intermittent experiment should have resulted in a higher Br^- peak velocity. However, this was not the case. From comparisons made at similar average water contents, Sharma and Taniguchi (1991) showed that the movement of the solute peak is much faster under continuous than under intermittent water application. Therefore the difference in Br^- peak movement between the steady state and intermittent experiments can be ascribed to the intermittency of water application. The intermittency effects observed are probably caused by (*i*) diffusion of solutes into pores with zero flux between drainage events, thus capturing it from leaching during subsequent flow events or (*ii*) hysteresis.

Under intermittent irrigation or rainfall, the periods between rainfall events allow solutes to diffuse into the surrounding aggregates or clusters of micropores along localized concentration gradients. During the next irrigation events, these solutes are protected against immediate leaching and would have to diffuse back into the main convective transport stream through larger pores (Kanchanasut and Scotter, 1982). This hydrodynamic dispersion mechanism retards the transport of solutes through the profile. In contrast, once solutes are present in streams of rapidly flowing solution through macropores under continuous irrigation, there would be limited opportunity for further diffusion into the surrounding aggregates or pores. Jones and Watson (1987) simulated solute concentration profiles numerically for intermittent leaching by including and excluding the effects of soil water hysteresis. According to their simulations, the solute concentration peak moved downward more quickly when the effect of hysteresis is omitted. Wierenga (1977) concluded that the use of steady or intermittent leaching had little or no effect on the location of the peak. However, he did not incorporate the effect of hysteresis in the intermittent leaching simulations.

4.3.3 Bromide and Nitrate Transport under Natural Rainfall

Soil sampling dates and data on the rainfall distribution during the experimental period are presented in Figure 4-6. Total precipitation (574 mm) from October 2000 to May 2001 was higher than the 463 mm average for this period.

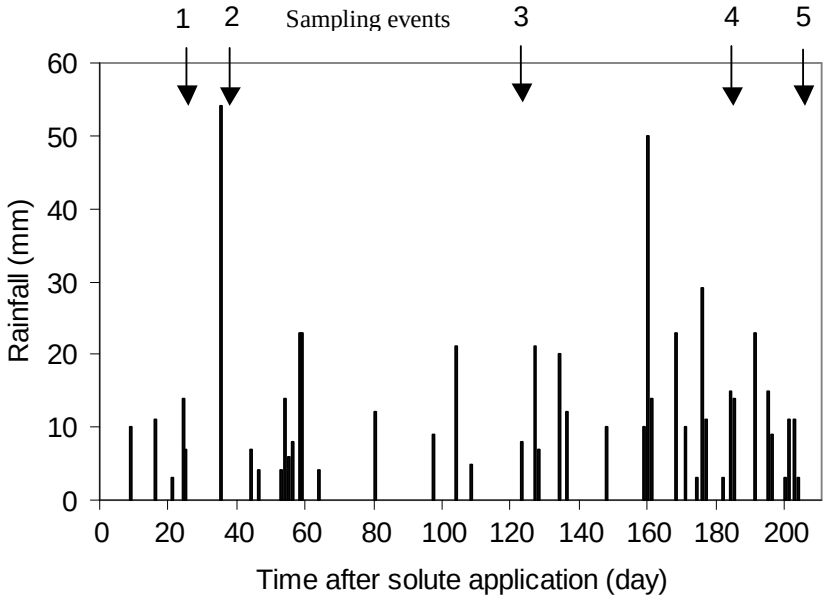

Figure 4-6 Daily rainfall distribution after Br^- and nitrate application.

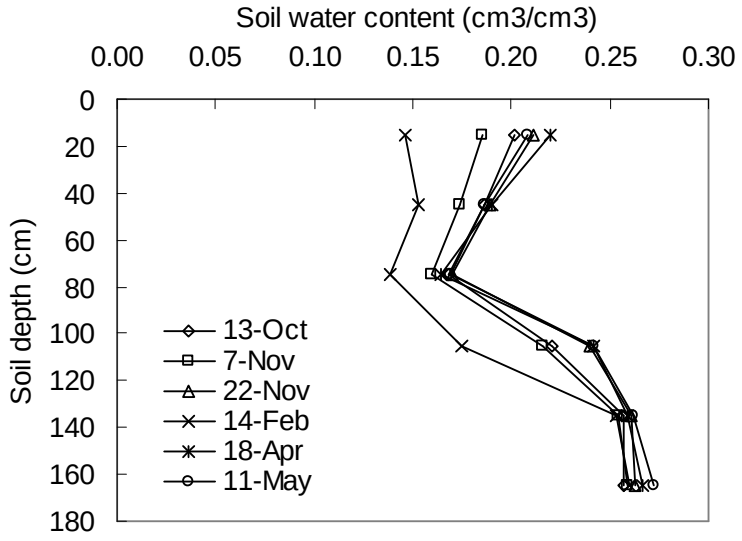

Figure 4-7 Water contents of the soil profile at soil sampling times.

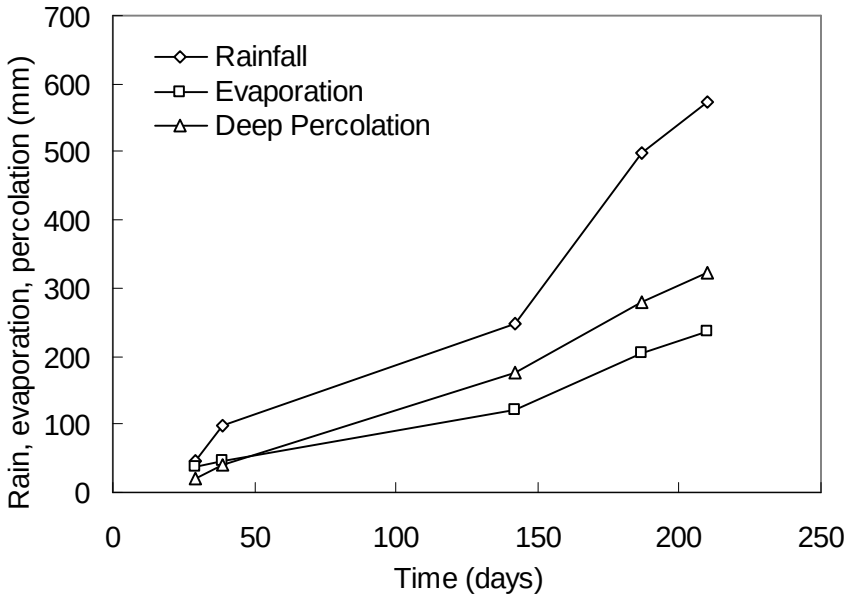

Figure 4-8 Cumulative rainfall, evaporation and deep percolation with time as calculated from a water balance.

Figure 4-7 shows the change in water content of the soil profile through infiltration and deep drainage. Average water content decreased from the surface up to a depth of 75 cm. Between 75 cm and 110 cm it increased steadily, it then remained nearly unchanged between 110 cm and the bottom of the sampling depth (160 cm). Soil water content

increased with depth. Since the hydraulic conductivity of the soil is relatively high, it might be that by the time the soil sample is taken, the infiltrate rainwater already had moved to deeper depths. The slight increase in clay content with might have also contributed to the retention of water at deeper depths. Although the amount of rainfall varied largely from short duration light showers to more than 50 mm d^{-1}, the variation in soil water contents with depth on different sampling dates were rather similar for most samplings. This indicates that the water storage ability at different depths is determined by soil physical properties rather than the amount of rainfall.

The soil water content was low during the 14 February sampling (Figure 4-7). This followed a long sampling interval with drier climatic conditions. From Table 4-4, it can be seen that this period experienced deep percolation losses, coupled with high evaporation and relatively less rain, which resulted in a lower water contents. Cumulative rainfall, estimated evaporation (Equation (4.2)), and deep percolation losses calculated using Equation (4.1) are shown in Figure 4-8.

Table 4-4 Water balance components and pore-water velocity

Day	Date (Interval)	P	E_v	ΔS	D_p	q	θ	v_w
		mm				(mm d^{-1})	(cm^3 cm^{-3})	(cm d^{-1})
29	13/10-11/11 (29)	45	37	-13	21	0.72	0.212	0.34
39	12/11-22/11 (10)	54	9	26	19	1.90	0.215	0.88
124	23/11-14/02 (85)	148	75	-62	135	1.59	0.205	0.78
187	15/02-18/04 (63)	252	83	65	104	1.65	0.206	0.80
210	19/04-11/05 (23)	75	32	-1	44	1.92	0.223	0.86
	Total/*Average*	574	236		323	*1.56*	*0.212*	*0.73*

Note: In Table 4-4, P is rainfall, E_v is evaporation from the soil surface, ΔS is the change in soil water storage, D_p is the deep percolation below the sampling depth (160 cm), q is the drainage flux, θ is the average volumetric water content of the soil profile, v_w is the pore-water velocity of the respective sampling intervals. The volumetric water content was the mean over the sampling interval. The pore-water velocity v_w was calculated as drainage flux divided by the volumetric water content. Negative ΔS values indicate water loss from the profile over that interval.

From the components of the water balance presented in Table 4-4, it can be seen that cumulative deep percolation exceeded cumulative evaporation except for the first two sampling dates. The first two samplings were just after the start of the rainy period. The rainfall during the first sampling period was distributed over the interval as small showers (Figure 4-6), hence evaporation was the dominant process. During the second sampling interval, however, heavier showers (Figure 4-6), including one of more than 50 mm,

resulted in a substantial average deep percolation rate. Although deep percolation exceeded evaporation following the 50 mm d^{-1} rain, the cumulative deep percolation for the entire sampling interval was less than the cumulative evaporation. It can be stated that only major rainfall events resulted in deep percolation and small showers resulted in only wetting the top soil that easily evaporated. Despite the rainfall during the third sampling interval (between 23 November and 14 February), the average deep percolation rate was low and the soil lost much water. This was due to the high evaporation that resulted from the dry and windy climatic conditions of the period (Table 4-4). During the fourth sampling interval (between 15 February and 18 April) rainfall was very high (Table 4-4) which resulted in an increase in deep percolation and soil water storage. During the final sampling interval (between 19 April and 11 May), evaporation was low and the average deep percolation rate was at its highest (Figure 4-8).

The water balance for the entire season showed that about 41 percent of the rainfall was lost through evaporation, 56 percent percolated below a potential root zone of 160 cm, about 3 percent was stored in the soil profile that was already wet when the experiment commenced. In general, it can be seen that the deep percolation exceeded evaporation during the experimental period. This small plot represented a typical flat area (as is the case in most of South Africa) in which runoff is low and much of the water during the rainy season infiltrates the soil surface, a part of it to be stored in the soil and a part of it percolating deep down to recharge the groundwater.

The percentage Br^- and NO_3^--N recovery for the different layers of the soil profile indicated that the distribution of these anions in the soil was strongly influenced by the amount of rainfall (Figure 4-9). Data from the first sampling on 11 November, one month after the KBr and KNO_3 applications, showed that some Br^- and NO_3^--N reached a depth of 100 cm. However, more than 80 percent of these anions were recovered from the top 20 cm layer of the profile (Figure 4-9). Although 45 mm of rainfall was recorded during this period, most of it was in the form of light showers (Figure 4-6), which was mostly lost through evaporation. On the date of the second sampling, 22 November, 65 percent of Br^- and 70 percent of NO_3^--N have moved to the second layer (20-40 cm) and about 17 percent of the NO_3^--N and 20 percent of the Br^- was already in the third layer (40-60 cm) and about the same percentage remained in the top layer (0–20 cm). All the rainfall during this period occurred in one day and downward movement of the chemicals was greatly enhanced. Large differences in depth of translocation and rate of solute movement were noted between the different rainfall amounts and frequencies.

These results indicated that an intense rain shower on a wet soil generates deep percolation, which induces deeper transport of solutes than would be the case if the same

amount of rainfall occurred over a longer period as intermittent moderate/light showers. Moreover, low frequency rains are often accompanied by extensive drying of the soil creating larger soil water deficits, conditions that promote soil infiltration rate.

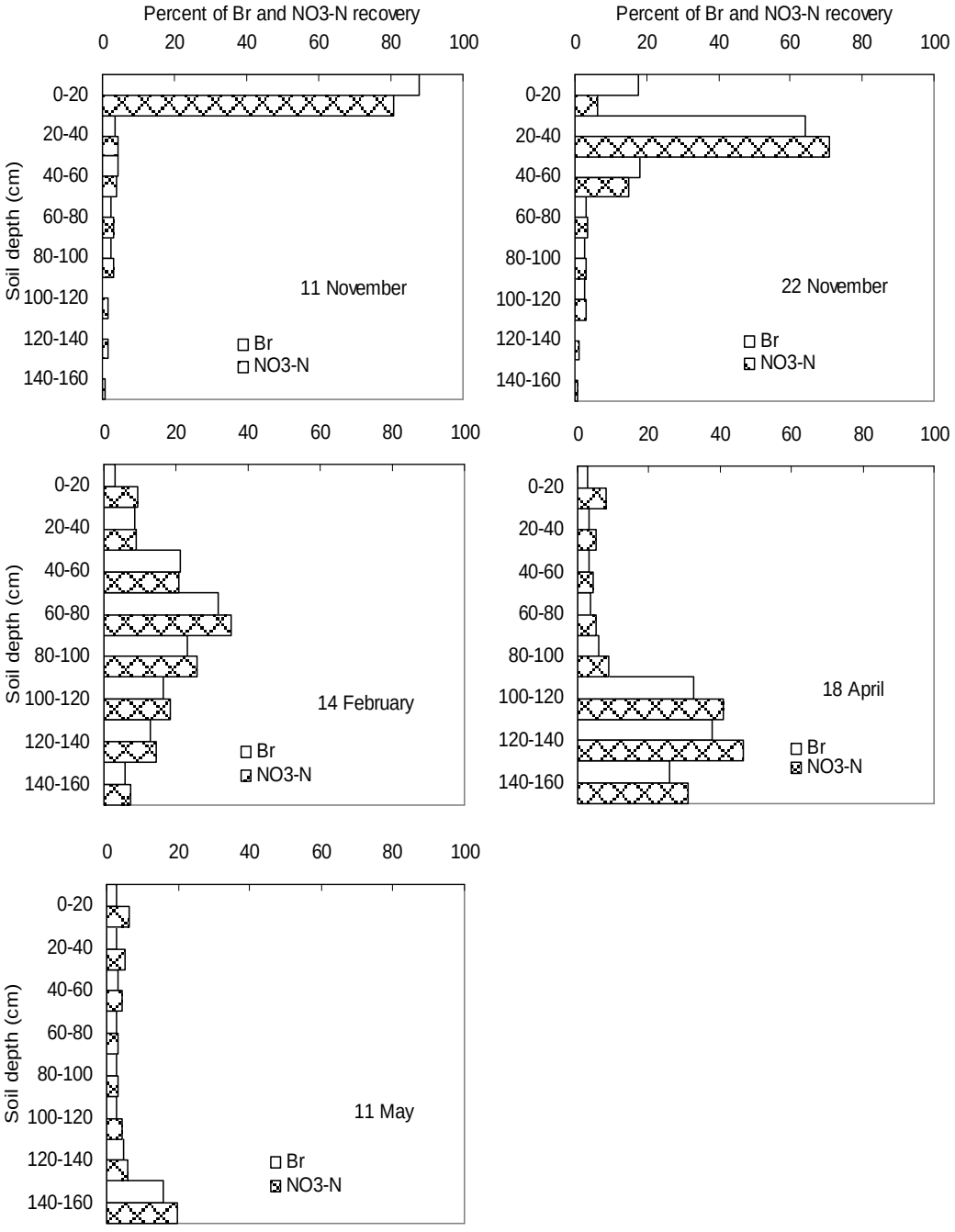

Figure 4-9 Pattern of Br^- and NO_3^--N distribution on different dates after KBr and KNO_3 were applied on 13 October 2000.

No significant deep percolation below the maximum rooting depth was observed during the first sampling events. By the third sampling event and 247 mm rain, a large volume of deep percolation moved past the maximum sampling depth. The concentration peaks of Br^- and NO_3^--N were half-way between the soil surface and the maximum sampling depth of 160 cm and the concentration profile was almost symmetrical (Figure 4-9). About 5 percent of the solutes have then moved below the maximum depth of sampling. By 18 April, almost all the applied Br^- and NO_3^--N was leached below 100 cm depth and a significant amount of these solutes moved past the maximum sampling depth. However, the mass of Br^- and NO_3^--N recovered at that sampling was still high (Table 4-5). On the last date of sampling, 5 May, only about 37 percent of the Br^- and 52 percent of the NO_3^--N remained within the sampled depth of the soil profile. Of this, 20 percent was in the bottom layer (140–160 cm) and the concentration peak reached the maximum sampling depth of 160 cm.

The preceding observations have practical significance for N fertilizer management. Since the maximum rooting depth of most crops grown in this area is limited to the maximum sampling depth used in this experiment, the NO_3^--N not recovered could be taken as leached and not available for crops. From Figure 4-9, it can be observed that the leaching potential of this soil, when wet and uncropped was very high. Leaching is especially serious when a nitrate application is followed by heavy rainfall. A single high rainfall event on these moderately permeable soils can generate a large volume of deep percolation, which in turn result in deeper movement of NO_3^--N the soil profile. While the reduced availability of fertilizer N to plants, due to leaching below the rooting depth, represents an economic loss to the grower, the NO_3^- that moved into deeper layers of the soil profile also pose an environmental threat to groundwater resources. Split application of fertilizer N during the growing season of the crop is recommended to reduce the economic loss of fertilizer and groundwater pollution. The NO_3^--N concentration of groundwater samples from a nearby borehole was found to be 27.96 mg/l. This is higher than the World Health Organization (WHO) limit of 10 mg/l. Since the area is an agricultural area, several NO_3^--N generating activities might be the source of this NO_3^--N contamination of the ground water of which fertilizer is one.

The results of this study suggested that Br^- and NO_3^--N have similar transport properties and patterns in the soil profile. Figure 4-10 depicts the relationship between the concentrations of Br^- and NO_3^--N 124 days after the starting the experiment. The high degree of correlation (r = 0.936) indicates that the two anions exhibit similar transport properties in this soil profile. This correlation coefficient, r, for the samples taken on days 29, 39, 187 and 210 after the start of the experiment was 0.999, 0.955, 0.995 and 0.931,

respectively. This might not be representative of conditions that occur when crops are grown, because when crops are grown, the presence of root competition for available Br^- and NO_3^--N reduces the Br^- and NO_3^--N that is available for leaching. Other processes like mineralization, denitrification, and loss through volatilisation of ammonia can also affect the relationship. However, NO_3^--N losses of as high as 60 percent have been reported in some areas even under cropped conditions (Hong *et al.*, 1992).

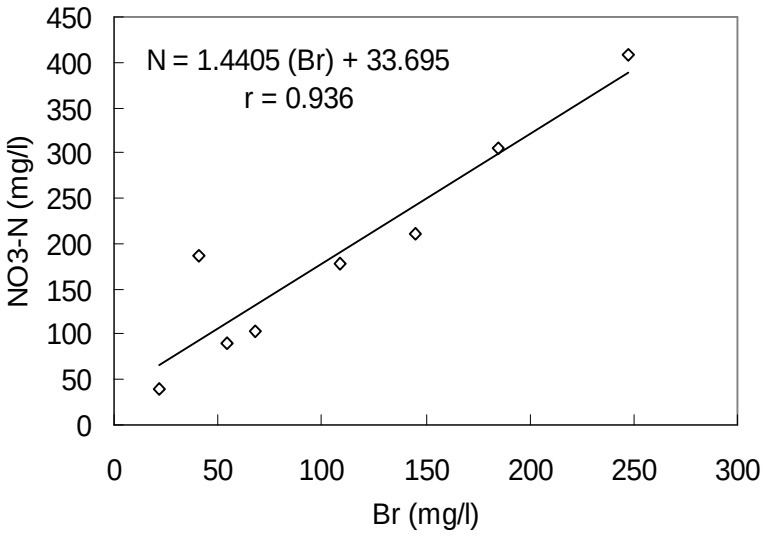

Figure 4-10 Relationship of Br^- and NO_3^--N concentrations in the soil sample taken from different depths 124 days after chemicals application.

The masses of Br^- and NO_3^--N recovered expressed as percentages of the total applied mass of Br^- and NO_3^--N were calculated as $r(\%) = 100m_i/M$, where M = the total mass of Br^- and NO_3^--N applied at the soil surface which were 18.7 mg of Br^- and 27.7 mg ofNO_3^--N for the sampled area of 4.2 cm diameter. The solute mass in the 20 cm long soil core relative to the solute input is given by the ratio of the recovered Br^- or NO_3^--N mass in the core to the applied Br^- mass (18.7 mg) and NO_3^--N mass (27.7 mg). The sum of the recovered masses of Br^- and NO_3^--N from the cores for all the depths expressed as percentages of the amounts applied are presented in Table 4-5.

Table 4-5 Br^- and NO_3^--N percentage masses recovered from soil cores taken at different times, Equation (3-25)

Time (d)		29	39	124	187	210
Recovery (%)	**Br**	99.8	109.0	123.4	114.7	37.6
	NO_3^--N	99.5	104.2	140.7	149.5	52.1

The average recovery was 96.9 percent for Br^- and 109.2 percent for NO_3^--N (Table 4-5). Average recovery of less than or greater than 100 percent might be due to spatial variability of the soil properties, and deep leaching beyond the maximum sampling depth. The background concentrations and the release of organic nitrogen in the soil through mineralization might have caused NO_3^--N recovery in excess of 100 percent. At the day of the last sampling event, significant percentages of the solutes have moved past the maximum depth of sampling, as can be observed from the low percentage of recovery. If this sampling event is excluded, the percentage recoveries were 111.7 percent for Br^- and 123.5 percent for NO_3^--N. The rate at which Br^- and NO_3^--N were moving in the soil profile was determined from the positions of the peak concentration and the centre of mass of the moving plume.

From the water balance data in Table 4-4, deep percolation amounted to 323 mm. For the 210 day duration of the experiment, this gives a mean drainage rate of 1.54 mm d^{-1}. The pore water velocity v_w is the ratio of the drainage flux and the average volumetric water content of 0.212 which gives a mean pore water velocity of 0.73 cm d^{-1}. The pore water velocity also resembles the pore-water velocity in cases where solute transport occurs as piston flow.

The velocity of the concentration peak was determined as a function of the arrival time of the concentration peak of Br^- and NO_3^--N pulse at various depths in the soil profile using Equation (3.27). The result is shown in Table 4-6. The velocity was high for the second sampling interval, that is between 29-39 days after the chemicals were applied to the plot. This observation could be attributed to the single high rainfall event that occurred during this sampling interval. The average concentration peak velocities for both the Br^- and NO_3^--N were 0.93 cm d^{-1}.

Table 4-6 Br^- and NO_3^--N concentration peak velocities determined using Equation (3.27)

Depth, z	Time, t	Difference		Velocity, v_s	v_s/v_w
(cm)	(d)	z_i-z_{i-1} (cm)	t_i-t_{i-1} (d)	(cm d^{-1})	
0	0				
10	29	10	29	0.34	0.47
30	39	20	10	2.00	2.74
70	124	40	85	0.47	0.64
130	187	60	63	0.95	1.30
150	210	20	23	0.87	1.19
			Average	0.93	1.27

The velocities of the solute centre of mass, v_s, determined using Equation (3.29) for the different sampling depths are presented in Table 4-7, where $\overline{z}$ is the depth of the centre of mass of the Br^- and NO_3^--N concentration profiles. The average centre of mass velocities over the whole period were 0.93 cm d^{-1} for Br^- and 0.89 cm d^{-1} for NO_3^--N. Negative values indicate that the solute had already moved beyond the maximum sampling depth at the last sampling date. These negative values were not included in the calculation of the average centre of mass velocities.

Table 4-7 Br^- and NO_3^--N centre-of-mass velocities determined according to Equation (3.29)

	Br^-					NO_3^--N				
Time (d)	29	39	124	187	210	29	39	124	187	210
$\overline{z}$ **(cm)**	15	32	82	117	107	22	40	80	112	98
$\Delta\overline{z}$ **(cm)**		16	50	35	-10		18	40	32	-14
Δt **(d)**		10	85	63	23		10	85	63	23
v_s **(cm d^{-1})**		1.65	0.58	0.56	-0.45		1.80	0.47	0.51	-0.59

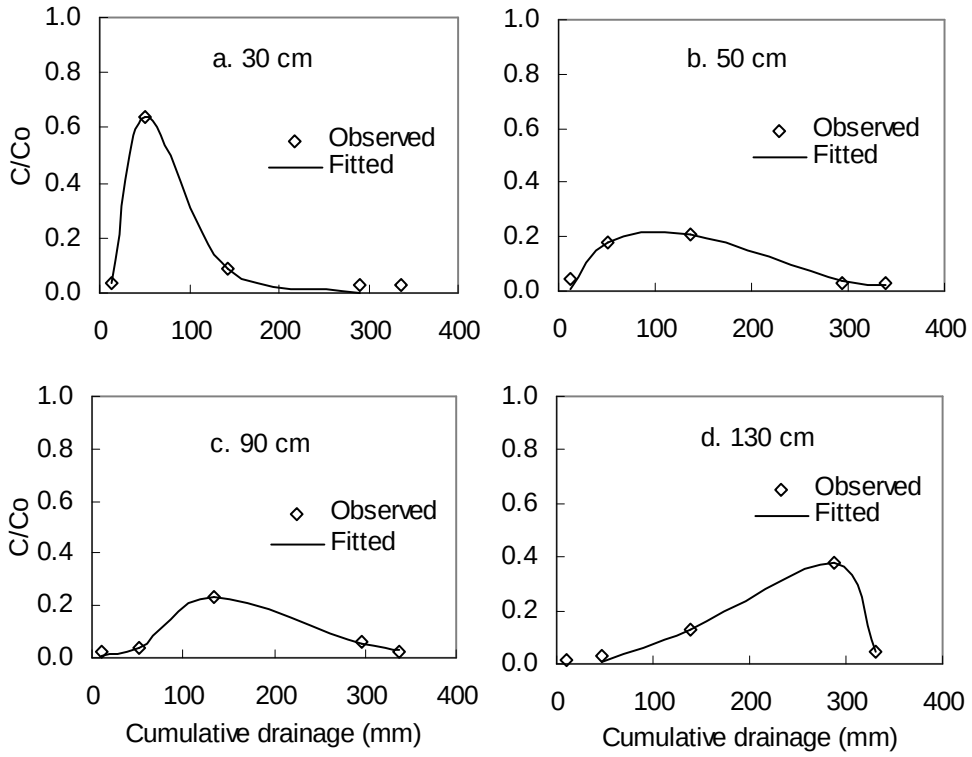

Figure 4-11 Observed and CDE fitted breakthrough curves as a function of the cumulative drainage at different depths of the soil profile.

The observed Br^- concentration profiles were fitted to the convection-dispersive (CDE) and stream tube model (STM) using the CXTFIT program. The analytical solutions of these models as used in the CXTFIT program are based on steady state conditions. Several researchers (Wierenga, 1977; Jury *et al.*, 1982; Sharma and Taniguchi, 1991; Meyer-Windel *et al.*, 1999) have shown that models developed for steady state conditions can be used to model transient conditions when cumulative drainage is used as independent variable instead of time. The concentration data was fitted to both the convective-dispersive and stream tube models. However, not much difference was observed between the results of these models. Therefore, only the fitted curves of the convective-dispersive model were presented in Figure 4-11. It can be observed from the figure that there was much tailing at deeper depths. Considering that (*i*) the experiment was conducted in the field under natural soil and climatic conditions and (*ii*) the drainage was calculated from other soil profile water balance components, the agreement between the observed and model predicted values were very good (high coefficient of determination).

The transport parameters determined with the convective-dispersive model and stochastic stream tube model are presented in Table 4-8. The average pore-water velocity for the CDE was 0.83 cm d^{-1} and for the STM it was 0.81 cm d^{-1}. The pore-water velocity or the pore-water velocity determined from the soil water balance was 0.73 cm d^{-1} (Table 4-4). The Br^- velocities determined from the displacement of concentration peaks and the centres of mass was 0.93 cm d^{-1} (Tables 4-6 and 4-7). The average dispersion coefficients were 9.95 cm^2 d^{-1} and 9.18 cm^2 d^{-1}, according to the convective-dispersive and the stream tube models respectively.

Table 4-8 The deterministic (v, D, α) and stochastic ($\langle v \rangle$, $\langle D \rangle$, α) transport parameters determined from the breakthrough curves given in Figure 4-11 ($\rho_{vD} = 1$)

Soil depth (cm)	Convective-dispersive model				Stream tube model				
	v (cm d^{-1})	D (cm^2 d^{-1})	α (cm)	r^2	$\langle v \rangle$ (cm d^{-1})	$\langle D \rangle$ (cm^2 d^{-1})	α (cm)	σ_v	r^2
30	0.79	4.55	5.76	0.995	0.80	3.24	4.05	0.26	0.995
50	0.65	6.86	10.55	0.954	0.62	6.62	10.67	0.28	0.953
90	0.89	10.48	11.77	0.987	0.85	10.67	12.55	0.46	0.987
130	0.98	17.90	18.3	0.994	0.95	16.20	17.05	0.34	0.994

The average pore-water velocity (determined from water balance, CDE and STM) was 0.79 cm d^{-1}. The ratio between Br^- velocity (v_s = 0.93 cm d^{-1}) and the average pore-water velocity (v_w = 0.79 cm d^{-1}) was used to assess if there was bypass flow during this

experiment. This ratio was found to be 1.18, which indicates 18 percent bypass transport. The solutes moved slightly faster than that would have been expected from the pore-water velocity. Bypass flow is not common in sandy soils. Considering the fact that the experiment was conducted over a season, with drying and wetting, slight preferential flow cannot be ruled out.

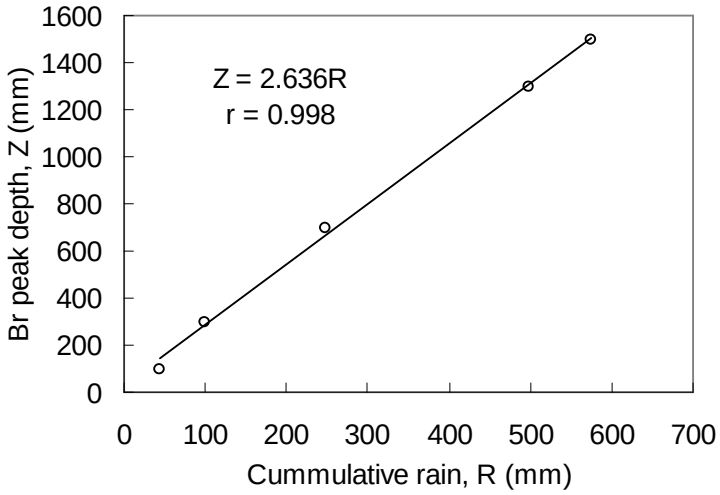

Figure 4-12 Depth of Br^- concentration peak as a function of cumulative rainfall at a mean volumetric soil water content of 0.212.

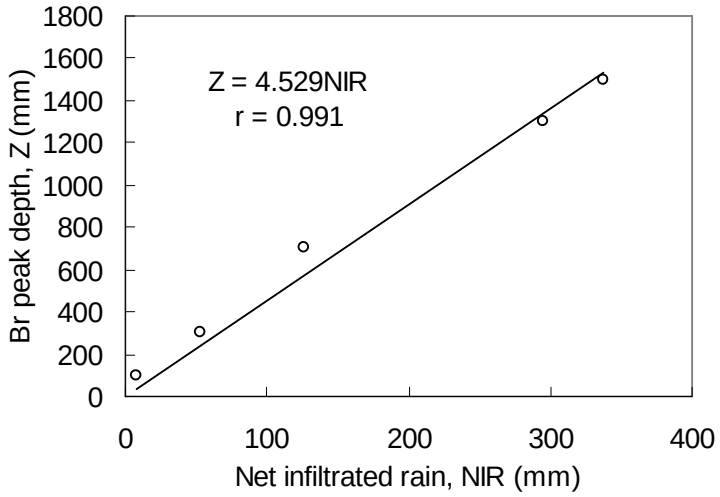

Figure 4-13 Depth of Br^- concentration peak as a function of cumulative net infiltrated rainfall at a mean volumetric soil water content of 0.212.

The depths of the concentration peaks of Br^- and NO_3^--N were plotted against the cumulative rain (Figure 4-12). The concentration peaks move by about 2.64 mm for every

mm of rainfall at an average soil profile volumetric water content of 0.212. Figure 4-13 displays the positions of the peaks as a function of cumulative net infiltrated rain (NIR). The NIR was calculated as the difference between rainfall and evaporation. If the ordinate of this graph were time, the slope of the depth of the peak versus time curve would define a mean solute velocity. In a truly steady-state experiment, the only difference between a graph of the peak depth versus time or versus NIR would be the scale of the ordinate axis. However, as a result of the variations in rainfall and evaporative water flux, transient condition prevails during the experiment. Thus, NIR is a more direct factor than time in governing the transport process. The slope of the fitted straight line in Figure 4-13 is the average transport velocity in terms of the net rain.

4.4 CONCLUSIONS

Two field experiments were conducted to investigate the translocation of Br^- and Br^- plus NO_3^--N respectively, under transient conditions. From the analytical analysis of the data it was found that the CXTFIT steady state models using cumulative drainage beyond a certain depth, instead of time, for simulating transient non-reactive solute transport seems to be justified. This result is of importance for prediction purposes in studies of groundwater pollution, which may require calculations over long periods. Results from this study could be applied to nutrient management in the root zone for agricultural production systems where intermittent conditions, caused by irregularties in the rainfall and irrigation events are dominant throughout the growing season.

Continuous irrigation or rainfall (approaching steady-state flow conditions) did lead to slightly higher nutrient leaching losses than an equivalent amount of irrigation/rainfall which is applied intermittently. Soil nutrients that are located within soil aggregates or clusters of micropores are, however, likely to be less rapidly leached by continuous leaching due to the flow of water mainly through macropores bypassing the intra-aggregate solute.

The reasonable mass recovery estimates obtained, as well as the correlation between Br^- and nitrate measurements, provide assurance of the quality of the data. Bromide and nitrate showed similar transport patterns. The Br^- concentration profile is indicative of potential NO_3^--N movement patterns and presents a worst-case scenario regarding NO_3^--N leaching loss.

Assuming one-dimensional flow and transport and no biochemical processes which could add or remove nitrogen to or from the soil, the experimental results indicated that by the end of the 210 day season, much of the Br^- (63%) and NO_3^--N (50%) was leached below

the 160 cm sampling depth. This indicates that there is a substantial potential for NO_3^--N leaching below the crop rooting depth in the area during wet years in uncropped fallow fields. Therefore, leaching of fertilizer-N during wet seasons could be a serious crop production and environmental constraint on this and similar soils of the area. Shallow rooted crops grown on these soils could be more at risk of facing nitrogen deficiency than deep-rooted crops.

The potential for leaching can be the greatest early in the crop season, when the consumptive use of water and plant uptake of soil nitrate are low and the water contents of soil profiles are minimally depleted. This suggests that it would be advantageous to minimize early or pre-season applications of nitrogen fertilizers and split the application into several smaller ones, throughout the growing season and in response to the needs of a crop.

CHAPTER 5

COMPARISON OF BROMIDE AND NITRATE TRANSPORT UNDER BARE AND CROPPED SOIL CONDITIONS

5.1 INTRODUCTION

In an attempt to ensure food security in the country, the Ethiopian government is promoting high-input agriculture. Fertilizer, in particular nitrogen fertilizer, represents an important component of the input. However, farmers apply fertilizer without even rudimentary preliminary information of the nutrient status of the soil. The application of excessive amounts of nitrogen can enhance the probability of NO_3^--N leaching from the root zone during periods of high rainfall or irrigation. The fact that there were no reported cases of NO_3^--N groundwater pollution in the country does not necessarily imply that the problem was not there. In developing nations, there is lack of research regarding this aspect. In addition, besides its effect on the subsurface environment, NO_3^--N leaching is an economic loss to the farmer. There is no information available that specifically documents and characterizes the downward movement of solutes either on bare or cropped soils in the Dire Dawa area or even in the country as a whole for that matter.

Among the many transformations and transportations that nitrogen experiences in the soil-plant system, leaching frequently represents the greatest loss of NO_3^--N from the system with a significant effect on soil fertility and crop production (Cameron and Hyanes *et al.*, 1986). The leached NO_3^--N can also affect the quality of groundwater and cause *methaemoglobinaemia* (blue baby syndrome) in infants and cancer in adults that drink the water (Menzer, 1991). However, in studying leaching of NO_3^--N, it is often difficult to separate NO_3^--N derived from fertilizer and that derived from other sources. Changes in NO_3^--N concentration caused by nitrification and/or denitrification cannot always be separated from the leaching component without using costly techniques such as fertilizers labelled with ^{15}N (Silvertooth *et al.*, 1992).

Due to the anionic character of NO_3^--N, its movement in the soil is often compared with other conservative anions that are present in minimal background concentrations and similarly charged. Cl^- and Br^- are two such chemically and biologically conservative anions often used to evaluate the anionic mobility of solutes, such as NO_3^--N. As discussed in Chapter 4, Br^- is commonly used in tracer studies for this purpose. Most studies of the solute transport in soils are conducted under continuously flooded conditions on bare soils. Not much is consequently known of solute leaching in the

presence of crops (Iragavarapu *et al*., 1998). According to few studies conducted under cropped conditions, Br^- is readily absorbed by plants, although it is not a required nutrient. For example, Jemison and Fox (1991) found that maize (*Zee mays L.*) can take up as much as 38% of the applied Br^-, while Owens *et al*. (1985) showed that a mixture of orchardgrass (*Dactylis glomertata L.*) and Kentucky bluegrass (*Poa ptatensis L.*) can take up 30% of the applied Br^- (168 kg ha^{-1}). The presence of crops, therefore, can significantly attenuate a Br^- profile in the field.

The objectives of this study were (i) to compare field observed Br^- and NO_3^--N leaching under bare and maize cropped soil conditions and determine the effect of maize crop on leaching, (ii) to characterize spatial and temporal variation of Br^- and NO_3^--N concentration/movement in the soil and plant, (iii) to determine the potential for NO_3^--N leaching under the given climatic and soil conditions and (iv) to compare the deep percolation determined using different methods.

The description of the experimental site, experimental set up and procedures for laboratory analysis are given in Section 5.2. This is followed by the discussion on the soil water balance and deep percolation equations in Section 5.3. The results of the experiment are analysed and discussed in Section 5.4.

5.2 FIELD INVESTIGATIONS

5.2.1 Site Description and Design of Experiments

The sets of experiments to be descried in this chapter were all conducted at the Dire Dawa field experimental farm of the Alemaya University in Eastern Ethiopia from March to May 2001. The farm is located at (9.26^o N, 41.8^o E) with an altitude of 1210 m. The climate of the area is semi-arid with monthly mean minimum and maximum temperatures of 16^oC and 32^oC and a mean annual rainfall of 650 mm with two rainy seasons: July–August and March–May. The soil is sandy loam.

Six plots with areas of (500 x 500) cm^2 each and separated 100 cm from one another, were prepared on uncultivated land. The area was first ploughed to clear it of weeds and grass roots. The plots were levelled to prevent run off, and erosion from one part of the plot to another. The inner (300 x 300) cm^2 area of the plots was isolated from the surrounding soil with galvanized metal sheets inserted to a depth of 20 cm with 20 cm above the soil surface. This helped to prevent lateral subsurface flow from the plots to the surrounding soil and to prevent runoff into and from the plots. Three of the plots were left bare and the other three planted with maize. The bare plots were sprayed with herbicides several times during the season to prevent weed growth. Tensiometers were installed at

depths of 30 cm and 90 cm in all plots. A soil profile was opened near the plots to a depth of 200 cm and soil samples were taken at depth intervals of 20 cm for texture analysis. The particle size distributions of the soil at the different depths were determined with the hydrometer method and the bulk density from core samples with a diameter of 5.0 cm and a length of 5.1 cm taken from the sides of the opened soil profile. The particle size distributions and bulk densities of the soil profile are presented in Table 5-1. Soil samples were also taken to determine the background concentrations of Br^- and NO_3^--N.

Table 5-1 Particle size distribution, textural class and bulk density of the soil profile at the experimental farm of the Alemaya University

Depth (cm)	Soil separates (%)			Textural class (USDA)	Bulk density ($g\ cm^{-3}$)*
	Sand	Silt	Clay		
0-20	70	18	12	Sandy loam	1.37±0.06
20-40	75	13	12	Sandy loam	1.42±0.05
40-60	83	10	7	Loamy sand	1.31±0.03
60-80	74	16	10	Sandy clay loam	1.32±0.04
80-100	56	23	21	Sandy clay loam	1.34±0.07
100-120	52	27	21	Sandy clay loam	1.17±0.04
120-140	54	26	20	Sandy clay loam	1.35±0.19
140-160	53	27	20	Sandy clay loam	1.14±0.09

* Mean of 6 values ± standard deviation

5.2.2 Application of Chemicals and Water

Potassium bromide and calcium ammonium nitrate (CAN) were used as sources of bromide and nitrogen respectively. Potassium bromide was applied at a rate of 200 kg ha^{-1} (135 kg Br ha^{-1}) and the calcium ammonium nitrate at a rate of 800 kg ha^{-1} (224 kg N ha^{-1}). The chemicals were dissolved in water and sprayed onto the plots using perforated buckets on 15 February 2001. Before the start of the actual leaching, 20 mm of water was applied just to wet the top few cm of the soil. This facilitated the conversion of ammonium-N to NO_3^--N before leaching started. On 1 March 2001, an early maturing maize (*Zea mays* L.) variety was planted in rows at a density of 5 plants per square meter. The plots were irrigated frequently to counter the effects that the high temperature and windy conditions at the site had on the maize plants. The water used for this purpose was pumped from a nearby borehole and stored in a reservoir to which a gate valve with metering gauge was attached. A plastic hose fitted with a perforated spraying device to maintain uniform application and minimize erosion and displacement of the chemicals, was used for this purpose.

5.2.3 Sampling and Chemical Analysis of Soil and Plants

Soil samples were taken during the growing season, mostly on a weekly basis, to a maximum depth of 160 cm. An auger type coring tube, 20 cm long and 4.2 cm diameter, was used for soil sampling. The inner (300 x 300) cm^2 of the plots was used for soil sampling. The soil samples were taken at two randomly selected positions in each of the plots during a sampling period. Samples taken from the same depths were mixed to get a composite sample. The core sampler was cleaned with water before re-insertion for the next depth of sampling. Following retrieval of the cores, the resultant holes were backfilled with soil from outside the plot. About 100 g of composite soil sample taken from a given depth was put in paper bags for gravimetric water content determination by drying it for 24 h at 105^0C. The remaining soil sample was put in polyethylene bags for Br^- and NO_3^--N analysis. The procedures described in Chapter 3 were again used to analyse the soil samples for their Br^- and NO_3^--N concentrations.

The amount of Br^- and NO_3^--N taken up by the maize was determined from the above-ground samples of the plants taken at the same time as the soil samples. The number of plants in the inner (300 x 300) cm^2 area of each plot was 46. The plant samples were taken from the area outside the inner (300 x 300) cm^2 of the planted plots to keep the number of plants in the inner area the same throughout the growing season. The sampled plants were shredded, weighed and oven-dried at 70^oC to determine their dry matter content (DM) for subsequent chemical analyses. The leaves, stalks and grain parts of the maize plant samples taken at harvesting were analysed separately. Oven-dried plant samples were ground, passed through a 0.25 mm sieve, and sealed in plastic bags for chemical analysis. Bromide concentration was determined using ion chromatography. One gram of the prepared plant sample was mixed with 50 ml of distilled water and shaken on a laboratory shaker for one hour. The suspension was filtered and analysed for Br^- concentration. Nitrogen content of the plant material was determined using the Kjeldahl Method.

The dry mass of the plants taken for bromide and nitrogen analysis was multiplied by 46 to obtain the total dry matter mass of the plants on a given plot, which was then converted to a per-hectare basis. The mass of bromide and nitrogen taken up was calculated using the plant dry matter and the respective concentration of the anions.

5.3 DATA ANALYSIS

5.3.1 Soil Water Balance

The percolation of water beyond the root zone, also referred to as deep percolation rate, is

often estimated with the soil profile water balance relation, which assumes in the case of bare soil the form

$$R_r = P + I - E_V - \Delta S \tag{5.1a}$$

and for soils planted with crops

$$R_r = P + I - E_T - \Delta S \tag{5.1b}$$

where R_r = deep percolation, P = rainfall, I = irrigation, ΔS = change in storage, E_V = evaporation, E_T = evapotranspiration.

Evaporation of water from bare soil is controlled by the energy available at the surface and by the ability of the soil to conduct water to the surface. When the soil surface is wet (after rainfall or irrigation), evaporation proceeds at a potential or energy-limiting rate EV_p and when visibly dried by the soil-limiting rate EV_s. Potential evaporation or the energy-limiting evaporation rate was calculated with the equation proposed by Priestley and Taylor (1972).

$$EV_p = a\left(R_n\right)s/\left(s+\gamma\right) \tag{5.2}$$

and the soil-limiting or actual evaporation rate from the bare plots from the equation of Ritchie (1972).

$$EV_s = C\,t^{-1/2} \tag{5.3}$$

where R_n is the net radiation, s the derivative of the saturated vapour pressure-temperature relation, γ the psychrometric constant, a a constant (= 1.37 ± 0.08) t the time (in days from the start of the soil limiting phase) and C a temperature dependent coefficient given by (Jackson *et al.*, 1976) as

$$C = 1.27 + 0.034T + 0.0009T^2$$

with T the temperature (°C). Evapotranspiration was determined with the well-known Modified Penman-Monteith Equation, as described by Allen *et al.* (1998). Since the soil surface was usually dry on the day following irrigation, the soil-limiting phase of evaporation was assumed to start on this day. The change in soil water storage over a given time interval was determined from the soil water content data at the beginning and end of the sampling interval.

The climatic and meteorological parameters needed for the calculations (rainfall, temperature, relative humidity, wind speed and sunshine hour) were obtained from the

weather station at Dire Dawa Airport near the experimental site.

Another approach to compute the deep percolation is to use conservative tracers (such as Br), which appears to provide more robust estimates of the percolation in arid regions, because of the small fluxes involved (Gee and Hillel, 1988). This approach is based on the observation that the percolation rate at a given depth, *z*, must be equal to the flux of water at that depth, *q*, which is related to the pore-water velocity of the water through Equation (3.26). If one therefore assumes that the pore-water velocity in the soil column is constant, the deep percolation rate at the depth *z* can be expressed as

$$R_{cv}(z) = v\theta(z) = (z/t)\theta(z) \tag{5.4}$$

where $\theta(z)$ is the volumetric water content at the depth *z* and *t* the time that it will take the water, or a conservative tracer, to move from the soil surface to the depth *z*. If one therefore knows the water content at the depth *z* and the time at which a particle of water or solute arrives at *z*, Equation (5.4) can be used to estimate the percolation rate at *z*. The opposite is of course also true, i.e., one can use the inverse of Equation (5.4)

$$t(z) = [z\,\theta(z)]/R_{cv}(z) \tag{5.5}$$

to determine the time it will take the particle to reach a given depth *z*.

There is reason to believe that Equation (5.4) may yield reasonable estimates for the deep percolation rate in the case of bare soils, but that it will completely overestimate the rate in soils covered with plants, where the velocity is controlled by the root zone density and the distribution of the roots and therefore not a constant. Indeed, one would expect the downward flux, $q(z)$, across the root zone to vary from a maximum at the soil surface to a minimum at the bottom of the root zone, i.e.,

$$P + I \geq q(z) \geq R_r \tag{5.6}$$

This applies in particular to arid and semi-arid conditions, (P < 300 mm y^{-1}) where $q(z)$ can vary from two to four orders of magnitude across the active root zone (Tyler and Walker, 1994).

To derive a more realistic estimate for the deep percolation consider again a homogenous soil profile subjected to a constant flux of water, ($P + I$) at the soil surface and a constant downward flux, R_r, at the bottom of the root zone at $z = z_r$. Let $q_r(z)$ represents the rate at which water is lost from the profile through withdrawal by plant roots, evaporation and soil storage as a function of *z* and *R* the percolation rate at that depth. The cumulative loss of water from the profile over a depth *z* can then be expressed as

$$E_L = E_T(z) + \Delta S(z) = \int_0^z q_r(z)dz \equiv P + I - R(z) \tag{5.7}$$

and that over the root zone as

$$E_{Lr} = E_T + \Delta S = \int_0^{z_r} q_r(z)dz \equiv P + I - R_r$$

and the pore-water velocity of the water at the depth z can then be expressed through Equation (5.7) as

$$\begin{aligned} v(z) &= \frac{R}{\theta(z)} = \frac{P+I}{\theta(z)} - \frac{1}{\theta(z)}\int_0^z q_r(z)dz \qquad (0 < z \le z_r) \\ v(z) &= \frac{R_r}{\theta(z)} \qquad\qquad (z > z_r) \end{aligned} \tag{5.8}$$

which can be used to determine the time it will take the water to reach a depth z, provided $q_r(z)$ is known. This time

$$t(z) = \int_0^z [(P + I - 1)\int_0^z q_r(z)dz]^{-1}\theta(z)dz \tag{5.9}$$

will also be the time it will take a conservative tracer to travel to the depth z and is therefore also known as the travel time of such a solute.

A simple application of Equation (5.8) arises in the case of uniform root water extraction. This is the case when $\Delta S(z)$ and $R(z)$ are constant with $R(z) = R_r$, in which case the root extraction function, $q_r(z)$, can be expressed as

$$q_r = \frac{P + I - R_r}{z_r} = \frac{A_r - R_r}{z_r} = \frac{Q_r}{z_r} \tag{5.10}$$

A more realistic model of root extraction is the exponential function given by Raats (1974)

$$\begin{aligned} q_r(z) &= q_m \exp(-\eta z / z_r) \quad (0 < z \le z_r) \\ q_r(z) &= 0 \qquad\qquad\qquad\quad (z > z_r) \end{aligned} \tag{5.11}$$

where q_m is a parameter that theoretically presents the value of $q_r(z)$ at the soil surface (z = 0) and η a constant (Tyler and Walker, 1994). A large value of η implies that root extraction and evaporation rates occur near the soil surface, while a small value of implies that the extraction rate approaches the uniform extraction rate. The parameter η is likely to be large for most arid and semiarid regions, because of the high density of shallow roots and the high rates of evapotranspiration in these regions.

The most natural way to determine q_m and η will be to derive them from field observations. However, this can be a formidable task. The following discussion will therefore be limited to the case where the extraction of water over the root zone given by Equation (5.11) is equal to that given by Equation (5.10), which implies that

$$q_m = \frac{\eta Q_r}{z_r (1 - e^{-\eta})} \tag{5.12}$$

An interesting application of Equations (5.10) and (5.11) is to derive the travel times associated with the two extraction models from Equation (5.9). If it is assumed that $\theta(z)$ is a constant, θ, say, the travel time for the uniform extraction rate in Equation (5.10) can be expressed as

$$t(z) = -\frac{z_r \theta}{Q_r}\left[\ln\left(1 - \frac{zQ_r}{A_r z_r}\right)\right] \quad (A_r = P + I) \tag{5.13}$$

and for the exponential extraction rate in Equation (5.10) as

$$t(z) = B(z_r, \eta, A_r, R_r, \theta)\ln[F(z, z_r, \eta, A_r, Q_r)]$$

$$B(z_r, \eta, A_r, R_r, \theta) = \frac{z_r [\exp(\eta) - 1]\theta}{\eta [R_r \exp(\eta) - A_r]} \tag{5.14}$$

$$F(z, z_r, \eta, A_r, Q_r) = \frac{A_r \exp(\eta z / z_r)[\exp(\eta) - 1] + Q_r \exp(\eta)[1 - \exp(\eta z / z_r)]}{A_r [\exp(\eta) - 1]}$$

which reduce to the expression for uniform extraction in the case where $\eta \to 0$. It is important to note that this equation assumes an exponential decrease of the rate of uptake with depth, similar to the equations of Raats (1974).

The deep percolation estimated using the observed Br^- travel times and travel times determined using the uniform and exponential root extraction models (Equations (5.13 and 5.14)) was compared with the deep percolation determined from the water balance (actual deep percolation). After calculating the travel time, t_a using Equations (5.13 and 5.14), the deep percolation was estimated using the constant velocity model, Equation (5.4). The relative error, *RE*, between the actual deep percolation and that calculated using Equation (5.4) is given by

$$RE = \frac{\hat{R}}{R} = \frac{z(t)\theta}{t_a R} \tag{5.15}$$

where R is the actual deep percolation rate obtained from the water balance and used to

calculate the travel times and $\hat{R}$ is the estimated deep percolation from Equation (5.4) using the travel times calculated using Equations (5.13) and (5.14).

5.3.2 Bromide Mass Balance

One of the approaches to determine the deep percolation of water is using tracer mass balance method (Allison and Hughes, 1978). In this study, it was assumed that the only source of Br^- would be the applied KBr solution at the beginning of the experiment. Therefore, on average the flux of Br^- through the soil surface is equal to the flux of Br^- beneath the root zone, thus

$$(P + I)C_{p+i} = RC_r \tag{5.16}$$

where ($P + I = A_r$) is the rainfall plus irrigation flux at the soil surface with a Br^- concentration C_{p+i} and R is the deep percolation rate with Br^- concentration of C_r.

5.3.3 Water and Solute Movement in the Soil

The pore-water velocity was determined from the deep percolation rate and the soil water content using Equation (3.26). The Br^- concentration profiles at different times of the growing season were fitted to the CDE model to determine the transport parameters: the pore-water velocity and dispersion coefficient. The actual convection rate of the solutes was determined from the velocity of the concentration peak, Equation (3.27) and the velocity of the centre of mass, Equation (3.29). The average pore-water velocities were compared with the actual Br^- and NO_3^--N velocities to see if there is any bypass flow. Each plot was analysed separately and the average value was taken to describe the transport under a given treatment.

5.4 RESULTS AND DISCUSSION

5.4.1 Soil Water Balance

The total rainfall during the experimental period (March to May 2001) was 203 mm, which was lower than the 20-year (1979-1998) normal of 269 mm for this period at Dire Dawa. As the rainfall was not sufficient to grow the maize, the experimental plots had to be irrigated. The irrigation of both the bare and maize plots was reduced after a high rainfall event during the second sampling interval, but was afterwards increased steadily for the maize plots until the crop entered its final growth stage, when the rate was reduced again.

The average water balances over the 100 cm depth root zone for the bare and maize plots

are summarized in Tables 5-2 and 5-3. Negative values for the change in storage imply that the soil water content at the end of the interval was lower than at the beginning of the interval. The cumulative water balance components are also presented in Figure 5-1 as a function of days after the plating of the maize crop.

Table 5-2 Average values of the water balance components of the soil profiles for the bare plots at different days after planting (DAP)

Time interval	DAP	P	I	E_v	ΔS	R_r	$\sum R_r$
				mm			
1 Mar-13 Mar	13	7.4	70.0	41.0	30.8	5.6	5.6
14 Mar-23 Mar	23	84.4	55.0	38.0	59.4	42.0	47.6
24 Mar-2 Apr	33	33.2	0.0	34.3	-16.0	14.9	62.5
3 Apr-10 Apr	41	4.4	35.0	26.9	5.2	7.3	69.8
11 Apr-18 Apr	49	9.9	35.0	32.3	6.6	6.0	75.8
19 Apr-26 Apr	57	13.7	35.0	22.8	12.8	13.1	88.9
27 Apr-3 May	64	3.9	35.0	31.5	5.6	1.8	90.7
4 May-10 May	71	28.1	30.0	26.2	14.9	17.0	107.7
11 May-17 May	78	17.3	40.0	27.9	13.7	15.7	123.4
18 May-24 May	85	0.2	50.0	28.1	10.0	12.1	135.5
25 May-7 Jun	98	0.1	50.0	39.8	4.9	5.4	140.9
	Total	202.6	435.0	348.8	147.9		

Table 5-3 Water balance components for the maize plots at different days after planting (DAP)

Time interval	DAP	P	I	E_T	ΔS	R_r	$\sum R_r$
				mm			
1 Mar-13 Mar	13	7.4	70.0	41.4	32.3	4.0	4.0
14 Mar-23 Mar	23	84.4	55.0	38.8	55.2	45.4	49.4
24 Mar-2 Mar	33	33.2	0.0	43.7	-18.3	7.8	57.2
3 Apr-10 Apr	41	4.4	34.0	35.7	1.2	1.5	58.7
11 Apr-18 Apr	49	9.9	48.0	38.5	7.0	12.4	71.1
19 Apr-26 Apr	57	13.7	62.0	40.3	7.9	27.5	98.6
27 Apr-3 May	64	3.9	64.0	41.8	18.7	7.4	106.0
4 May-10 May	71	28.1	65.0	38.3	23.8	31.0	137.0
11 May-17 May	78	17.3	52.0	41.6	-13.3	41.0	178.0
18 May-24 May	85	0.2	60.0	34.8	7.9	17.5	195.5
25 May-7 Jun	98	0.1	55.0	42.6	5.7	6.8	202.3
	Total	202.6	565.0	437.5	128.1		

As shown by these tables and Figures 5-2 and 5-3, the soil profiles of the bare plots retained more water than the profiles of the maize plots. This was most likely due to the higher evapotranspiration losses from the maize plots compared to the evaporation losses

from the bare plots. However, the cumulative deep percolation below the effective root zone (100 cm) of the maize plots was higher than that below the bare plots (22% of the water applied in the case of the bare plots and 27% in the case of the maize plots). The higher volume of irrigation water applied to the maize plots therefore caused a higher rate of deep percolation. In addition to the hot and windy climatic condition, the light irrigation might have contributed to the higher evaporation/evapotranspiration compared with the deep percolation component.

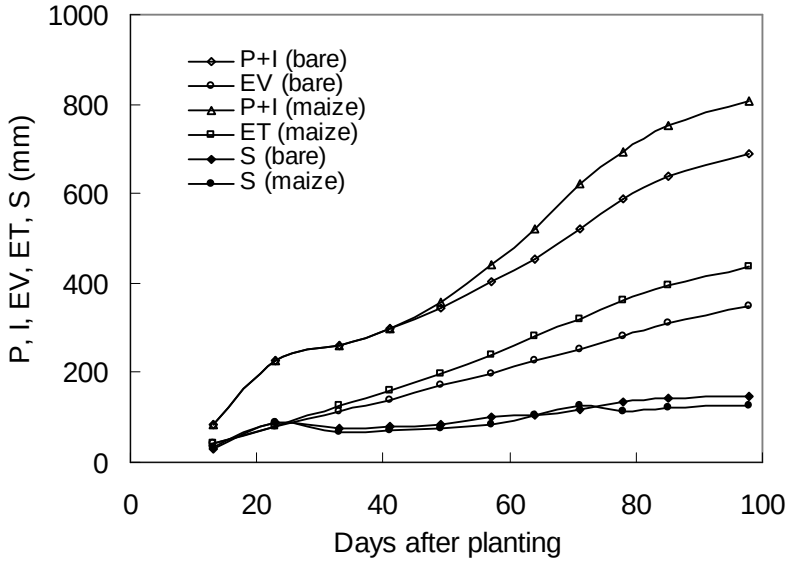

Figure 5-1 Cumulative rainfall (P), irrigation (I), evaporation (E_V) and evapotranspiration (E_T) and soil water storage (S) of the bare and maize plots.

The soil water content profiles for the bare and maize plots at different times of the growing season are presented in Figures 5-2 and 5-3 respectively. In the root zone (up to 100 cm), the soil water content for the bare plots was higher than that of the maize plots. This means that the evapotranspiration rate from the maize crop was higher than the evaporation rate from the bare plots over the root zone. However, the water content of the maize plots was higher than that of the bare plots below the root zone, because more water was applied to the maize plots than to the bare plots. The high soil water content observed on the 23rd of March was due to the high rainfall during this period. It is interesting to note that the maximum soil water content of the bare plots occurred at a depth of approximately 90 cm for all sampling periods except the first one, but that the maxima for the maize plots occurred at depths that varied from 90 cm to 130 cm.

The behaviour of the soil water content in the maize plots was probably caused by the fact that irrigation water was applied at small volumes at short time intervals, which limited the maize roots to the upper 100 cm of the soil, since maize roots can penetrate as deep as 200 cm (Allen *et al*., 1998).

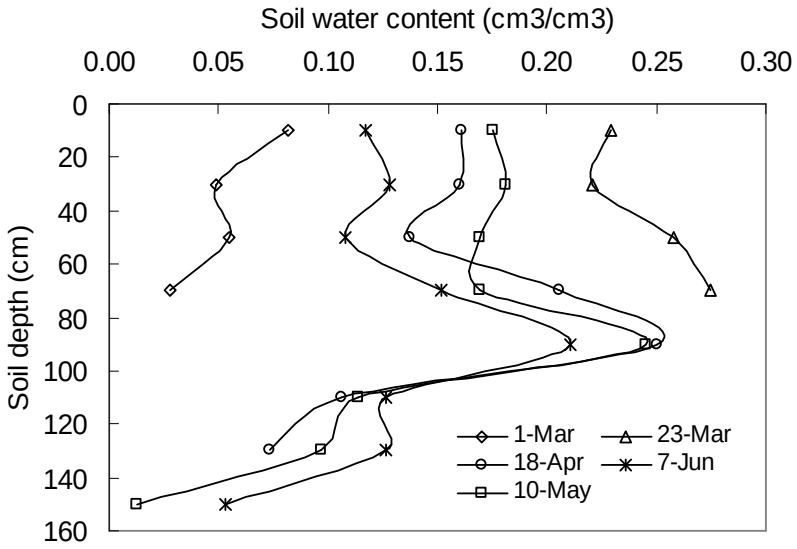

Figure 5-2 Soil profile water content of bare plots at different times of the experimental period.

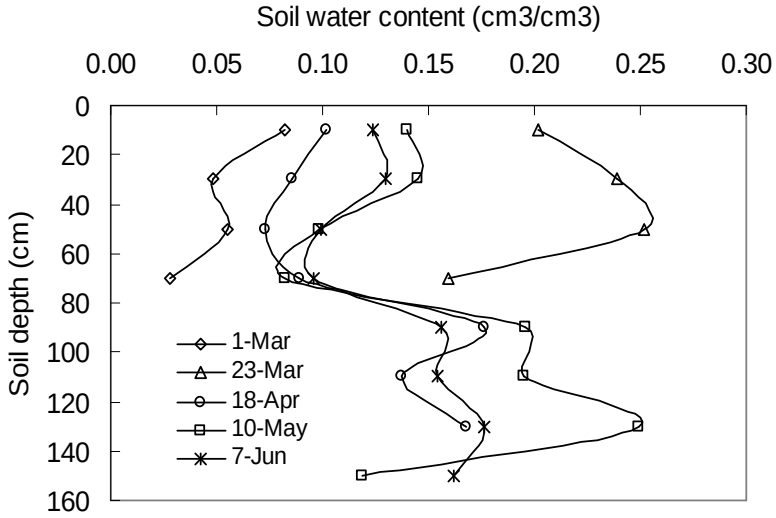

Figure 5-3 Soil profile water content of maize plots at different times of the experimental period.

The soil water suction heads observed with the tensiometers installed at depths of 30 cm and 90 cm for the bare and maize plots are presented in Figure 5-4. As shown in these graphs, the suction heads in the bare plots were lower than that of the maize plots. The suction head at 30 cm remained approximately the same throughout the experimental period in the bare plots. The suction heads at the other depths all increased sharply approximately 50 days after planting the maize. At this time, the suction head in the maize plots at 30 cm increased considerably and even approached that at a depth of 90 cm, which is an indication that the maize experienced a water stress at the time. The increase in irrigation rate after this period clearly alleviated the water stress considerably. The hydraulic gradients between the two tensiometers in Table 5-4, nevertheless shows that there was no upward flux of water between the two tensiometers during the experiment and that the hydraulic gradient between the tensiometers in the maize plots was always higher than that of the bare plots.

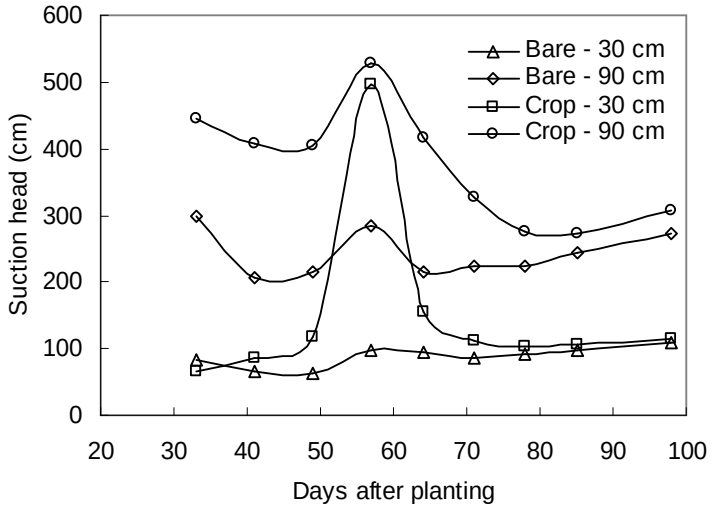

Figure 5-4 Soil water suction heads at different times of the season.

Table 5-4 Hydraulic gradients between the tensiometers at 30 and 90 cm depths during different time intervals

Plots	Time interval (day/month)								
	24/3-2/4	3/4-10/4	11/4-18/4	19/4-26/4	27/4-3/5	4/5-10/5	11/5-17/5	18/5-24/5	25/5-7/6
	Hydraulic gradient								
Bare	1.36	1.24	1.26	1.31	1.20	1.23	1.22	1.24	1.27
Maize	1.64	1.54	1.48	1.05	1.44	1.36	1.29	1.28	1.32

5.4.2 Bromide and Nitrate Concentrations

The change in Br^- concentration in the soil profile of the bare and maize plots at selected times during the growing season is presented in Figures 5-5 and 5-6. The quantity of water applied (rain plus irrigation) during the experiment, 637.6 mm and 767.6 mm for the bare and maize plots respectively, were higher than the mean annual rainfall of 650 mm. The Br^- peak, nevertheless, was not leached out of the 160 cm depth, but progressed to 90 cm and 130 cm on the bare and maize plots at the end of the experiment. From Figures 5-5 and 5-6, it can be seen that the depths of the centres of mass of the bromide concentration profiles depend on the time during the growing season, i.e. closer to the soil surface during the early stages of the growing season, and deeper in the profile later.

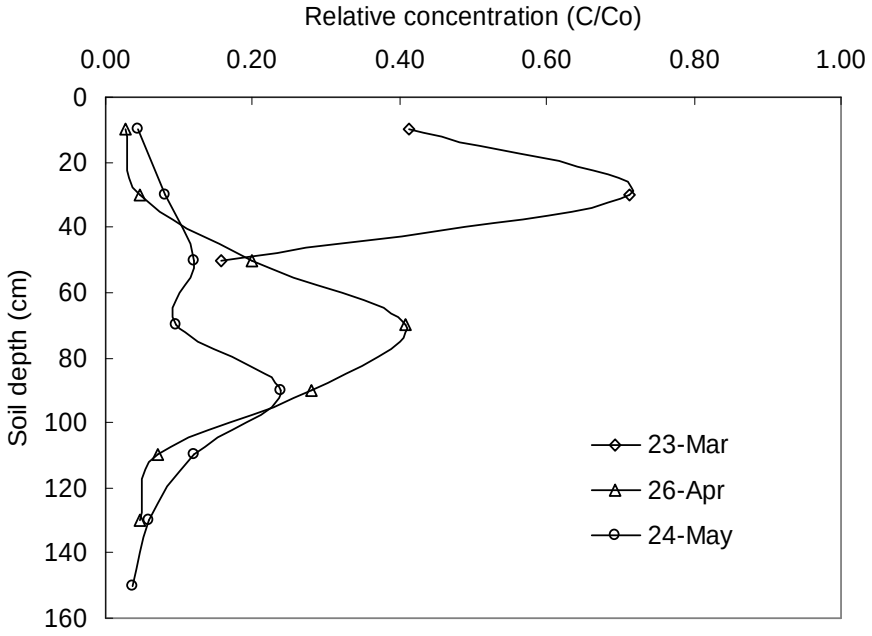

Figure 5-5 Change in Br concentration with depth during the season for the bare plots.

Nitrates in soils and groundwater can originate from a number of sources such as geological origin, precipitation, animal wastes, mineralisation of organic-N and fertilization. While NO_3^--Ns are probably leached from most geological formations, it is not unusual for relatively large amounts of plant-available N to be present in the soil below minor vegetation such as grass (Paltineanu *et al.*, 1980). Such resident nutrients will only be leached slowly from the top eluvial horizon and then accumulate in the lower illuvial horizon, especially under the semiarid conditions at the test site. This phenomenon was most likely responsible for the gradual increase in the NO_3^--N in the concentration profiles of the bare and maize plots during the growing season as presented in Figures 5-7 and 5-8 respectively. Because the maximum sampling depth was

progressively increased during the season. This accumulation of residual NO_3^--N with depth made it difficult to follow the downward movement of the peak of applied NO_3^--N.

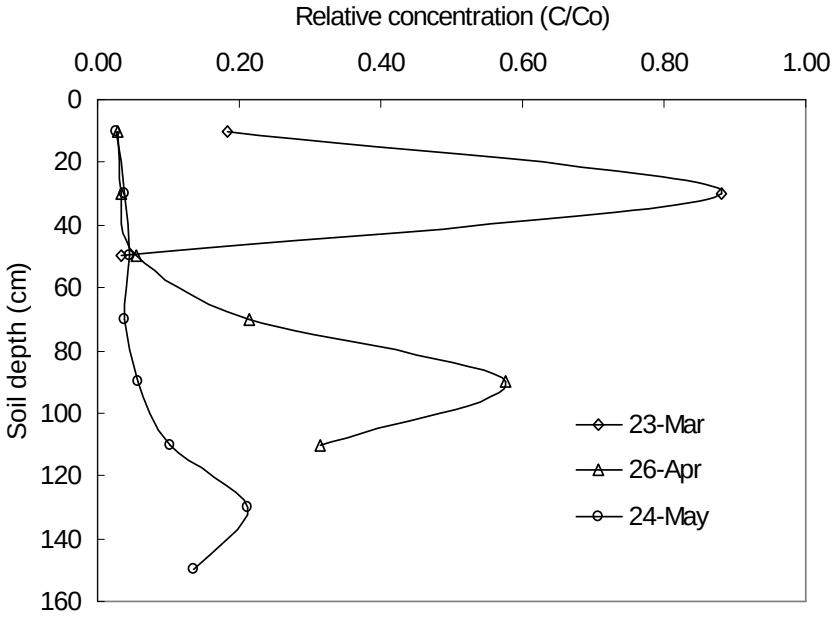

Figure 5-6 Change in Br concentration with depth during the season for maize plots.

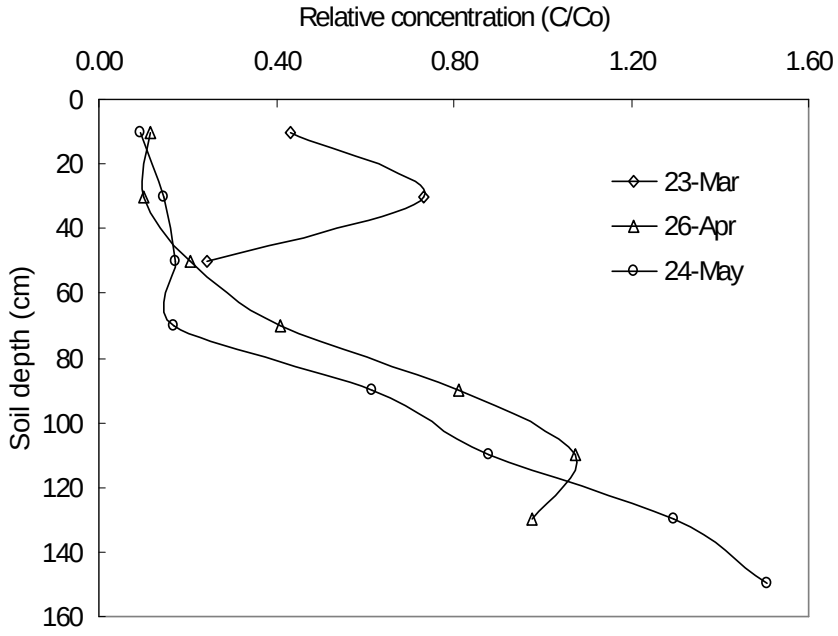

Figure 5-7 Change in NO_3^--N concentration with depth during the growing season for the bare plots.

An interesting feature of the NO_3^--N profiles in Figures 5-7 and 5-8 is that the concentration of NO_3^--N in the soil profiles of the bare plots was higher than that in the soil profiles of the maize plots and that the difference increased with depth. The concentration profiles in Figure 5-9 illustrates this behaviour more vividly.

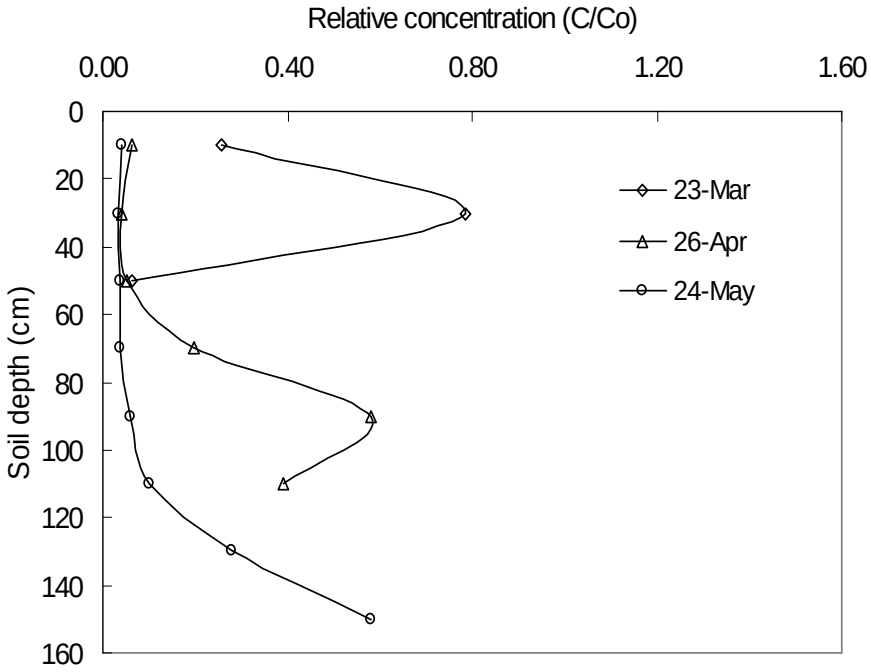

Figure 5-8 Change in NO_3^--N concentration with depth during the growing season for the maize plots.

There are two phenomena that caused the behaviour of the previously described profiles—the uptake of NO_3^--N by the maize and the variation in soil texture with depth. As shown in Table 5-1, the top 100 cm of the soil profile consists of sandy loam, but then change to a sandy clay loam which would retard the water flow and leaching of chemicals.

The average relative concentrations of Br^- and NO_3^--N on bare and maize plots are presented in Figure 5-9. The relative concentration of Br^- was lower than that of NO_3^--N on both bare and maize plots. The difference increased with depth. This implies that the background concentration of NO_3^--N was much higher than that of Br^-. In the upper 100 cm, Br^- and NO_3^--N concentration profiles are very close to each other. Below 100 cm depth, the concentration of Br^- decreased while that of NO_3^--N was increasing. Lower concentrations at shallower depths were due to the maize crop uptake of both Br^- and NO_3^--N. The trend of Br^- with depth on bare plots was similar to that on maize plots and the trend of NO_3^--N on bare plots was similar to that on maize plots. The maize crop has

significantly attenuated the peak of NO_3^--N concentration. The distinct concentration peak of Br^- is absent for NO_3^--N except for minor peaks at the Br^- peak depths.

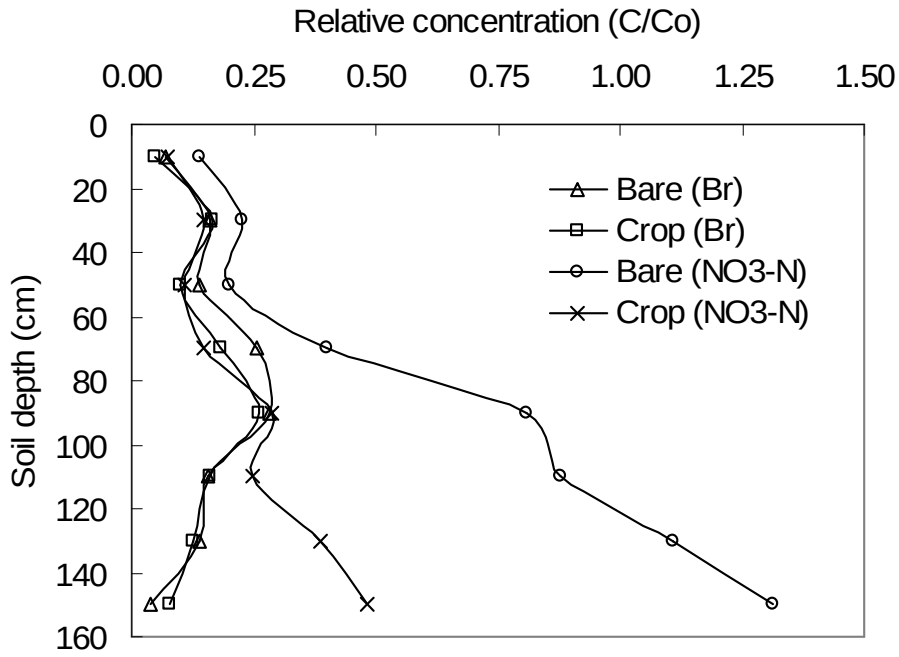

Figure 5-9 Profiles of the average Br^- and NO_3^--N concentrations in the bare and maize plots during the growing season.

The average seasonal depth of the centre of mass of Br^- and NO_3^--N obtained by integrating the concentration profiles in Figure 5-9 is presented in Table 5-5. As could have been expected from the preceding discussion, the centres of mass of both the Br^- and the NO_3^--N were located at deeper depths for maize plots than for bare plots. The high background concentration of NO_3^--N at deeper depths resulted in the centre of mass of NO_3^--N to be deeper than that of Br^- in both the bare and the maize plots.

Table 5-5 Depths of the centres of mass for the Br^- and NO_3^--N concentration profiles in Figure 5-9

	Depths of centres of mass (cm)							
	Bare plots				**Maize plots**			
	1	2	3	**Average**	1	2	3	**Average**
Br^-	68.1	68.4	75.2	70.6	80.0	73.2	77.7	76.9
NO_3^--N	82.5	83.8	87.8	84.7	91.8	82.6	83.9	86.1

5.4.3 Variations in the Recovered Masses of Bromide and Nitrate

The average recovered masses of Br^- and NO_3^--N at different sampling times, expressed as percentages of the masses applied at the beginning of the experiment, are given in Table 5-6. As could have been expected, a higher mass of the applied Br^- was recovered from the bare plots than from the maize plots, 98.5% in the case of the bare plots and 86.8% in the case of the maize plots. The average recovery of NO_3^--N from the bare and maize plots was 308.8% and 124.5% respectively. This high recovery is due to the high background concentration of NO_3^--N in the soil as explained in Section 5.4.2.

Average soil Br^- and NO_3^--N concentrations can mask individual differences within fields. It is therefore necessary to take the variability of the recovered mass into account in sampling procedures aimed at the assessment of solute concentrations for regulatory purposes. In this study the spatial variability of the recovered masses of Br^- and NO_3^--N at various sampling dates was described by simple descriptive statistics, as presented in Tables 5-7. As discussed above, there was no loss of Br^- and NO_3^--N beyond the maximum sampling depth of 160 cm in this experiment The observed variations in the concentrations were most likely caused by factors such as soil heterogeneity and differential leaching rates, while microbial transformation could have contributed significantly to the observed variations in the NO_3^--N concentrations.

Table 5-6 Average percentage recovered masses of Br^- and NO_3^--N at different sampling times during the field investigations

Days after planting	Average recovered masses (%)			
	Bare plots		Maize plots	
	Br^-	NO_3^--N	Br^-	NO_3^--N
13	128.3	140.5	109.9	110.5
23	109.8	169.3	124.5	124.8
33	89.8	150.4	69.0	90.4
41	79.7	205.7	113.3	117.5
49	111.5	337.5	122.0	147.2
57	122.4	384.3	74.0	131.0
64	120.6	403.9	67.0	144.1
71	81.9	435.8	69.4	113.4
78	79.3	362.5	111.9	194.4
85	68.8	382.3	64.5	117.2
98	91.2	425.1	29.1	78.6
Mean	98.5	308.8	86.8	124.5
St. Dev.	20.6	117.1	30.9	30.9
CV	20.9	37.9	35.6	24.8

The spatial variability of recovered solute masses is common (Biggar and Nielsen, 1976; Cameron *et al*., 1979; Nielsen *et al*., 1980; Rice *et al*., 1986; Silvertooth *et al*, 1992). For example, Cameron *et al*. (1979), using eight sampling times from six replicate plots, observed minimum, maximum and average CVs of 23.9%, 100.8%, 41.6% respectively for the percentage NO_3^--N recovered. They reported, the minimum, maximum and average recoveries for chloride in this same experiment to be 36.6%, 125.3% and 75.3% respectively. In a field experiment with Br^-, Rice *et al*. (1986) observed 40% to 350% variation in the amount of recovered Br^- and attributed this large variation to a non-uniform application of Br^- during the experiment. The relatively lower variability observed in this study might be due to the smaller area considered and the limited number of samples.

Table 5-7 Minimum, maximum and average coefficients of variations of recovered Br^- and NO_3^--N masses for the respective plots at different times of sampling

	Coefficient of variation (%)					
	Bare plots			Maize plots		
	Minimum	Maximum	Average	Minimum	Maximum	Average
Br^-	7.8	101.8	38.1	17.0	52.4	37.0
NO_3^--N	17.9	71.6	32.6	12.4	68.4	36.6

5.4.4 Crop Uptake of Bromide and Nitrate

A summary of the dry matter, Br^- and NO_3^--N plant tissue concentration, determined as described in Section 5.2.3 is presented in Table 5-8, which shows that the maize plant Br^- concentrations ranged from 1.28 to 5.12 g kg^{-1} during the growing season with an average of 2.56 g kg^{-1}. These results agree with that of Iragavarapu *et al*. (1998) who found a Br concentration of 1.9 g kg^{-1} in maize plants harvested from a soil to which 197 kg Br ha^{-1} has been applied. Since it is known that Br concentrations higher than 4.6 g kg^{-1} is toxic to live stock (Knight and Reina-Guerra, 1976), the Br concentrations in Table 5-8 suggest that it may be perilous to feed live stock with young maize plants, grown on soil rich in Br or treated with Br.

As illustrated in Figure 5-10 both the Br^- and NO_3^--N concentrations increased rapidly at early growth ages of the plants and then decreased as the plants matured. This trend has also been observed by Jemison and Fox (1991). From Figure 5-11, it can be observed that the mass of bromide and nitrogen taken up by the crop increased during the growing season.

Table 5-8 Average dry matter mass, bromide and nitrogen content of maize at different times of the growing season

Sampling date	Dry matter (kg ha^{-1})	Br conc. (g kg^{-1})	N conc. (g kg^{-1})	Br uptake (kg Br ha^{-1})	N uptake (kg N ha^{-1})	N uptake/ Br uptake
02 April	425	3.44	21.83	1.46	9.28	6.36
10 April	1629	5.02	26.33	8.18	42.89	5.24
18 April	2563	5.12	24.37	13.12	62.46	4.76
03 May	3208	1.57	21.87	5.04	70.16	13.92
10 May	4174	1.87	18.00	7.81	75.13	9.62
17 May	5503	2.29	14.65	12.60	80.62	6.40
24 May	7038	1.28	14.12	9.00	99.38	11.04
31 May	9456	1.83	10.39	17.30	98.25	5.68
07 June	**(at harvest)**					
Leaf	2356	1.18	13.04	2.78	30.72	11.05
Stem	1285	2.26	14.23	2.91	18.28	6.28
Grain	5432	0.96	17.48	5.21	94.95	18.22
Total	9073	1.47	14.92	10.90	143.95	13.14

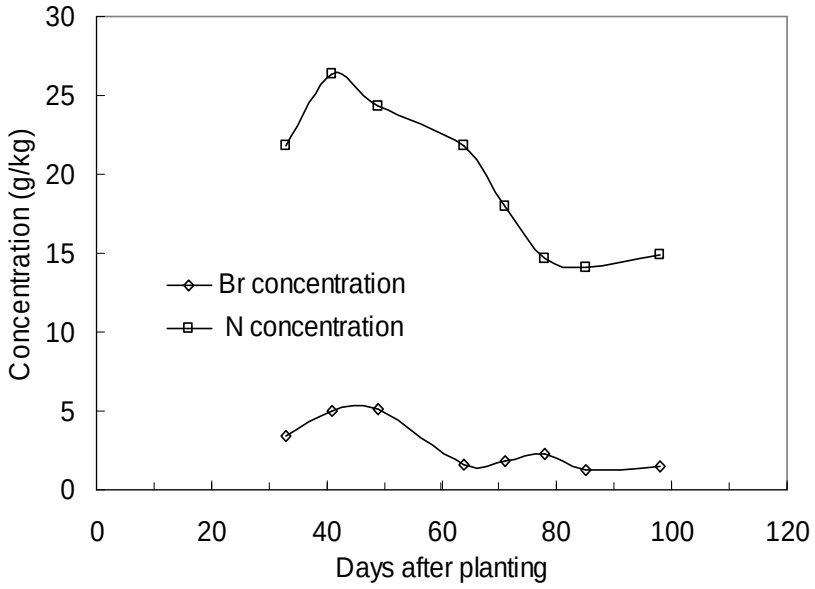

Figure 5-10 Maize plant tissue bromide and nitrogen concentrations during the growing season.

The uptake of Br and NO_3^--N by the maize at physiological maturity was 10.9 kg ha^{-1} and 143.9 kg ha^{-1} respectively. This implies that the maize recovered 64.2% of the 224 kg ha^{-1} NO_3^--N and 8.1% of 135 kg ha^{-1} Br applied as fertilizer to the soil at the beginning of the experiment. The latter result agrees very much with the 8 to 10% observed by

Iragavarapu *et al*. (1998), but differ considerably from the 40% observed by Jemison and Fox (1991) and also significantly from 2 to 3% observed by Gish and Jury (1982) or the zero uptake observed by Gish and Coffman (1987).

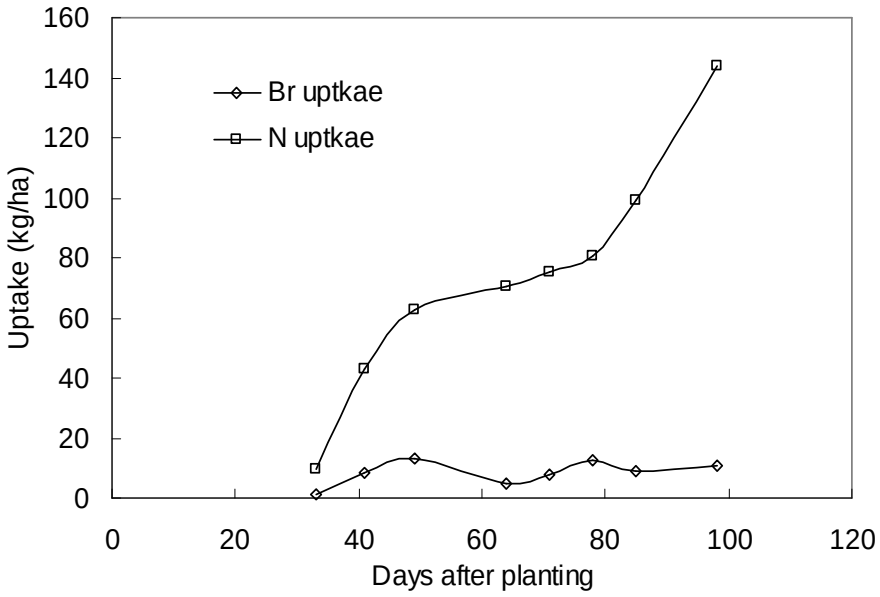

Figure 5-11 Maize plant Br and NO_3^--N uptake during the growing season.

Since 86.8% of the Br^- was recovered from the soil in the maize plots, see Table 5-6, 94.9% of the applied mass of Br^- was recovered from the soil and maize. The difference between this figure and the almost 100% recovery rate of Br from the bare soil plots (Table 5-6) was probably taken up by maize roots which was not measured. For NO_3^--N, it is not possible to determine what percentage of the nitrogen taken up by the crop came from the applied fertilizer and background concentration in the soil unless labelled (N-isotope) fertilizer is used.

5.4.5 Bromide and Nitrate Movement in the Soil

As mentioned in Chapter 3, convection is the most important component of solute transport processes because convection, rather than dispersion, determines the position of the peak concentration in a soil profile. The velocities of Br^- and NO_3^--N determined from concentration peak and centre of mass movements were compared with the pore-water velocity. The pore-water velocity was determined using the soil water balance and also from the fitting of Br^- leaching data to the analytical solution of the CDE model using the CXTFIT. Dispersion coefficient of Br^- movement was also determined from this fitting.

Pore-water velocity from the soil water balance was determined as the ratio of Darcian flux (q) and the volumetric soil water content (θ). In the Dire Dawa field experiment, the cumulative deep percolation from bare and maize plots was 140.9 mm and 202.3 mm respectively (Tables 5-2 and 5-3). The duration of the experiment was 98 days. The Darcian flux (q) was, therefore, 1.44 mm d^{-1} and 2.06 mm d^{-1} respectively for the bare and maize plots. The average soil profile volumetric water content during the season was respectively 0.149 and 0.137 for bare and maize plots. The pore-water velocity (q/θ) is calculated to be 0.96 cm d^{-1} and 1.50 cm d^{-1} for bare and maize plots respectively, Equation (3.26). The higher deep percolation from the maize plots resulted in a higher pore-water velocity.

The CDE fitted parameters (v and D) to the Br^- concentration profiles at different times of the experiment in the bare and maize plots are presented in Table 5-9. The average velocity and dispersion coefficient values for the bare plots were 1.47 cm d^{-1} and 3.65 cm^2 d^{-1} respectively. These parameters were respectively 1.78 cm d^{-1} and 6.96 cm^2 d^{-1} for the maize plots. The fitting was not as good as the ones in Chapters 3 and 4. The average pore-water velocities, obtained from the water balance and Br^- concentration fittings, were therefore 1.21 cm d^{-1} for the bare plots and 1.64 cm d^{-1} for the maize plots.

Table 5-9 Transport parameters determined by fitting Br^- concentration profiles to the CDE model for the bare and maize plots

Time	Bare plots			Maize plots		
(d)	v (cm d^{-1})	D (cm^2 d^{-1})	r^2	v (cm d^{-1})	D (cm^2 d^{-1})	r^2
23	1.97	9.45	0.701	2.15	9.05	0.565
41	2.21	5.67	0.527	2.20	7.31	0.948
49	1.77	3.64	0.858	2.01	2.20	0.971
57	1.52	2.72	0.683	1.46	8.25	0.800
64	1.23	1.37	0.630	1.55	7.67	0.756
71	1.27	1.44	0.911	2.28	6.03	0.711
78	1.26	1.48	0.936	1.32	1.55	0.755
85	1.07	4.23	0.617	1.67	10.57	0.761
98	0.96	2.81	0.714	1.41	10.00	0.457

The actual solute velocity was determined from the displacement of the concentration peak and solute centre of mass. The velocity of concentration peak was calculated using the time it took for the peak to move from one depth to the next depth, Equation (3.27). The change in depth was divided by the change in time. The centre of mass velocity was calculated using Equation (3.29). Table 5-10 presents these velocities determined from the leaching of Br^- and NO_3^--N in the bare and maize plots.

Table 5-10 The average concentration peak and centre of mass velocities of Br^- and NO_3^--N on bare and maize plots

Velocity of Br^- (cm d^{-1})					
Bare plots			**Maize plots**		
Plot number	**Concentration peak**	**Centre of mass**	**Plot number**	**Concentration peak**	**Centre of mass**
1	1.26	1.06	1	1.62	1.54
2	1.08	0.97	2	1.84	1.38
3	1.08	1.08	3	1.57	1.68
Average	1.14	1.04	**Average**	1.68	1.53
St. Dev.	0.10	0.06	**St. Dev.**	0.14	0.15
CV (%)	8.77	5.77	**CV (%)**	8.33	9.80
Velocity of NO_3^--N (cm d^{-1})					
Bare plots			**Maize plots**		
Plot number	**Concentration peak**	**Centre of mass**	**Plot number**	**Concentration peak**	**Centre of mass**
1	1.03	1.11	1	1.57	1.77
2	1.12	1.21	2	1.60	1.77
3	1.29	1.37	3	1.47	1.68
Average	1.15	1.23	**Average**	1.55	1.74
St. Dev.	0.14	0.23	**St. Dev.**	0.08	0.44
CV (%)	12.17	18.70	**CV (%)**	5.16	25.29

It can be observed that the velocities of Br^- and NO_3^--N for the bare plots were lower than the corresponding velocities for the maize plots. The amount of water applied and the deep percolation for the maize plots were higher than that for the bare plots (Tables 5-2 and 5-3). The rate of solute transport increases with the net water flux and this was the reason for the higher velocity of Br^- and NO_3^--N on the maize plots. Towards the end of the experimental period, Br^- peaks have moved to 90 cm and 130 cm depths for the bare and maize plots respectively. The ratios between the actual solute velocities and the average pore-water velocities are presented in Table 5-11. The average pore-water velocities (v_w) were 1.21 cm d^{-1} and 1.64 cm d^{-1} for bare and maize plots. On average, the ratio (v_s/v_w) was close to one.

Table 5-11 The ratios between actual solute velocities and pore-water velocities (v_s/v_w) on bare and maize plots

	Br^-			NO_3^--N		
	Concentration peak	**Centre of mass**	**Average**	**Concentration peak**	**Centre of mass**	**Average**
Bare	0.94	0.86	0.90	0.95	1.02	0.99
Maize	1.02	0.93	0.98	0.95	1.04	1.00
Average	0.98	0.90	0.94	0.95	1.03	1.00

5.4.6 Deep Percolation Rate Determined using Different Root Water Extraction Models

Tracer-based rate of deep percolation is commonly calculated assuming a constant velocity from the time of tracer injection at the soil surface to the depth at which the deep percolation is to be determined. This constant velocity model ignores the transport process within the active root zone. In this section, the deep percolation calculated using a constant velocity model is compared with the deep percolation calculated using the assumptions of uniform and exponential root water extractions.

The observed and calculated travel times to 30, 50, 70, 90, 100, 110, and 120 cm depths are presented in Table 5-12. The input values for these equations are described as follows for the maize plots. The input water fluxes P and I were 2.07 and 5.76 mm d^{-1} respectively (Table 5-3). The cumulative deep percolation at the bottom of the effective root zone (100 cm) determined from the water balance was 2.06 mm d^{-1} (Table 5-3). The average soil water content of the root zone was 0.137. The λ constant in the exponential root water uptake was assumed to be 3. Considering the shallow roots of the maize crop, the light and frequent irrigations and the sandy nature of the top soil, this is a reasonable value. For larger values of λ, the bulk of the root extraction occurs near the soil surface, while small values of λ produce an extraction rate approaching the uniform extraction rate.

Table 5-12 Bromide travel times to different depths determined using different methods

Depth	Br peak movement	Uniform extraction	Exponential extraction
(cm)	Observed	Equation (5.13)	Equation (5.14)
30	16.33	5.93	7.36
50	29.00	10.91	15.00
70	45.00	17.22	24.91
90	61.67	25.84	36.76
100	69.84	31.70	43.25
110	78.00	39.51	50.04
120	85.12	51.21	57.06

Figure 5-12 presents the relation between the travel times and the root water extraction models. The uniform extraction shows the most rapid transport of the solute through the root zone. The exponential uptake shows longer travel time as the water extracted near the surface is high. However, at depths greater than the root zone the two models tend to predict similar travel times. Tyler and Walker (1994) stated that for fixed values of P, I, R, θ and z_r, the travel times calculated according to the piston flow assumption are much

higher than the travel times calculated using equations that take root water uptake into account.

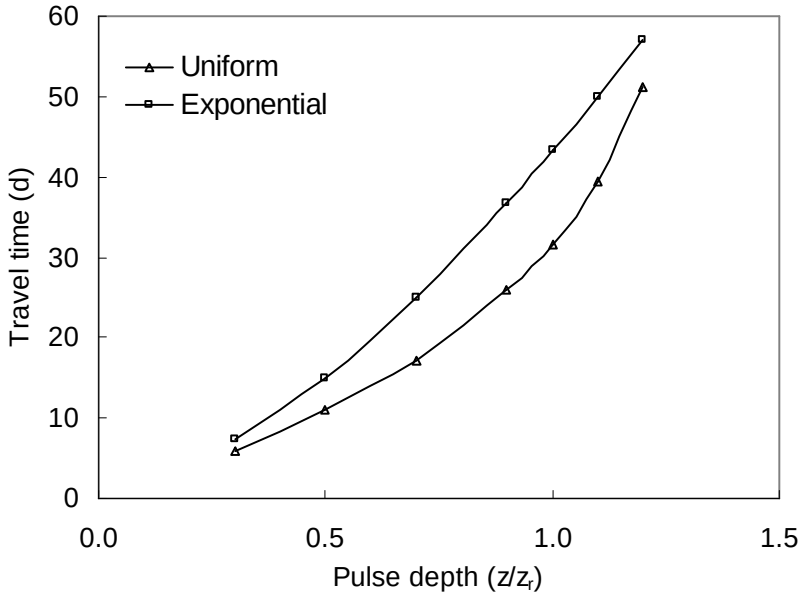

Figure 5-12 Comparison of travel times for the two root water extraction functions.

Table 5-13 Deep percolation determined by substituting travel times in Table (5-12) into Equation (5.4)

Depth	Deep percolation, $\widehat{R}$ (mm d^{-1})		
(cm)	Br peak movement	Uniform extraction	Exponential extraction
30	2.52	6.93	5.58
50	2.36	6.28	4.57
70	2.13	5.57	3.85
90	2.00	4.77	3.35
100	1.96	4.32	3.17
110	1.93	3.81	3.01
120	1.93	3.21	2.88

The travel times presented in Table 5-12 were used in Equation (5.4) to determine the deep percolation and the result is presented in Table 5-13. This deep percolation rate is then compared with the actual deep percolation rate used in determining these travel times (R = 2.06 mm/d) in order to evaluate the performance of Equation (5-4) in the determination of the deep percolation. It can be seen that the flux through the upper portion of the root zone is much higher than the actual deep percolation rate (2.06 mm d^{-1}). However, as the tracer moves to the bottom of the root zone, its instantaneous velocity

decreases asymptotically. The deep percolation estimated using the observed travel time of Br^- was closer to the actual deep percolation than the deep percolation estimated from the travel times calculated using uniform and exponential root extraction models. The deep percolation estimated from the travel time determined by the exponential root extraction model was closer to the actual deep percolation than the one calculated using the travel time determined by the uniform root extraction model.

Table 5-14 shows the relative error as a function of pulse depth for uniform and exponential root extractions, Equation (5.15). The relative error of the deep percolation estimated from the observed Br^- peak movement was also included. The relative errors shown in the table are relatively low compared to other studies conducted in arid environments. This was due to the high *R/(P+I)* ratio (= 0.26) in this small plot study. Using *R/P* values varying from 0.001 to 0.5, Tyler and Walker (1994) have shown that for large values of *R/P*, the relative errors in deep percolation estimation are small even when the tracer is still in the root zone. For deep percolation values approaching typical arid zones (*R/P* = 0.001 to 0.01), however, their estimated deep percolation was two to three orders of magnitude higher than the actual deep percolation. For example, for the *R/P* value of 0.1% they found the relative error to be 300 when uniform extraction is considered and for a strongly exponential extraction the error was 20. They observed that the errors persist well below the root zone, with errors of approximately 100% still present when the tracer pulse has reached twice the rooting depth.

Table 5-14 The relative error in deep percolation estimation under uniform and exponential root extractions

Depth	Relative error RE ($\widehat{R}$ /R)		
(cm)	Br peak movement	Uniform extraction	Exponential extraction
30	1.22	3.36	2.71
50	1.15	3.05	2.22
70	1.03	2.70	1.87
90	0.97	2.32	1.63
100	0.95	2.10	1.54
110	0.94	1.85	1.46
120	0.94	1.56	1.40

5.4.7 Deep Percolation Estimated from Bromide Mass Balance

Mass balance of tracers is often used to estimate deep percolation, especially in arid climates where the deep percolation to rainfall (*R/P*) ratio is low. The tracer mass balance principle was applied to the data of the controlled experiment of this study. In these maize plots, the term “deep percolation” refers to the percolation past the crop root zone.

The water input (rain plus irrigation) into the soil surface of the maize plots was 767.6 mm. Bromide was applied to the plots at a rate of 13.5 g m^{-2}. The Br^- concentration in the applied water was, therefore, 17.59 mg L^{-1}. The average concentration of recovered soil Br^- from the three maize plots at a 100 cm depth was 75.35 mg L^{-1}. From the tracer mass balance method of Allison and Hughes (1978), Equation (5.16), the deep percolation was calculated to be 179 mm. The average deep percolation rate is therefore 1.83 mm d^{-1} for the 98 days experimental period. The deep percolation calculated from the water balance was 27% of the applied water (Section 5.3.1) while the deep percolation according to the Br^- mass balance is 23% (179/767.6*100%) of the applied water. This difference is small, compared with other long-duration studies done in arid climates. The good agreement was due to the higher *R/P* ratio (where *P* includes irrigation) in this study. Tyler and Walker (1994) analysed the relative errors in deep percolation estimation, using *R/P* values varying from 0.1% to 50%. They observed that as the *R/P* approaches 50%, the error becomes smaller and concluded that for typical arid regions, tracers could be used effectively when the deep percolation exceeds 10% of the annual precipitation.

5.5 CONCLUSIONS

High background concentration of NO_3^--N together with its complex transformations in the soil can obscure the transport pattern of the applied nitrogen and make the study of the leaching process difficult. However, results of this study have indicated that while it is not possible to quantify the actual amount of NO_3^--N lost, a conserved tracer such as Br^- is very helpful in determining the worst case scenario of its leaching. However, specific issues regarding the fate of fertilizer N in a soil-plant system cannot be determined by using a physically, chemically and biologically conserved tracer such as Br^-.

The solute velocities were close enough to the pore-water velocities and it can be said that solute movement can be described by piston flow. The applied tracer Br^- and fertilizer NO_3^--N were not leached out of the root zone during the cropping season. It can take several years for the leached NO_3^--N to reach the groundwater.

The presence of crops cause attenuation of the concentration peaks of solutes such as fertiliser N. As Br^- is not an essential plant nutrient, the rate at which it is taken up by crops is lower than that of nitrogen and can not be used to quantify the crop uptake of nitrogen.

It has been observed that there is not much difference between deep percolation rates calculated using the constant velocity model and the deep percolation rates determined using uniform and exponential root water extraction models. This is attributed to the high

value of $R/(P+I)$ in this study.

The solute concentration profiles in this study are the results of the interaction of numerous factors including irrigation, rainfall, evaporation, hydrodynamic dispersion, diffusion, and exclusion of anionic solute from negatively charged minerals. Unlike laboratory experiments, field experiments give rise to difficulties in isolating the influence of a particular factor. Therefore, one should be cautious before extrapolating the results of laboratory experiments into the field.

The higher amount of soil water stored in the bare plots has an important implication for leaving a land fallow. Not only nutrient is restored but there is soil water conservation too.

CHAPTER 6

APPLICATION OF THE SOLUTE TRANSPORT PARAMETERS

6.1 INTRODUCTION

In the previous Chapters of this thesis, solute transport parameters were determined under steady and transient states. In this Chapter, these transport parameters will be used to investigate solute leaching to the water table and three-dimensional transport. In Section 6.2, the breakthrough times of solute concentration peaks at the water table depth will be estimated for different drainage rates with the CXTFIT program using transport parameters determined in the transient seasonal experiment of Chapters 4 and 5. In Section 6.3, the transport parameters determined in the steady state experiment of Chapter 3 will be used to investigate three-dimensional transport during the experiment using the 3DADE program.

6.2 CONCENTRATION PEAK BREAKTHROUGH TIME AT THE WATER TABLE

6.3.2 General

The average time required for a solute to reach groundwater table depends upon a number of factors. One of these factors is the nature of the solute. For example, a solute, which is easily adsorbed to the soil particles, takes longer time than a non-adsorbing solute. The soil cover also determines the net amount of water that enters and leaves the soil profile and consequently the solute transport. Evapotranspiration is higher and deep percolation is lower from a vegetated soil than from a bare soil. The soil type also controls the transport processes. Solute movement is faster in coarse-grained soils than in fine-grained soils if transport is assumed to occur only in the matrix (no preferential flow). The transport of agrochemicals such as nitrate, is therefore, different under different climate, soil and soil cover conditions.

Nitrate is very mobile and is easily displaced from its point of origin by infiltrating water. It is stable in soils except when biologically transformed by denitrification, which only occurs in very wet soils or soil aggregates (Broadbent and Clark, 1985). Although nitrate is rapidly taken up by plant roots, this phenomenon is restricted to the upper soil layers. Thus, whenever there is a source of nitrogen and an excess of water applied to the soil, nitrates have the potential to migrate to an underlying aquifer. Although it may take a shorter time for dissolved nitrates to reach a shallow aquifer, it will eventually also reach

a deep aquifer as long as water continues to enter the soil at a rate in excess of evaporative demand. Pratt *et al*. (1970) describe nitrate plumes that had moved far below the root zone of citrus groves over years, but had not yet reached the groundwater table. Indeed, they estimated that travel times in excess of 50 years would be required for the nitrate to reach groundwater in some locations. This explains why Ayers and Branson (1973) found groundwater with high nitrate levels under land developed over former citrus groves years after fertilization of the surface ceased.

6.3.3 Simulation of Solute Transport to the Water Table

One of the major goals of solute transport models is to predict the movement of contaminants such as nitrates to groundwater. In Chapter 4 it was observed that bromide and nitrate move similarly in the Bainsvlei soil. In this Section, transport parameters determined at shallow depths by fitting bromide concentration data to analytical models will be used to simulate the leaching of bromide to the water table at a deeper depth. This will be done using the transport parameters determined in Chapters 4 (Bainsvlei, South Africa) and 5 (Dire Dawa, Ethiopia). The quantity of water required to leach the solute to the groundwater table was also determined.

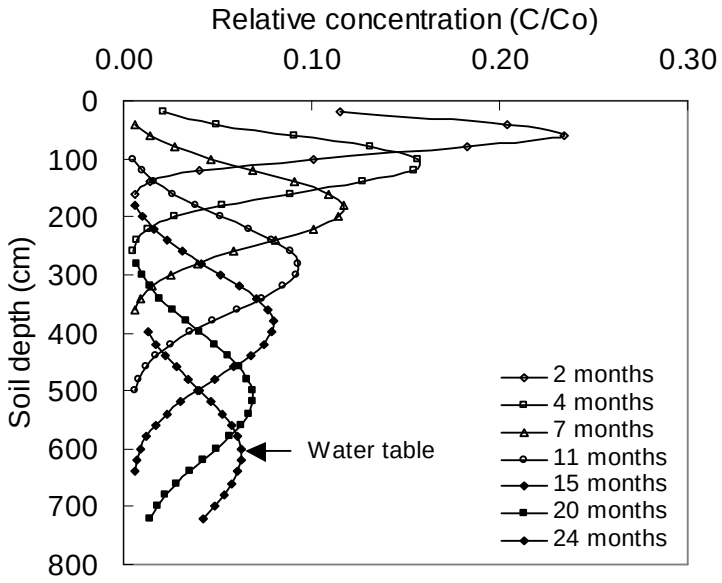

Figure 6-1 Simulated bromide concentration profiles using the CDE estimated average transport parameters (v = 0.83 cm d^{-1} and D = 9.95 cm^2 d^{-1}).

The transport parameters were determined from a tracer experiment conducted only in the upper 160 cm of the soil. However, the soil profile was relatively homogenous to a depth

of 300 cm (Table 2-1). A borehole log close to the study area also indicated a similar reddish soil to a depth of 1000 cm. Therefore, it is reasonable to use transport parameters determined in the upper 160 cm of the soil profile to estimate the travel time of solutes to reach the groundwater table at 600 cm depth at this site. The CXTFIT computer program was used to determine the concentration profiles.

The simulated concentration profiles using the average transport parameters of the CDE model in Table 4-8 (v = 0.83 cm d^{-1} and D = 9.95 cm^2 d^{-1}) are shown in Figure 6-1 for a bare soil with no runoff. According to this model, it will take the concentration peak 24 months to reach the water table at 600 cm depth, even though some solute already reached this depth after 15 months, or 23 months if the highest dispersion coefficient in Table 4-8 (D = 17.90 cm^2 d^{-1}) is used, see Figure 6-2.

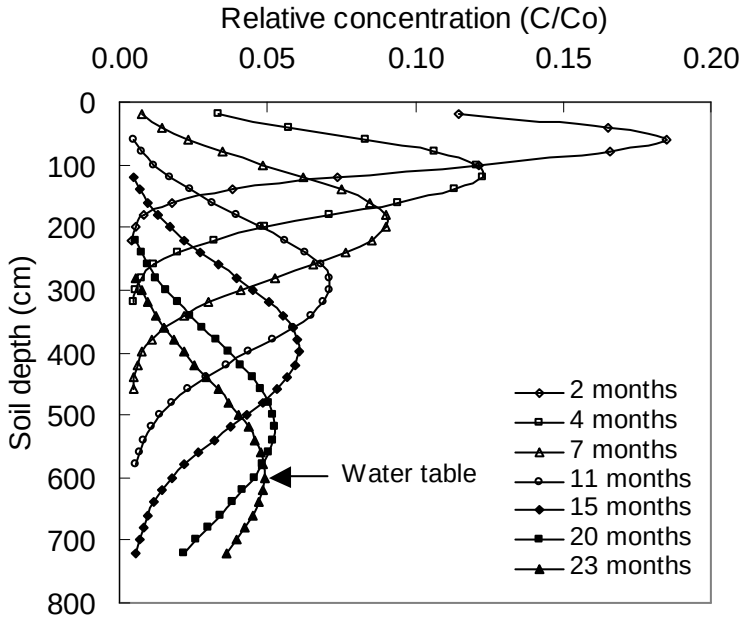

Figure 6-2 Simulated bromide concentration profiles using the CDE determined average velocity (v = 0.83 cm d^{-1}) and maximum dispersion coefficient (D = 17.9 cm^2 d^{-1}).

The time it takes the concentration peak to reach a given depth is therefore inversely related to the dispersion coefficient. This behaviour of the solute contradicts the notion that the centre of mass must travel with the same velocity, regardless of dispersion coefficient. The same phenomenon has also been observed by Chiang and Kinzelbach (1998), and Jury (1983), who investigated solute transport the one-dimensional CDE and the convective-lognormal transfer (CLT) models. His models were calibrated at 30 cm

depth (v = 3 cm d^{-1} and D = 15 cm^2 d^{-1}) and used to predict transport to a water table at 1 000 cm. The predicted time for 50% of the solute pulse to reach the water table was higher for the CDE. This might be due to the considerations in the models that the CDE assumes constant dispersion coefficient and the CLT assumes a linearly increasing dispersion coefficient with depth.

The rate at which a solute moves through the soil profile is essentially determined by the pore-water velocity of the water in the absence of preferential flow. The slight difference between the pore-water velocity for the sandy loam Bainsvlei soil observed in the field, 0.73 cm d^{-1}, and the value, 0.83 cm d^{-1}, derived from the CDE model for bromide may be due to minor cracks that developed in the soil during the experiment or experimental errors. Figure 6-3 presents the concentration profiles for bromide simulated with the observed pore-water velocity and the average dispersion coefficient. As could have been expected from the preceding discussion, the concentration peak now arrives after 27 months at the water table. This suggests that the pore-water velocity observed in the field may provide a conservative estimate of the time it will take the concentration peak of a solute to reach the water.

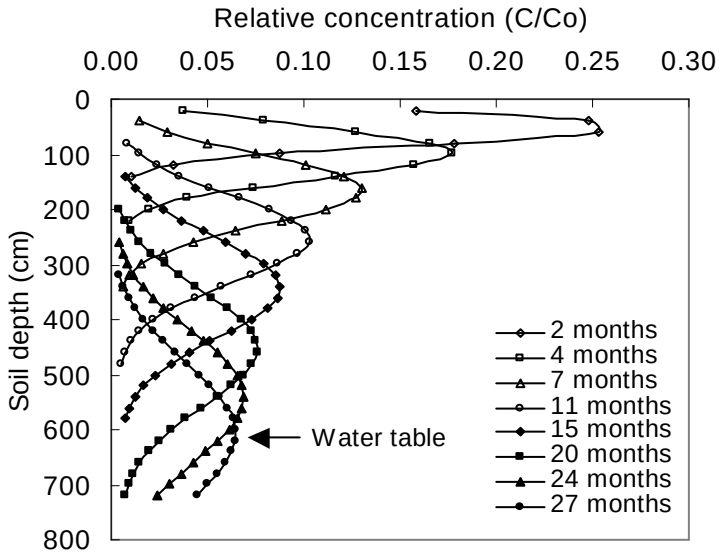

Figure 6-3 Simulated bromide concentration profiles using the pore-water velocity (v = 0.73 cm d^{-1}) and the CDE estimated average dispersion coefficient (D = 9.95 cm^2 d^{-1}).

The major driving force behind the movement of a solute beyond the root zone is the so-called recharge or deep percolation rate. Since plants take up water from the soil, one can expect that the deep percolation rate below a vegetated soil will be less than below a bare

soil. It may therefore be interesting to compare the time it will take a solute such as bromide to reach the water table at the test site under a vegetated soil and a bare soil.

A first rough estimate of the difference between the behaviour of a solute under bare and vegetated soils can be obtained by comparing the times it took the concentration peak to reach the groundwater table with the times it will take water to travel from the soil surface to the groundwater table for a given deep percolation rate. If the symbols L, q_c and θ_c are used to denote the depth to the water table, the deep percolation rate and water content for soils planted with crops respectively, these times can be computed from the equation

$$t = L\theta_c / q_c = L / v_c \qquad (6.1)$$

Since the deep percolation rate below crops was not investigated for the Bainsvlei soil, the value θ_c = 0.200 observed by Bennie *et al*. (1998) for the soil at the test site will be used for this investigation. The results for values of q_r ranging from 0.02 mm d^{-1} to 0.2 mm d^{-1}—the maximum value Bennie *et al*. (1998) observed for the deep drainage rate of the soil planted with crops at the Bainsvlei site—are given in Table 6-1. These results indicate that the adverse effects the mismanagement of agrochemicals (or other hazardous chemicals) have on the groundwater below a site planted with crops may not be noticed for a very long time after application of the chemical at the soil surface. This will especially be the case in arid areas with deep-seated aquifers and low precipitation rates.

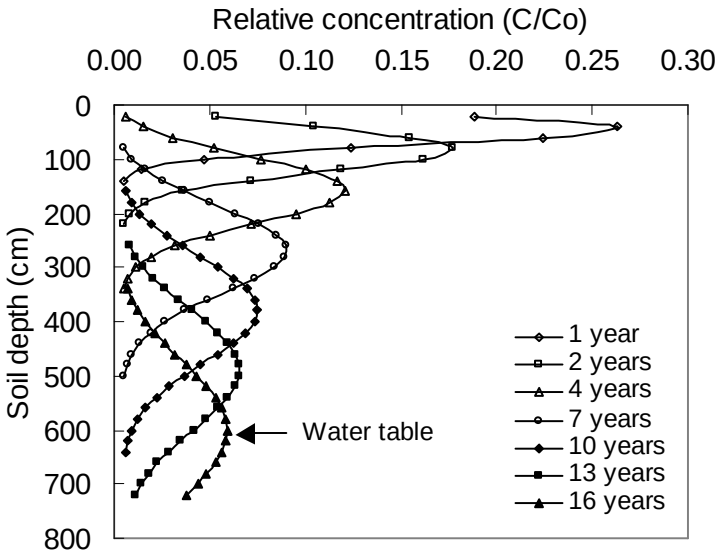

Figure 6-4 Simulated bromide concentration profiles using the pore water velocity (v = 0.10 cm d^{-1}) determined from soil water balances and the dispersion coefficient (D = 1.36 cm^2 d^{-1}) value determined from dispersivity relation.

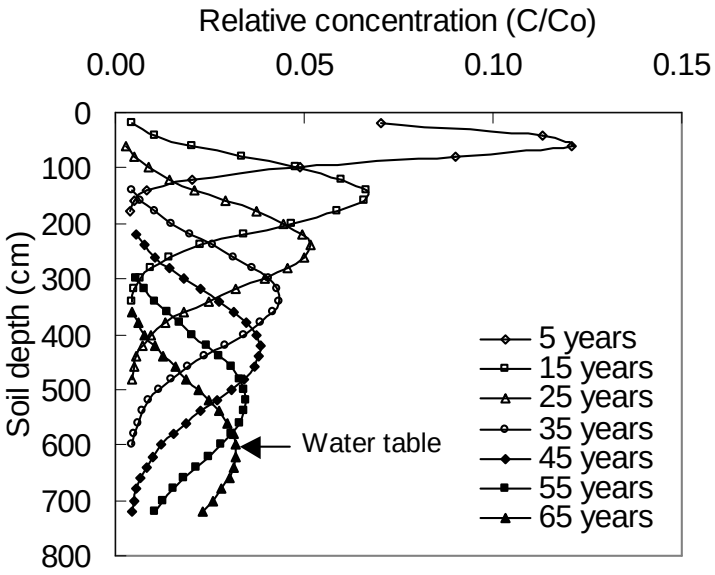

Figure 6-5 Simulated bromide concentration profiles using the pore water velocity (v = 0.025 cm d^{-1}) determined from soil water balances and the dispersion coefficient (D = 0.34 cm^2 d^{-1}) value determined from dispersivity relation.

Table 6-1 Concentration peak arrival time at the water table for different drainage rates

Drainage (mm/d)	0.20	0.15	0.10	0.05	0.03	0.02
Peak arrival time (years)	17	22	33	67	111	167

A more realistic estimate of the travel times of solutes can be obtained by using the CDE model in Equation (6.1) to compute the time that the concentration peak arrives at the groundwater table or aquifer. This can be done, for example by using the relation between the dispersion coefficient and the pore-water velocity in Equation (3.15) to derive a value for the dispersivity, α_L, from observations under bare soils and combine this with the deep percolation rate observed under vegetated soils. It must be kept in mind though that the value of α_L is scale-dependent. For example, Jury *et al*. (1991) have shown that while α_L varies from 0.5 cm to 2.0 cm when determined form packed laboratory columns to between 5 cm and 20 cm when determined in the field, while Fried (1975) obtained even larger values for α_L in regional groundwater investigations. It is therefore interesting to note that the dispersivity of 13.63 cm, derived from the observed pore-water velocity and average dispersion coefficient computed above for a bare Bainsvlei soil is in the range suggested by Jury *et al*. (1991). Figures 6-4 and 6-5 display the concentration profiles for the Bainsvlei soil simulated with this value of α_L, θ_c = 0.2 and q_r = 0.20 mm d^{-1} and 0.05 mm d^{-1}. It can be seen that it took 16 and 65 years respectively for the solute

concentration peaks to reach the water table at 600 cm depth for the drainage rates of 0.20 and 0.05 mm d^{-1}.

As mentioned above, the transport of a solute in the subsurface of the earth depends mainly on the pore-water velocity of the water, which in turn depends on the piezometric gradient. The possibility therefore exists that one can control the motion of a solute in unsaturated soils by limiting the volume of water applied to the surface. It may therefore be important to know how much water is needed to move a chemical through the unsaturated zone, also known as *the cumulative drainage*. Let q denotes the constant flux of water through a soil column with unit area and length L, θ the constant water content of the column and t_L the time it takes a conservative solute to move through the length of the column. The cumulative drainage, or *pore volume*, needed to displace a solute through the length L can then be expressed as

$$d_L = qt_L = L\theta \tag{6.2}$$

Consider, for example, the steady state experiment of Chapter 3, with the average soil water content of 0.259 and the transient state experiment with the average soil water content of 0.212 of Chapter 4. In these situations one will require respectively 1554 mm and 1272 mm of water to leach the Br^- from the 600 cm of soil above the water table at the Bainsvlei test site. The reason why more water is required to displace the Br^- during the steady state experiment than the transient state experiment is because the volume of water needed to displace a solute through a pore volume increases linearly with the water content of the soil. This behaviour of the solute suggests that it may be worthwhile to control the water applied to crops through irrigation by using a measure such as the Profile Available Water Capacity (PAWC) of Laker (1985).

The simulation of bromide concentration peak arrival time at the water table for the Bainsvlei soil was done under bare and cropped soil conditions under natural rainfall. Under irrigated condition, the drainage rate is generally higher. The bromide transport parameters determined at the Dire Dawa under irrigated condition (Chapter 5) were also used to simulate bromide concentration peak arrival time at the water table at a depth of 1000 cm at the experimental site. The simulated concentration profile curves are presented in Figures 6-6 and 6-7 for the bare and maize plots respectively. It can be seen that, it takes 23 months and 19 months for the concentration peak to reach the groundwater table under the bare and maize plot conditions. The difference in the arrival time was due to difference in the drainage rates which is 1.44 mm/d for the bare plots and 2.06 mm/d for the maize plots.

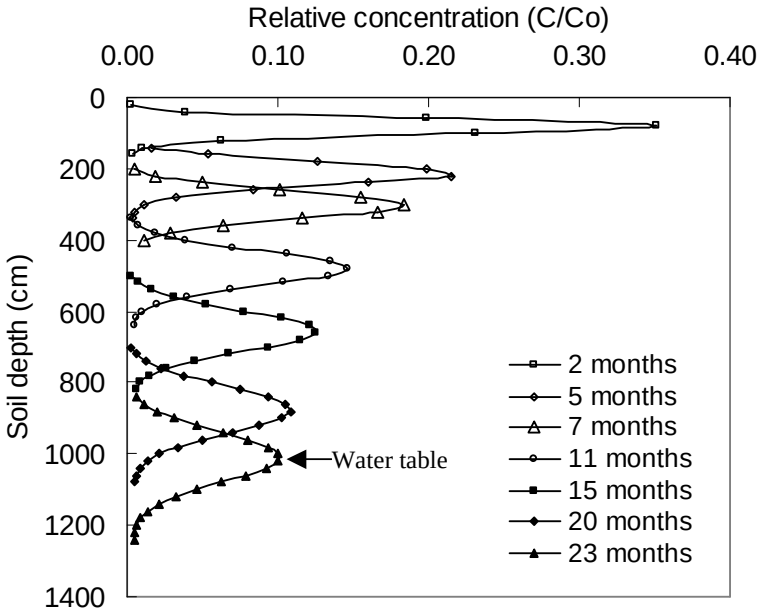

Figure 6-6 Simulated bromide concentration profiles using the pore-water velocity (v = 1.47 cm d^{-1}) and the CDE estimated average dispersion coefficient (D = 3.65 cm^2 d^{-1}).

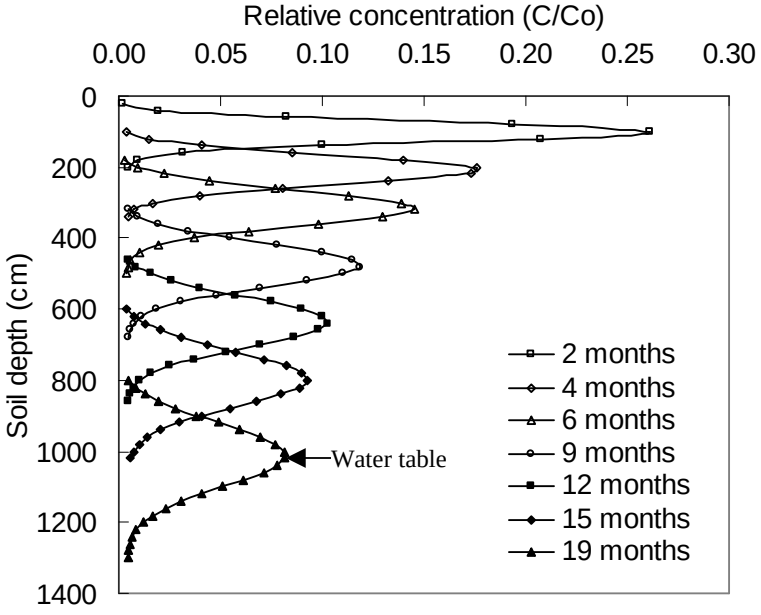

Figure 6-7 Simulated bromide concentration profiles using the pore-water velocity (v = 1.78 cm d^{-1}) and the CDE estimated average dispersion coefficient (D = 6.96 cm^2 d^{-1}).

6.3 THREE-DIMENSIONAL TRANSPORT

6.3.1 Introduction

As implied by the name, one-dimensional solute transport models in porous media only consider dispersion in one direction, while dispersion is a three-dimensional phenomenon. The true transport of solutes in soils therefore should preferably be studied with three-dimensional transport models. Unfortunately, field studies related to the three-dimensional nature of solute transport in soil are relatively rare (Ellsworth *et al*., 1991). The reason for this is not that three-dimensional models do not exist, but that the validation of the models through field observations is a formidable task. In fact, even the more elementary problem of predicting the mean solute position as a function of time is extremely difficult in the unsaturated zone (Jaynes *et al*., 1988; Butters *et al*., 1989). One of the difficulties in using three-dimensional models is the determination of the dispersion coefficient, **D**, which is a non-symmetric tensor. The practice to express **D** in terms of the three components of the pore-water velocity, ***v***, and *longitudinal* and *transverse* dispersivities, α_L and α_T, does not really simplify the matter, since both parameters are scale-dependent, and it is difficult to determine α_T from column experiments. It is known though that transverse dispersivity is usually smaller than the longitudinal dispersivity. The transverse dispersivities used in three-dimensional models is consequently often taken as a fraction (0.05 to 0.2) of the longitudinal dispersivity (Freeze and Cherry, 1979; de Marsily, 1986). This approach will also be followed in the discussion of the analytical solutions derived by Leij *et al*. (1991) for solute transport in a three-dimensional porous media and implemented in the code 3DADE below where the model is applied to the bromide experiments.

6.3.2 Three-Dimensional Simulation

The experimental and fitting procedures used in the bromide experiment used to determine the vertical component of the velocity and the longitudinal transmissivity are described in Chapter 3 and will not be repeated here. The source geometry used for the simulations is illustrated in Figure 6-8 and the initial and boundary conditions by

$$\begin{aligned} c(x,y,z,0) &= 0 \\ c(x,y,z,t) &= c_0 \qquad (|x|<a, |y|<b, z=0, t \le t_0) \\ &= 0 \qquad \text{Otherwise} \\ \partial c/\partial t\big|_{z\to\infty} &= 0 \end{aligned} \tag{6.3}$$

The transverse dispersion coefficients, D_x and D_y, required by the three-dimensional model equation

$$\frac{\partial c}{\partial t} = D_x \frac{\partial^2 c}{\partial x^2} + D_y \frac{\partial^2 c}{\partial y^2} + D_z \frac{\partial^2 c}{\partial z^2} - v \frac{\partial c}{\partial z} \qquad (6.4)$$

were taken as 10% of the longitudinal dispersion coefficients D_x.

The simulations in Figures 6-10, 6-11, 6-12, and 6-13 were performed using the CDE fitted parameters for the bromide experiments in Table 3-2 at 27.5 h. The initial concentration values were normalized relative to the initial input concentration as illustrated in Figure 6-9.

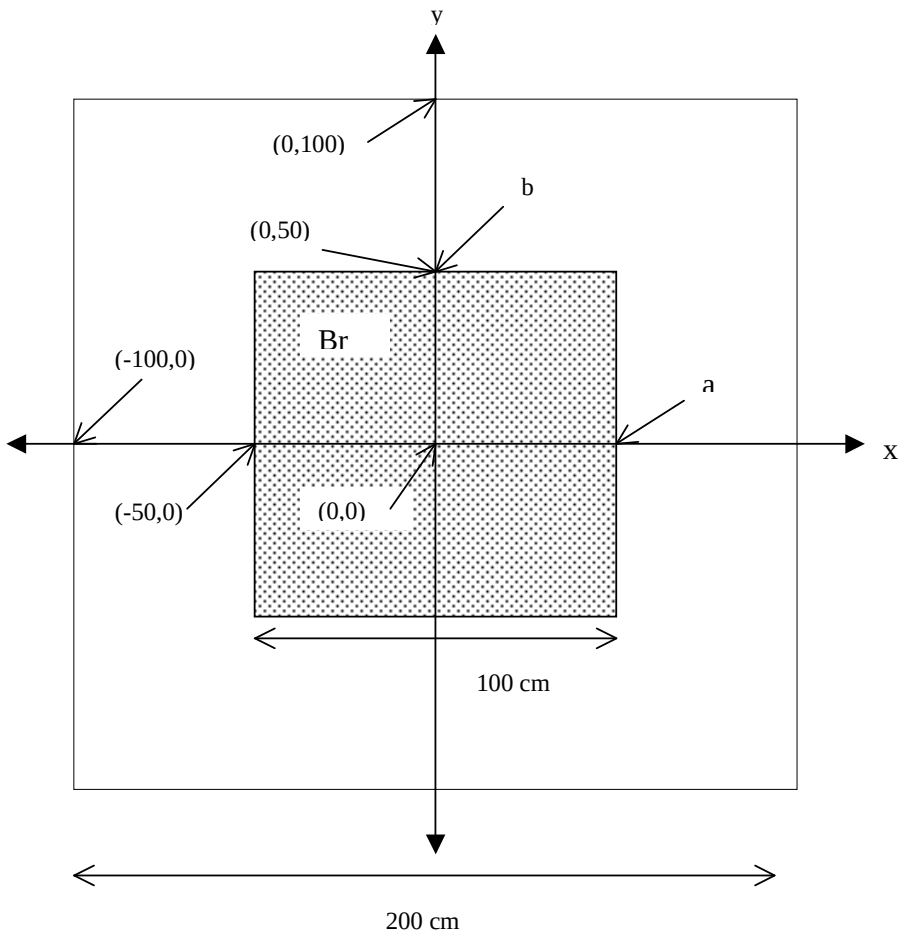

Figure 6-8 Plan view of the soil patch and the surrounding area used in the three-dimensional simulation of bromide transport.

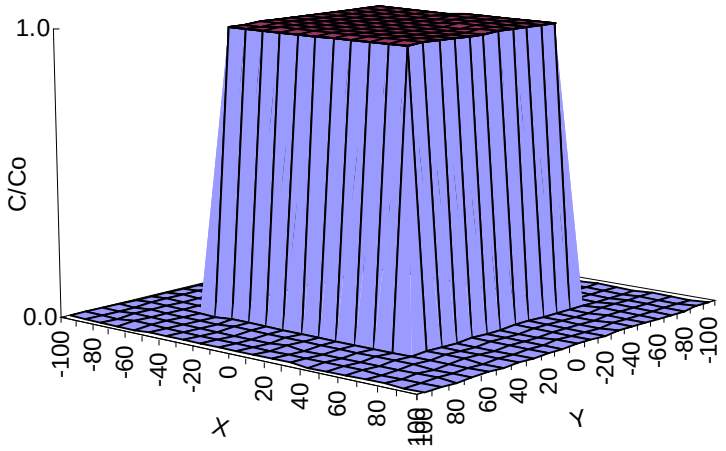

Figure 6-9 The initial bromide concentration in the X-Y plane at the soil surface used in the three-dimensional simulation with 3DADE.

Profiles of the simulated bromide concentrations at a few points in the *xy*-plane are presented in Figure 6-10. Simulated concentration profile at (40 cm, 40 cm) was almost the same as the simulated concentration profile at (0, 0) and therefore was not shown in this figure. Concentration profile simulated at (55 cm, 55 cm) was very low and is also not presented here. As shown by these profiles the peak concentration, which occurred at a depth of 50 cm, decreased rapidly from the inner (40 cm, 40 cm) square towards the boundary of the patch at (*x*, *y*, *z*) = (50 cm, 50 cm, 0 cm). The concentration profiles simulated at the coordinates (0, 0) and (45 cm, 45 cm) were very similar. However, the concentration decreased substantially at the farthest point of the plot (50 cm, 50 cm), which indicates that bromide concentration was uniform over the inner 80 cm x 80 cm plot area.

Simulated bromide concentration at different depths of the soil profile along the y-axis is presented in Figure 6-11. It can be observed that the concentration profiles at different depths have similar patterns and the curves are plateau especially in the inner (80 cm x 80 cm) area of the plot. The maximum concentration was at 50 cm depth. For ease of visualisation, the simulated concentrations were presented in a three-dimensional form in Figure 6-12. In Figure 6-12a it was intended to more clearly show concentration variation with depth (front side). The peak concentration was at 50 cm depth and it falls sharply at shallower depths and gradually at deeper depths. Almost all of the bromide was in the depth range of 30-90 cm at the time of sampling. In Figure 6-12b from the observation along the y-axis, it can be seen that bromide concentration was almost uniform in the

inner area (80 cm x 80 cm) of plot and decreases rapidly as one approaches the boundaries.

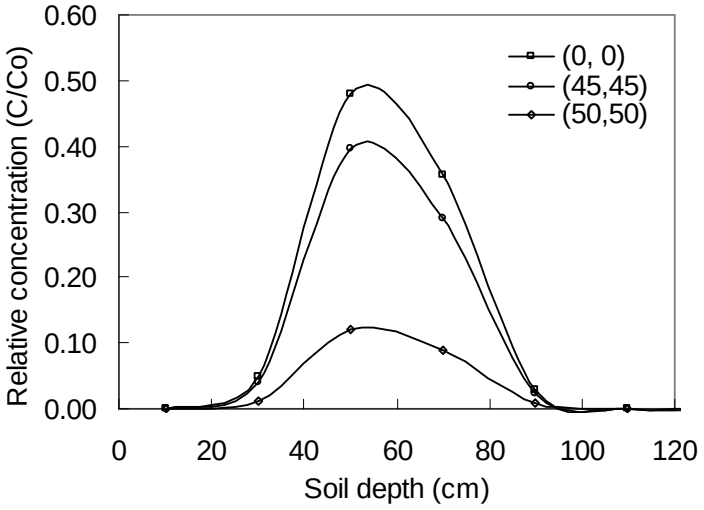

Figure 6-10 Simulated bromide concentration profiles as a function of depth at three points along a line through the centre of the plot and the corner.

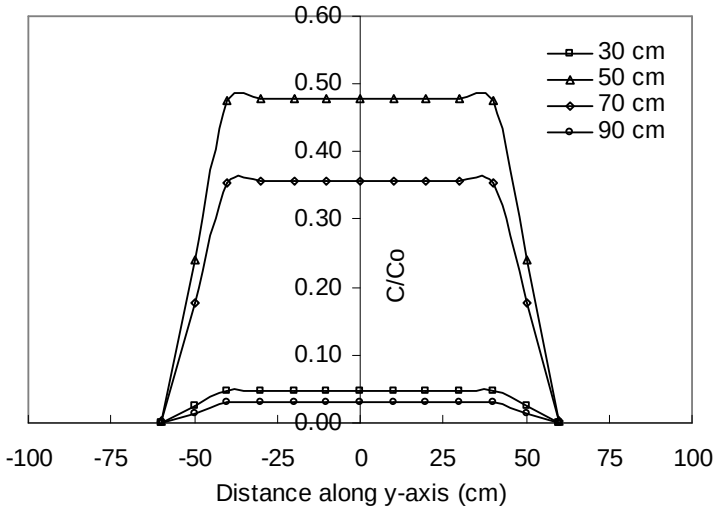

Figure 6-11 Simulated bromide concentrations at different depths of the soil profile along the y-axis.

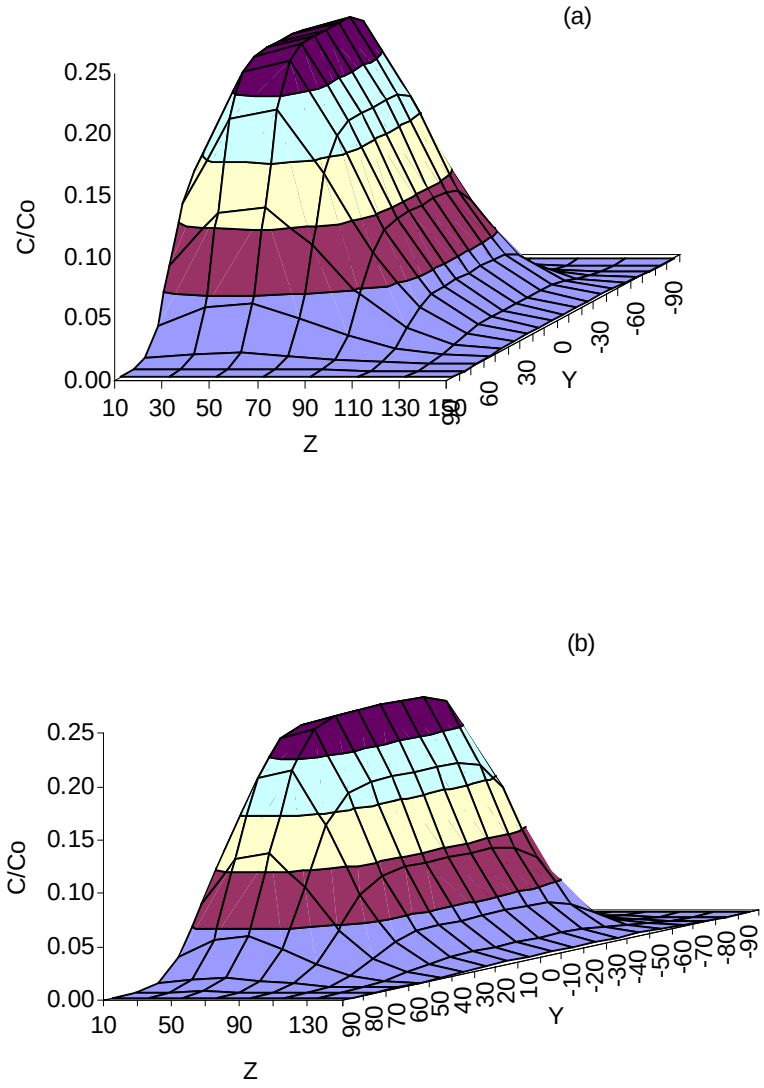

Figure 6-12 Three-dimensional representation of simulated bromide concentration at different depths of the soil profile along the y-axis.

In the previous sections, the simulations were done assuming the value of transverse dispersion coefficient to be 10 percent of the longitudinal one. Figure 6-13 shows the simulated concentration at 70 cm depth along the y-axis for two extreme values of D_y (5%D_z and 100%D_z). It can be observed that the two concentration profiles differ as one goes away from the centre of the plot. Under the assumption of $D_y = D_z$, concentration becomes non-uniform starting from distance of 20 cm from the centre of the plot. The bromide also spreads to a distance as far as 25 cm outside of the plot boundary.

Therefore since transverse dispersion causes tracers to spread outside of the experimental plot area and only samples takes close to the centre of the plot are representative of the plot, it is wise to take composite samples. This can be done by taking one sample close to the centre of the plot and the other close to the boundary of the plot as has been done in this study (Chapter 3).

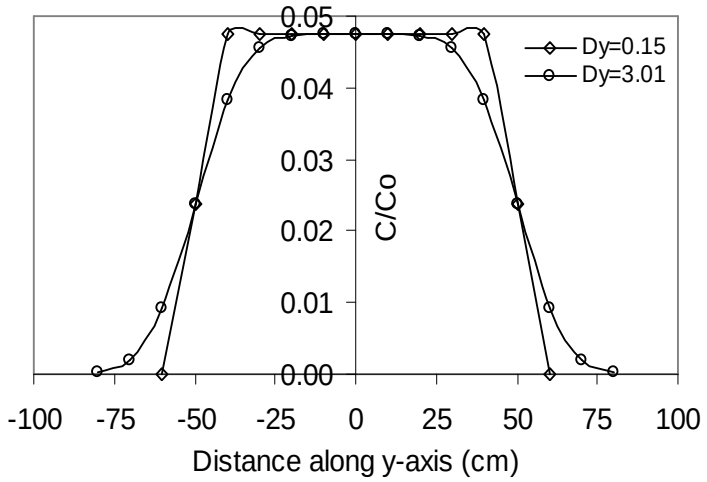

Figure 6-13 Simulated bromide concentrations using two values of transverse dispersion coefficients D_y (= 5%D_z and 100%D_z) where *Dz* is the longitudinal dispersion coefficient.

6.4 CONCLUSIONS

Transport parameters determined from tracer studies at shallow depths can be used to simulate solute transport to a deeper groundwater table. In the Bainsvlei soil it was found that it takes several years before a mobile chemical such as nitrate reaches the groundwater table under cropped soil and rainfed conditions. In cases where there is no data on solute transport parameters for a given soil, pore-water velocity calculated from drainage rata and soil water content, is a good estimate of the concentration peak movement especially in sandy and sandy loam soils. From the experiment on the Bainsvlei soil, it was observed that pore-water velocity could be used to get a somewhat conservative estimate of nitrate arrival time at the water table. Drainage rate can be obtained from water balance data: rainfall/irrigation, evaporation/evapotranspiration and change in soil water storage. If in addition to the pore water velocity we have dispersivity, it is possible to determine the relative concentration profile at different depths down to the water table using analytical models. Under irrigated conditions, where deep percolation

below the plant roots is high, it takes relatively shorter time for the solute concentration peak to reach the groundwater as indicated in the Dire Dawa experiment.

Determining transverse dispersion coefficient is relatively more difficult compared to the longitudinal one. However, once longitudinal dispersion coefficient is determined, assuming transverse dispersion coefficient to be a fraction of longitudinal dispersion coefficient (10%, for example), it is possible to simulate three-dimensional transport. From the simulation results when D_y is taken as 10%D_z, it was observed that bromide concentration is uniform over the inner (80 cm x 80 cm) of the (100 cm x 100 cm) plot area and decreases rapidly towards the boundary of the plot. When D_y was taken to be equal with D_z, the simulation results indicated that the concentration is uniform only in the inner (40 cm x 40 cm) of the plot area and the bromide spreads 25 cm outside of the plot area. Therefore, to avoid non-representative sampling during small plot tracer studies, it is advisable to take composite samples. This can be done by taking one sample close to the centre of the plot and another close to the boundary of the plot and mixing the two samples to get a single sample.

It is important to note that nitrate leached below the crop root zone may take several years to reach the groundwater. Even a once off application of nitrate can therefore affect the groundwater quality for many years.

CHAPTER 7

CONCLUSIONS AND RECOMMENDATIONS

7.1 INTRODUCTION

Concern about water quality and not only quantity is increasing as the quality of many of the world's surface and groundwater resources are dwindling due to pollution. The main sources of pollution are municipal solid and liquid wastes, industrial wastes, and agriculture. Animal wastes from feedlots and agrochemicals are the major agricultural pollution sources. The agrochemicals of importance in the pollution of groundwater sources include fertilizers, pesticides and herbicides. The use of fertilizers, especially nitrogen fertilizer, is increasing in developing countries with the hope of meeting the growing food and fibre demand of the increasing population. In some countries, there are no guidelines for the application of fertilizers per unit area for a given crop. Farmers consequently tend to apply large quantities of fertilizer, with the assumption that 'yield increases in direct proportion to the quantity of applied fertilizers'. The leaching of excess fertilizer, especially during periods of high rainfall or irrigation not only causes a loss to the farmer, but also poses a threat to the quality of the subsurface water. This leaching varies from one soil type to another and from one climate type to another.

Since nitrogen experiences complex and interdependent transformations in the soil, it is not easy to isolate and study the leaching component of this fertilizer. Conservative tracers, which are not produced in the soil, are therefore often used to study the maximum leaching potential of nitrogen in agricultural soils. This study investigated the movement of bromide and nitrogen under steady and transient state conditions in bare soils and soils planted with crops at two locations with different soil and climatic conditions. These experiments are briefly summarized in Section 7.2, while Sections 7.3 and 7.4 summarize some general conclusions and recommendations derived from the experiments.

7.2 SUMMARY

The first step in the investigation was to determine the hydraulic properties, such as bulk density, saturated hydraulic conductivity and saturated water content, of the Bainsvlei soil in South Africa *in situ*. The soil water content and matric potential were monitored at different depths of the soil profile with a neutron probe and a set of tensiometers. These observations and the models of Libardi *et al*. (1980), Chong *et al*. (1981), and van Genuchten (1980) were also used to estimate the unsaturated hydraulic conductivity of

different soil layers, which is very important for mass transport in the vadoze zone, where the pollution of groundwater resources usually originates. The values determined form these models were then compared with values derived from the 'internal drainage method' of Hillel *et al*. (1972) in terms of Willmott's index of agreement.

Leaching of solutes in the Bainsvlei soil was studied under steady state conditions using Br^- as a tracer and continuous application of water with a rainfall simulator at rates of 5.41 mm h^{-1} and 3.27 mm h^{-1} to a patch of soil. (100 x 100) cm^2. The concentration of Br^- was monitored by taking soil samples at different depths and times. Analytical solutions of the convective-dispersive and stochastic stream tube models in the CXTFIT program of Toride *et al*. (1995) were used to determine solute transport parameters.

The motion of water in natural soils is usually transient in nature, because of the non-uniformity of rainfall and evaporation. A transient state experiment was therefore also conducted by applying water at the beginning of each week for one month with sprinklers to another (200 x 200) cm^2 patch of soil. The solute transport parameters were again determined with the steady state models in CXTFIT, using cumulative drainage, instead of time, as the independent variable. The movement of Br^- and NO_3^--N were also compared on a bare plot in the Bainsvlei soil under natural rainfall and evaporation conditions for a period of 7 months.

Bromide and NO_3^--N movement was also investigated in six plots, three bare and three planted with maize, under natural climatic conditions at Dire Dawa, Ethiopia, from March 2001 to May 2001. Since the natural rainfall was not sufficient to sustain the maize, the plots were irrigated from time to time. Soil and plant samples were taken several times during the growing season and analysed for Br^- and NO_3^--N concentration.

7.3 CONCLUSIONS

The comparison of the different models for the computation of the unsaturated hydraulic conductivities showed that the model of van Genuchten (1980) described the hydraulic conductivity of the Bainsvlei soil better than the power-function-based models of Chong *et al*. (1981) and the 'simplified methods of Libardi' (Libardi *et al*., 1980).

Solute transport in the weekly structured Bainsvlei soil did not show preferential transport and can therefore be considered as piston flow. The transport parameters obtained from the deterministic convective-dispersive equation and stochastic stream tube models did not differ significantly in the experiments performed on the Bainsvlei soil. A sensitivity analysis of the results confirmed that convection determines the position of the peak

concentration during leaching, while dispersion determines the spreading of the solute. As could have been expected, an increase in the intensity of rainfall caused an increase in the leaching rate.

The continuous application of rainfall resulted in higher leaching rates than the intermittent application of the same volume of water in the Bainsvlei soil. The Br^- therefore moved deeper into the soil column under steady state conditions than transient conditions. It can generally be said that the rate at which a solute leaches from a soil is therefore determined by the volume of water applied and the frequency with which the water is applied.

It was found that Br^- and NO_3^--N move very similarly in the Bainsvlei soil. At the end of a rainy season, half of the applied NO_3^--N leached below the sampling depth of 160 cm in this soil. These results and the observation that the NO_3^--N concentration in water taken from a borehole on the farm was almost three times higher than the WHO health limit, indicate that NO_3^--N leaching in the area is very high.

The high natural concentration of nitrogen in the soils at Dire Dawa, made it impossible to trace the movement of applied NO_3^--N in the experiment carried out there. However, Br^- concentration profiles revealed distinct peaks on both bare and maize plots. In this experiment, the solutes did not leach out of the sampling depth of 160 cm, which represents the root zone of vegetables and field crops, even though the total amount of water applied during the study period was higher than the mean annual rainfall in the area.

The previous results indicate that it can take several years before applied agrochemicals reach the groundwater. For example, substitution of the transport parameters determined from the tracer experiments and drainage fluxes under cropped conditions on the Bainsvlei soil into the CDE model, showed that it will take an agrochemical 16 y to reach the groundwater table at a depth of 600 cm under a drainage flux of 0.20 mm d^{-1} and 65 y for a flux of 0.05 mm d^{-1}.

The leaching of solutes is always a three-dimensional phenomenon in the field. It was therefore thought worthwhile to investigate the validity of the one-dimensional models used in this study, by simulating the leaching observed during the steady state experiment at Bainsvlei with the three-dimensional model 3DADE of Leij and Bradford (1994). Since it is very difficult to determine the transverse dispersion coefficient in the field, no attempt was made to determine it in this investigation. The transverse dispersion coefficient used in the model was consequently simply equated to one-tenth of the

longitudinal dispersion coefficient derived from the one-dimensional tracer experiments—a common assumption in groundwater investigations. This model showed that the concentrations remained fairly constant within the inner (80 x 80) cm^2 of the patch used in the experiment, but then decreased significantly and spread beyond the boundary of the patch. It is therefore very important that special attention be given to the selection of sampling positions in field investigations of solute transport and analysing the results with one-dimensional models.

The experiments performed at Bainsvlei indicated that Br^- could be used with confidence as a substitute for nitrogen in studies of the leaching of nitrogen and perhaps other agrochemicals that do not adsorbed to the soil. However, the experiments at Dire Dawa clearly showed that it couldn't be used to study biological, chemical, and physical reactions of the chemicals with the soil or crops.

Nitrate contamination of groundwater can be minimised by carefully controlling the timing and mass of nitrogen applied, efficient irrigation systems, and other management practices that reduce leaching of nitrate. Since leaching is proportional to the deep percolating rate of water, the infiltration and percolation of water could be reduced through efficient agricultural water management practices. Other management practices that could reduce the leaching losses of nitrate include the synchronization of the application of the nitrogen with the crop's needs and reducing the excessive application of nitrogen through a soil or a plant-tissue nitrogen test.

One approach to reduce the leaching of nitrate (or any other fertilizer) is to analyse the quantitative effects local conditions (e.g. soil, crop rotation, groundwater depth and climate) may have on the potential yield of a crop and develop what may be called a *crop development stage-specific fertilization scheme* (CDSSFS), similar to existing climatologically based irrigation scheduling models. Such a scheme can be developed by determining the potential yield of the crop as a function of the soil and climatic conditions, and then split the application of the fertilizer over the growing season of the crop. This may entail a determination of the soil texture, regular tests for residual fertilizers in the soil and the installation of water and other meters to accurately record the volume of irrigation water applied and the weather conditions. The observations and models discussed in this thesis could be very useful in developing such a CDSSFS.

7.4 RECOMMENDATIONS

The experiments at Dire Dawa have shown that crops and the natural background content of a chemical could influence the transport of an agrochemical significantly. It is

therefore suggested that the experiments at the Bainsvlei site be repeated under cropped soil conditions to verify the relation between the leaching of Br^- and NO_3^--N observed for bare soil, before applying the relation in practice. The same investigation could also be used to study the deep percolation flux and its dependence on the distribution of crop roots in detail. Such experiments could also be used to further elucidate the dependence of the rate at which a crop takes up a fertilizer as a function of the vegetative phase of the plants, the supply of water and perhaps the microclimate in general.

The preliminary three-dimensional model used in this study to simulate the motion of a solute in the field indicated that transverse dispersion might have a significant effect on the leaching of an agrochemical. It is therefore recommended that more attention should be paid to three-dimensional dispersion and matrix diffusion in future studies of the leaching of agrochemicals. One approach that could be followed for this purpose would be to take three samples—one near the centre of the experimental plot, one near the boundary of the plot and one slightly outside the boundary of the plot. Such samples could also be used to determine to what extent can the leaching of agrochemicals be modelled with one-dimensional models.

REFERENCES

Agrawal, R.P., Jhorar, B.S., Dhankar, J.S. and Raj, M. (1987) Compaction of sandy soils for irrigation management. *Irrig. Sci.*, 8, 227-232.

Allen, R.G., Pereira, L.S., Raes, D. and Smith, M. (1998) *Crop evpotranspiration-Guidelines for computing crop water requirements*. FAO Irrig. and Drain. Paper No. 56, FAO, Rome, Italy, 300 pp.

Allison, G.B., and Hughes, M.W. (1978) The use of environmental chloride and tritium to estimate total recharge to an unconfined aquifer. *Aust. J. Soil Res*., **16**, 181-195.

Amoozegard-Fard, A., Nielsen, D.R. and Warrick, A.W. (1982) Soil solute concentration distributions for spatially varying pore-water velocities and apparent diffusion coefficients. *Soil Sci. Soc. Am. Proc*., **46**, 3-8.

Ashraf, M.S., Izadi, B., King, B. (1997) Transport of bromide under intermittent and continuous ponding conditions. *J. Environ. Qual*., **26,** 69-75.

Ayers, R.S. and Branson, R.L. (1973) Nitrates in the upper Santa Ana River basin in relation to groundwater pollution. *Cal. Agr. Exper. Stn. Bull*. **861**, 1-60.

Baker, J.L. and Laflen, J.M. (1982) Effects of corn residue and fertiliser management on soluble nutrient runoff losses. *Trans ASAE*, **25**, 344-348.

Bandarayake, W.M., Butters, G.L., Hamdi, M., Prieksat, M. and Ellsworth, T.R. (1999). Irrigation and tillage management effects on solute movement. *Soil and Tillage Res*. **46**, 165-173.

Beese, F., and Wierenga, P.J. (1980) Solute transport through soil with adsorption and root water uptake computed with a transient and a constant flow model. *Soil Sci*., **129**, 245-252.

Bennie, A.T.P., Strydom, M.G. and Very, H.S. (1998) The application of computer models for agricultural water management on ecotope level (Africans). Pp 42-45. *In*: Report No 625/1/98. *Water Research Commission*, Pretoria, South Africa.

Bicki, T.J. and Guo, L. (1991) Tillage and simulated rainfall intensity effect on bromide movement in an argiudoll. *Soil Sci. Soc. Am. J*., **55**, 794-799.

Biggar, J.W. and Nielsen, D.R. (1976) Spatial variability of the leaching characteristics of a field soil. *Water Resour. Res*., **12**, 78-84.

Black, T.A., Gardner, W.R. and Thurtell, G.W. (1969) Prediction of evaporation, drainage and soil water storage for a bare soil. *Soil Sci. Soc. Am. Proc*., **33**, 655-660.

Botha, J. F. (1986) Modelling contaminant transport using site specific data from Vaalputs. In: Proceedings of the *International Conference on the treatment and containment of radioactive waste, and it disposal in arid environments, Radwaste'86.*

L. C. Ainslie (eds.) Cape Town. 149–162. Atomic Energy Corporation of South Africa, P.O. Box 582, Pretoria.

Botha, J.F. (1988) *RIEN. A program to fit water retention data*. Institute for Groundwater Studies, The University of the Orange Free State, South Africa.

Botha, J. F. (1996) *Principles of Groundwater Motion*. Unpublished Lecture Notes. Institute for Groundwater Studies, University of the Orange Free State, P.O. Box 339, Bloemfontein 9300.

Bouwer, H. and Jackson, R.D. (1974) *Determining soil properties*, In Drainage for Agriculture, ed. J. van Schilfgarde. Agronomy., **17**, 611-672.

Bowman, R.S. (1984) Evaluation of some new tracers for soil water studies. *Soil Sci. Soc. Am. J*., **48**, 987-993.

Bowman, R.S. and Rice, R.C. (1986) Transport of conservative tracers in the field under intermittent flood irrigation. *Water Resour. Res*., **22**, 1531-1536.

Brenner, H. (1962) The diffusion model of longitudinal mixing in beds of finite length. Numerical values. *Chem. Eng. Sci*., **17**, 229-243.

Bresler, E. and Dagan, G. (1979) Solute dispersion in unsaturated heterogeneous soil at field scale: II. Applications, *Soil Sci. Soc. Am. J*., **43**, 467-472.

Bresler, E. and Dagan, G. (1981) Convective and pore scale dispersive solute transport in unsaturated heterogonous fields. *Water Resour. Res*., **17**, 1683-1693.

Broadbent, F.F. and Clark, F.E. (1965) *Denitrification*. In: J.W. Bartholomew and F.E. Clark (Eds.), Soil Nitrogen, Agronomy Monograph **10**, American Society Agronomy, Madison, WI.

Bronswijk, J.J.B, Hamminga, W. and Oostindie, K. (1995) Field-scale solute transport in a heavy clay soil. *Water Resour. Res.*, **31**, 517-526.

Butters, G.L. and Jury, W.A. (1989) Field scale transport of bromide in an unsaturated soil: 2. Dispersion modelling. *Water Resour. Res*., **25**, 1583-1589.

Butters, G.L., Jury, W.A. and Ernst, F.F. (1989) Field scale transport of bromide in an unsaturated soil. 1. Experimental methodology and results. *Water Resour. Res*., **25**, 1575-1581.

Cameron, D.R., Kowalenko, C.G. and Campbell, C.A. (1979) Factors affecting nitrate-nitrogen and chloride leaching variability in a field plot. *Soil Sci. Soc. Am. J*., **43**, 455-460.

Cameron, K.C. and Haynes, R.J. (1986) *Retention and movement of nitrogen in soils*. Pp. 166-241. *In*: Mineral nitrogen in the plant/soil system, Haynes, R.J. ed. New York, Academic Press.

Chiang, W. and Kinzelbach, W. (1998) Processing Modflow: A simulation system for modeling groundwater flow and pollution.

Chong, S.K., Green, R.E., and Ahuja, L.R. (1981) Simple in situ determination of hydraulic conductivity by power function description of drainage. *Water Resour. Res*., **17**, 1109-1114.

Claassens, A.H. and van Der Watt, H.V.H. (1993) An inexpensive, portable rain simulator: construction and test data. *S. Afr. J. Plant Soil.*, **10**, 6-11.

Cleary, R.W. and Adrian, D.D. (1973) Analytical solution of the convective-dispersive equation for cation adsorption in soils. *Soil Sci. Soc. Am. Proc*., **37**, 197-199.

Clothier, B.E. and Green, S.R. (1994) Root zone processes and efficient use of irrigation water. *Agric. Water Mgmt*., **25**, 1-12.

Dagan, G. (1993) *The Bresler-Dagan model of flow and transport: Recent theoretical developments. In*: Water flow and solute transport in soils, edited by D. Russo and G. Dagan, Springer-Verlag, Berlin, Heidelberg.

Dagan, G. and Bresler, E. (1979) Solute dispersion and in unsaturated heterogeneous soil at field scale, 1, Theory. *Soil Sci. Soc. Am. J*., **43**, 461-467.

Danckwerts, P.V. (1953) Continuous flow systems Chem. Eng., **2**, 1-13.

Davidson, J.M., Stone, L.R., Nielsen, D.R. and Larue, M.E. (1969) Field measurement and use of soil water properties. *Water Resour. Res*., **5**, 1312-1321.

De Marsily, C. (1986) *Quantitative hydrogeology: Groundwater hydrology for engineers*. Academic press, Inc.

Ellsworth, T.E., Jury, W.A., Ernst, F.E. and Shouse, P.J. (1991) A three dimensional field study of solute leaching through unsaturated soil. I. Methodology, mass balance, and mean transport. *Water Resour. Res*., **27**, 951-966.

Fleming, J.B. and Butters, G.L. (1995) Bromide transport detection in tilled and non-tilled soil: Solution samplers vs. soil cores. Soil Sci. Soc. Am. J., **59**, 1207-1216.

Flury, M. and Papritz, A. (1993) Bromide in the natural environment: Occurrence and Toxicity. *J. Environ. Qual*., **22**, 747-758.

Freeze, R.A. and Cherry, J.A. (1979) *Groundwater*. Prentice-Hall, Inc.

Fried, J.J. (1975) Groundwater Pollution. Elsevier, New York.

Fuller, K.D. and Moolman, J.H. (1989) An evaluation of simplified field methods used for estimating soil hydraulic conductivity. *S. Afr. J. Plant Soil*., **6**, 64-69.

Gardner, W.R., Hillel, D.I. and Benyamini, I. (1970) Post irrigation movement of soil water: I. Redistribution. *Water Resour. Res*., **6**, 851-861.

Gee, G.W. and Hillel, D. (1988) Groundwater recharge in arid regions: Review and critique of estimation methods, Hydrol. Process., **2**, 255-266.

Gish, T.J. and Coffman, C.B. (1987) Solute transport under no-till corn. *Trans. ASAE*., **30**, 1358-1363.

Gish, T.J. and Jury, W.A. (1982) Estimating solute travel times through a crop root zone. *Soil Sci*., **133**, 124-130.

Hillel, D., Krentos, V.D. and Steylianou, Y. (1972) Procedure and test of an internal drainage method for measuring soil hydraulic characteristics *in situ*. *Soil Sci*., **114**(5), 395-400.

Hong, C.W., Katyal, J.C. and Vlek, P.L.G. (1992) Losses and utilization of nitrogen by sorghum as affected by depth of a swelling clay soil. *J Agron Crop Sci*., **168,** 263-271.

Iragavarapu, T.K., Posner, J.L. and Bubenzer, G.D. (1998) The effect of various crops on bromide leaching to shallow groundwater under natural rainfall conditions. *J. Soil and Water Cons*., **53**, 146-151.

Izadi, B., King, B., Westermann, D. and McCann, I. (1993) Field scale transport of bromide under variable conditions observed in a furrow irrigated field. *Trans. ASAE*, **36**, 1679-1686.

Jackson, R.J., Idso, S.B. and Reginato, R.J. (1976) Calculation of evaporation rates during the transition from energy-limiting to soil-limiting phases using albedo data. *Water Resour. Res*., **12,** 23-26.

Jardin, P.M., Wilson, G.V. and Luxmoore, R.J. (1990) Unsaturated solute transport through a forest soil during rain storm events. *Geoderma*, **46**, 103-118.

Jarvis, N.J., Bergstrom, L. and Dik, P.E. (1991) Modelling water and solute transport in macroporous soil. II. Chloride breakthrough under non-steady flow. *J. Soil Sci*., **42**, 71-81.

Javandel, I., Doughty, C. and Tsang, C.-F. (1984) *Groundwater Transport: Handbook of Mathematical Models*. Water Resources Monographs Series. Vol. 10. American Geophysical Union, Washington, D.C.

Jaynes, D.B. (1991) Field study of bromacil transport under continuous flood irrigation. *Soil Sci. Soc. Am. J*., **55**, 658-664.

Jaynes, D.B. and Rice, R.C. (1993) Transport of solutes as affected by irrigation method. *Soil Sci. Soc. Am. J*., **57**, 1348-1353.

Jaynes, D.B., Bowman, R.S. and Rice, R.C. (1988) Transport of conservative tracer in the field under continuous flood irrigation. *Soil Sci. Soc. Am. J*., **52**, 618-624.

Jaynes, D.B, Rice, R.C. and Bowman, R.S. (1988) Independent calibration of a mechanistic-stochastic model for field scale solute transport under flood irrigation. *Soil Sci. Soc. Am. J*., **52**, 1541-1546.

Jemison, J.M., Jr., and Fox, R.H. (1991) Corn uptake of bromide under greenhouse and field conditions. *Commun. Soil Sci. Plant Anal*., **22**, 283-197.

Jones, A.J. and Wagenet, R.J. (1984) In situ estimation of hydraulic conductivity using simplified methods. *Water Resour. Res*., **20**, 1620-1626.

Jones, M.J. and Watson, K.K. (1987) Effect of soil water hysteresis on solute movement during intermittent leaching. *Water Resour. Res*., **23**, 1251-1256.

Jury, W.A. (1982) Simulation of solute transport using a transfer function model. *Water Resour. Res*., **18**, 363-368.

Jurry, W.A. (1983) Chemical transport modelling: current approaches and unresolved problems. In: D.W. Nelson, D.E. Elrich, and K.K. Tanji (Eds.), *Chemical mobility and reactivity in soil systems*. Special publication No. **42**. American Society of Agronomy, Madison, WI.

Jury, W.A. and Fluhler, H. (1992) Transport of chemicals through soils: Mechanisms, models and field applications. *Adv. Agron*., **47**, 141-201.

Jury, W.A., Gardner, W.R. and Gardner, W.H. (1991) *Soil Physics*. John Wiley, New York.

Jury, W.A. and Roth, K. (1990) *Transfer functions and solute movement through soils: Theory and Applications,* Birkhauser, Basel, Switzerland.

Jury, W.A., Sposito, G. and White, R.E. (1986) A transfer function model of solute transport through soil, 1, Fundamental concepts. *Water Resour. Res*., **22**, 243-247.

Jury, W.A., Stolzy, L.H. and Shouse, P. (1982) A field test of the transfer function model for predicting solute transport. Water Resour. Res., **18**, 369-375.

Kanchanasut, P. and Scotter, D.R. (1982) Leaching patterns in soil under pasture and crop. *Aust. J. Soil Res*., **20**, 193-202.

Kelly, B.P. and Pomes, M.L. (1998) Preferential flow and transport of nitrate and bromide in claypan soil. *Groundwate*r, **36**, 484-494.

Knight, H.D. and Reina-Guerra, M. (1976) Intoxication of cattle with sodium bromide-contaminated feed. *Am. J. Vet. Res*., **38**, 407-409.

Kung, K.J.S. (1990) Influence of plant uptake on the performance of bromide tracer. *Soil Sci. Soc. Am. J*., **54**, 975-979.

Kutilek, M. and Nielsen, D.R. (1994) *Soil Hydrology*. CATENA VERLAG.

Laker, M.C. (1985). The utilization of heavier soils for irrigation and using the water storage capacities of soils to reduce design peaks. SABI congress, Christiana (South Africa), Pp. 12.

Lapidus, L. and Amundson, N.R. (1952) Mathematics of adsorption in beds. IV. The effect of longitudinal diffusion in ion exchange chromatographic columns. *J. Phys. Chem*., **36**, 984-988.

Leij, F.J. and Bradford, S.A. (1994) 3DADE: *A computer code for evaluating three-dimensional equilibrium solute transport in porous media*. U.S. Salinity Lab. Research Rep. 134. Riverside, CA.

Leij, F.J., Skaggs, T.H., and van Genuchten, M.Th. (1991) Analytical solutions for solute transport in three-dimensional semi-infinite porous media. *Water Resour. Res*., **27**, 2719-2733.

Libardi, P.L., Reichardt, K., Nielsen, D.R., and Biggar, J.W. (1980) Simple field methods of estimating soil hydraulic conductivity. *Soil Sci. Soc. Am. J*., **44**, 3-7.

Lindstrom, F.T. (1976) Pulsed dispersion of trace chemical concentration in saturated sorbing porous medium. *Water Resour. Res*., **12**, 229-238.

Luckner, L. and Shestakow, W. M. (1991) *Migration Processes in the Soil and Groundwater Zone*. Lewis Publishers, Inc., Chelsea, Michigan.

McLay, C.D.A., Cameron, K.C. and McLaren, R.G. (1991) Effect of time of application and continuity of rainfall on leaching of surface-applied nutrients. *Aust. J. Soil Res*., **29**, 1-9.

Meek, B.D., Rechel, E.R., Carter, L.M., Detar, W.R. and Urie, A.L. (1992) Infiltration rate of a sandy loam soil: Effects of traffic, tillage, and plant roots. *Soil Sci. Soc. Am. J*., **56**, 908-913.

Menzer, R.E. (1991) *Water and soil pollutants*. Pp . 872-902 *In*: Casarett and Doull's toxicology: the basic science of poisons, 4th ed., Amdur, M.D.; Doull, J.; Klaassen, C.D. *ed*. New York, MacMillan Publishing Company.

Meyer-Windel, S., Lennartz, B.. and Widmoser, P. (1999) Bromide and herbicide transport under steady-state and transient flow conditions. *European Journal of Soil Science*, **50**, 23-33.

Myers, J.L. Wagger, M.G. and Leidy, R.B. (1995) Chemical movement in relation to tillage system and simulated rainfall intensity. *J. Environ. Qual*., **24**, 1188-1192.

Nachabe, M.H., Ahuja, L.R. and Butters, G. (1999) Bromide transport under sprinkler and flood irrigation for no-till soil condition. *J. Hydrol*., **214**, 8-17.

Nachabe, M.H. and Morel-Seytoux, H.J. (1995) Modelling the displacement of resident soluble salt during infiltration. *Soil Sci*., **160**, 243-249.

Nielsen, D.R., Biggar, J.W. and Erh, K.T. (1973) Spatial variability of field measured soil water properties. *Hillgardia*, **42**, 215-259.

Nielsen, D.R, Biggar, J.W., Macintyre, J.and Tanji, K.K. (1980) *Field investigation of water and nitrate-nitrogen movement in yolo soil. In*: Soil nitrogen as a fertiliser or pollutant. International Atomic Energy Agency, Viena, 1980.

Nielsen, D.R., van Genuchten, M. Th. and Biggar, J.W. (1986) Water flow and solute transport processes in the unsaturated zone. *Water Resour. Res*., **22**, 895-1085.

Onken, A.B., Wendt, C.W., Hargrove, R.S. and Wilke, O.C. (1977) Relative movement of bromide and nitrate in soil under three irrigation systems. *Soil Sci. Soc. Am. J*., **41**, 50-52.

Owens, L.B., van Keuren, R.W. and Edwards, W.M. (1985) Groundwater quality changes resulting from a surface bromide application to a pasture. *J. Environ. Qual*., **14**, 543-548.

Palentineanu, I.C., Hera, C., Palentineanu, R., Bologa, M, Canarache, A., Postolache,

T. and Apostol, I. (1980) *Irrigation water and fertiliser application efficiencies for reduction of water and N losses and for water pollution control*. In: Soil Nitrogen as Fertiliser or Pollutant. Proceedings and Report of a Research Coordination Meeting Piracicaba, 3-7 July 1978. International Atomic Energy Agency, Viena, 1980.

Patel, M.S. and Singh, N.T. (1980) Changes in bulk density and water intake rates of coarse textured soil in relation to different levels of compaction. *J. Indian Soc. Soil Sci.*, **29**, 110-112.

Persson, M., and Berndtsson, R. (1999) Water application frequency effects on steady-state solute transport parameters. *J. Hydrol*., **225**, 140-154.

Porro, I., Wierenga, P.J., and Hills, R.G. (1993) Solute transport through large uniform and layered soil columns. *Water Resour. Res*., **29**, 1321-1330.

Pratt, P.F., Jones, W.W. and Hunsaker, V.E. (1970) Nitrate in deep soil profiles in relation to fertilizer rates and leaching volumes. *J. Environ. Qual*., **1**, 97-120.

Priestley, C.H.B. and Taylor, R.J. (1972) On the assessment of soil heat flux and evaporation using large parameters. *Mon. Weather Rev*., **100**, 81-92.

Raats, P.A.C. (1974) Steady flows of water and salt in uniform profile with plant roots. *Soil Sci. Soc. Am. J*., **38**, 717-722.

Rawitz, E., Burns , S. and Etkin, H. (1980) *Fate of fertilizer nitrogen in irrigated fields under semiarid conditions*. In: Soil Nitrogen as Fertiliser or Pollutant. Proceedings and Report of a Research Coordination Meeting Piracicaba, 3-7 July 1978. International Atomic Energy Agency, Viena, 1980.

Rhoades, J.D. (1982) *Soluble salts*. p. 167-178. In: A.L. Page *et al*. (ed.) Methods of soil analysis. Part 2. 2nd ed. Agron. Monogr. 9. ASA and SSSA, Madison, WI.

Rice, R.C., Bowman, R.S. and Jaynes, D.B. (1986) Percolation of water below an irrigated field. *Soil Sci. Soc. Am. J*., **50**, 855-859.

Rice, R.C., Jaynes, D.B. and Bowman, R.S. (1988) Preferential flow of solutes and herbicides under irrigated fields. *ASAE* pap. 88-2634.

Ritchie, J.T. (1972) Model for predicting evaporation from a row crop with incomplete cover. *Water Resour. Res*., **8**, 1204-1213.

Rose, C.W., Chichester, F.W., Williams, J.R. and Ritchie, J.T. (1982) Application of an approximate analytical method of computing solute profiles with dispersion in soils. *J. Environ. Qual*., **11**, 151-155.

Roth, K., Jury, W.A., Fluhler, H. and Attimger, W. (1991) Transport of chloride through unsaturated field soil. *Water Resour. Res*., **27**, 2533-2541.

Russo, D., Jury, W.A. and Butters, G. (1989) Numerical analysis of solute transport during transient irrigation. *Water Resour. Res*., **25**, 2109-2118.

Sharma, M.L., Cresswell, I.D. and Watson, J.D. (1985) *Estimation of natural groundwater recharge from the depth distribution of an applied tracer*. Proceedings of the 21st international Association of Hydraulic Research, Melbourne, pp. 65-70.

Sharma, M.L. and Taniguchi, M. (1991) Movement of a non-reactive solute tracer during steady and intermittent leaching. *J. Hydrol*., **128**:323-334.

Silvertooth, J.C., Watson, J.E., Malcuit, J.E.and Doerge, T.A. (1992) Bromide and nitrate movement in an irrigated cotton production system. *Soil Sci. Soc. Am. J*., **42**, 386-391.

Sisson, J.B., Ferguson, A.H., and van Genuchten, M.T. (1980) Simple method for predicting drainage from field plots. *Soil Sci. Soc. Am. J.*, **44**, 1147-1152.

Smith, S.J. and Davis, R.J. (1974) Relative movement of bromide and nitrate through soils. *J. Environ. Qual*., **3**, 152-155.

Soil Classification Working Group (1991) Soil Classification. A Taxonomic System for South Africa. Dept. of agricultural development, Pretoria, South Africa. 262 pp.

Sposito, G., Jury, W.A., and Gupta, V.K. (1986) Fundamental problems in the stochastic convective-dispersion model of solute transport in aquifers and field soils. *Water Resour. Res*., **22**, 77-88.

Star, J.L., DeRoo, H.C., Frink, C.R. and Parlange, J.Y. (1978) Leaching characteristics of a layered field soil. *Soil Sci. Soc. Am. J.*, **42**, 386-391.

Sudicky, E. (1986) A natural gradient experiment on solute transport in a sandy aquifer: Spatial variability of hydraulic conductivity and its role in the dispersion process. *Water Resour. Res*., **22**, 2069-2082.

Toride, N., and Leij, F.J. (1996a) Convective-dispersive stream tube model for filed-scale solute transport: I. Moment analysis. *Soil Sci. Soc. Am. J*., **60**, 342-352.

Toride, N., and Leij, F.J. (1996b) Convective-dispersive stream tube model for filed-scale solute transport: II. Examples and calibration, *Soil Sci. Soc. Am. J*., **60**, 352-361.

Toride, N. and Leij, F.J. and van Genuchten, M. Th. (1995) *The CXTFIT code for estimating transport parameters from laboratory and field tracer experiments*. U.S. Salinity Lab. Research Rep. 138. Riverside, CA.

Tyler, S.W. and Walker, G.R. (1994). Root zone effects on tracer migration in arid zones. *Soil Sci. Soc. Am. J*., **58**, 25.31.

van de Pol, R.M., Wierenga, P.J. and Nielsen, D.R. (1977) Solute transport in a field soil. *Soil Sci. Soc. Am. J*., **41**, 10-13.

van Genuchten, M. T. (1980) A Closed-form equation for predicting the hydraulic conductivity of unsaturated Soils. *Journal of the American Society of Soil Science.* **44**, 892–898.

van Genuchten, M.T., F.J. Leij and Yates, S.R. (1991) The *RETC* code for quantifying the hydraulic functions unsaturated soils. *Report No. EPA/600/2-91/065*. R.S. Kerr

Environmental Research Laboratory, U.S. Environmental Protection Agency, Ada. OK. 85 p.

van Genuchten, M. Th. and Alves, W.J. (1982) *Analytical solutions of the one-dimensional convective-dispersive solute transport equation*. U.S. Dept. of Agriculture, Tech. Bull. No. 1661. 151 pp.

van Genuchten, M. T. and Nielsen, D. R. (1985) On describing and predicting the hydraulic properties of unsaturated soils. *Annales Geophysicae*. **3**, 615–628.

van Ommen, H.C., van Genuchten M.Th., van der Molen, W.H., Dijksma, R. and Hulshoh, J. (1989) Experimental and theoretical analysis of solute transport from a diffuse source of pollution. *J. Hydrol*., **105**, 225-251.

Ward, A.L., Kachanoski, R.G., von Bertoldi, A.P. and Elrick, D.E. (1995) Field and undisturbed column measurements for predicting transport in unsaturated layered soil. *Soil Sci. Soc. Am. J*., **59**, 52-59.

Watson, K.K., Sardana, V. and Jones, M.J. (1987) *Numerical analysis of the effect of periodicity on solute movement during intermittent leaching*. In: Irrigation and Water Allocation. Symposium held during the 19th General Assembly of the IUGG, Vancouver, B.C., 9-22 August 1987. IAHS Pub. No. 169, pp. 81-90.

White, R.E., Dyson, J.S., Gerstl, Z. and Yaron, B. (1986) Leaching of herbicides through undisturbed cores of a structured clay soil. *Soil Sci. Soc. Am. J*., **50**, 1050-1055.

Wierenga, P.J. (1977) Solute distribution profiles computed with steady-state and transient water movement models. *Soil Sci. Soc. Am. J*., **41**, 1050-1055.

Wierenga, P.J., Shaffer, M.J., Gomez, S.P. and O'Connor, G.A. (1975) Predicting ionic distributions in large soil columns. *Soil Sci. Soc. Am. Pro*., **39**, 1080-1084.

Wild, A. and Babiker, I.A. (1976) The asymmetric leaching pattern of nitrate and chloride in a loamy sand under field conditions. *J. Soil Sci*., **27**, 467-477.

Williams, A.E., Johnson, J.A., Lund, L.J. and Kabala, Z.J. (1998) Spatial and temporal variations in nitrate contamination of a rural aquifer, California. *J. Environ. Qual*., **27**, 1147-1157.

Willmott, C.J. (1981) On the validation of models. *Phys. Geogr*., **2**, 184-194.

SUMMARY

The pollution of surface and subsurface water is a serious problem worldwide. To clean up a once polluted groundwater source is very difficult and costly, if not impossible. Almost all the sources responsible for groundwater pollution originate in the vadose zone of the subsurface. A better understanding of the movement of chemicals in the vadose zone under different conditions can therefore contribute significantly to prevent the pollution of groundwater resources. One particularly important pollutant of groundwater sources in agricultural areas is nitrogen. However, it is very difficult to study the movement of this chemical in agricultural soils, because of its complex and interdependent transformations in the soil. The major aim of this thesis was to compare the movement of bromide and nitrogen in the Bainsvlei soil of South Africa and a soil of Ethiopia, under steady state, transient state and cropped soil conditions, with the view to use bromide as a substitute tracer for nitrogen.

The hydraulic properties of the Bainsvlei soil were determined *in situ*. Different simplified models were used to determine the hydraulic conductivity of the soil, and the performance of the models was evaluated. A steady state experiment was conducted using bromide tracer and a rainfall simulator to determine solute transport parameters using deterministic and stochastic models. Parameters determined from the deterministic convective-dispersive equation and the stochastic stream tube model were similar. It was observed that this soil did not exhibit preferential flow. From the experiments conducted to determine the effect of intensity and continuity of water application on solute transport, it was observed that increasing the intensity and continuity of rainfall/irrigation increases leaching in this soil. The experiments conducted on a bare plot under natural rainfall conditions suggested the leaching of a fertilizer could be minimized if the fertiliser is not applied in batch mode at the beginning of the growing season of a crop, but split over the growing season of the crop.

The study of the movement of bromide and nitrate was repeated with the alluvial sandy loam of Dire Dawa, Ethiopia. Two sets of plots were used for this purpose. One set was left bare and the other planted with maize. No clear conclusions could be reached from this study because of the high natural background nitrate concentration of the soil, which obscured the positions of the concentration peaks. Nevertheless, the experiment did show that the maize uptake attenuated the movement of both chemicals in the soil and that the rate at which maize plants take up nitrogen depends on the vegetative stage of the plants. When combined with the results of the leaching experiment on the bare plot, these results

indicate that it would be more economical, and environmental friendly, if a farmer applies the fertilizer not in batch mode at the beginning of the growing season, but split it over the growing season, dependent on the vegetative phase of the crop and weather conditions.

OPSOMMING

Die besoedeling van oppervlak- en ondergrondse water is 'n wêreldwye probleem. Die skoonmaak van 'n besoedelde grondwaterbron is uiters moeilik en duur, indien nie onmoontlik nie. Bykans alle bronne verantwoordelik vir grondwater besoedeling ontstaan in die onversadigde sone onder die grondoppervlak. Indien die beweging van chemikalieë onder verskillende toestande in die onversadigde sone dus beter verstaan kan word, kan dit lei tot 'n aansienlike verbetering in pogings om grondwaterbesoedeling te verhoed. Een belangrike bron van grondwaterbesoedeling in landbou gebiede is stikstof. Dit is egter baie moeilik om die beweging van stikstof in landbougronde te bestudeer, aangesien dit komplekse en interafhanklike transformasies in die grond ondergaan. Die hoofdoel van hierdie tesis is om die beweging van bromied en stikstof in die Bainsvlei grond van Suid Afrika en ook in ’n grond van Ethiopië te vergelyk onder ewewigs-, oorgangs- en beplante grond toestande, met die doel om bromied as 'n plaasvervanger vir stikstof in studies van die beweging van stikstof te gebruik.

Die hidrologiese kenmerke van die Bainsvlei grond is op die terrein bepaal. Verskeie vereenvoudigde modelle is gebruik om die hidroliese geleiding van die grond te bepaal, en die effektiwiteit van hierdie modelle is ondersoek. 'n Ewewigstoestand eksperiment is gedoen, met bromied as spoorder en ’n reënval simuleerder om die massa transport parameters van die grond met behulp van stochastiese en deterministiese modelle oplossing te bepaal. Parameters bepaal met behulp van die deterministiese konvektiewe dispersiewe vergelyking en die stochastiese stroombuis model het nie veel verskil nie. Daar is ook gevind dat hierdie grond nie voorkeurvloei vertoon nie. Uit eksperimente met die doel om die effek van die intensiteit en kontinuiteit van water op die massa transport te bepaal, is gevind dat ’n toename in intensiteit en kontinuiteit van reënval of besproeiing die loging in hierdie grond laat toeneem. Die eksperimente wat uitgevoer is op 'n skoon perseel onder natuurlike reënval, dui daarop dat die loging van kunsmis geminimaliseer kan word indien die kunsmis deelsgewys oor die groeiseisoen van 'n oes toegedien word, in plaas van eenmalig aan die begin van die seisoen.

Die studie van die beweging van bromied en stikstof is herhaal met die alluviale sanderige kleigrond van Dire Dawa, Ethiopië. Twee stelle persele is vir hierdie doel gebruik. Een stel is skoon gelaat, terwyl die ander met mielies beplant is. Geen duidelike gevolgtrekkings kon

bereik word uit hierdie studie nie. Die rede hiervoor is dat die hoë natuurlike agtergrond nitraatkonsentrasie van die grond die posisies van die konsentrasie pieke verskuil het. Die eksperiment het nietemin bewys dat die opname van die mielies die beweging van beide chemikalieë in die grond verminder het, en dat die hoeveelheid stikstof wat die mielieplante op ’n bepaalde tydstip opneem, deur die vegetatiewe stadium van die plante bepaal word. Hierdie resultate, gekombineer met die resultate van die logingseksperiment op die skoon perseel, dui aan dat dit meer ekonomies sowel as meer omgewingsvriendelik sal wees as ’n boer die kunsmis deelsgewys oor die groeiseisoen in afhanklikheid van die ontwikkelingstadium van die gewas en die weersomstandighede toedien, in plaas van 'n enkele toediening aan die begin van die seisoen.